

AD-A008 987

ROTARY SWAGING OF PRECISION BARRELS

A. L. Hoffmanner, et al

TRW, Incorporated

Prepared for:

Rock Island Arsenal

September 1974

DISTRIBUTED BY:

NTIS

National Technical Information Service
U. S. DEPARTMENT OF COMMERCE

**Best
Available
Copy**

UNCLASSIFIED

SECURITY CLASSIFICATION OF THIS PAGE (When Data Entered)

REPORT DOCUMENTATION PAGE		READ INSTRUCTIONS BEFORE COMPLETING FORM
1. REPORT NUMBER R-TR-74-050	2. JOINT ACCESSION NO.	3. RECIPIENT'S CATALOG NUMBER AD-ACC8 987
4. TITLE (and Subtitle) Rotary Swaging of Precision Barrels		5. TYPE OF REPORT & PERIOD COVERED Technical Report
		6. PERFORMING ORG. REPORT NUMBER ER-7623-F
7. AUTHOR(s) A.L. Hoffmanner and K. R. Iyer		8. CONTRACT OR GRANT NUMBER(s) DAAF03-73-C-0005
9. PERFORMING ORGANIZATION NAME AND ADDRESS TRW Inc., 23555 Euclid Avenue Cleveland, Ohio 44117		10. PROGRAM ELEMENT, PROJECT, TASK AREA & WORK UNIT NUMBERS AMS CODE 552D.11.80700.01
11. CONTROLLING OFFICE NAME AND ADDRESS CDR. Rock Island Arsenal GEN Thomas J. Rodman Laboratory, SARRI-LR Rock Island, Illinois 61201		12. REPORT DATE September 1974
14. MONITORING AGENCY NAME & ADDRESS (if different from Controlling Office)		13. NUMBER OF PAGES 101
		15. SECURITY CLASS. (of this report) UNCLASSIFIED
15a. DECLASSIFICATION/DOWNGRADING SCHEDULE		
16. DISTRIBUTION STATEMENT (of this Report) Approved for public release, distribution unlimited.		
17. DISTRIBUTION STATEMENT (of the abstract entered in Block 20, if different from Report)		
18. SUPPLEMENTARY NOTES Reproduced by NATIONAL TECHNICAL INFORMATION SERVICE US Department of Commerce Springfield, VA. 22151		
19. KEY WORDS (Continue on reverse side if necessary and identify by block number)		
1. Rotary Swaging 2. Statistical Design 3. Residual Stresses 4. Fabrication 5. Barrels		
20. ABSTRACT (Continue on reverse side if necessary and identify by block number) The objective of this program was to optimize the relevant process variables and heat treatments for the fabrication of Cr-Mo-V, 7.62mm, M21 rifle barrels by rotary swaging. This program was based on a statistical-experimental investigation of the relevant process variables and heat treatments to determine their effects on bore quality and dimensional precision. The results quantitatively defined the relations between process and tooling design parameters and product quality. Excellent bore quality with dimensional		

UNCLASSIFIED

SECURITY CLASSIFICATION OF THIS PAGE(When Data Entered)

20. CONT

precision of 0.0001 inch and straightness of 0.0005 inch/foot was obtained in a nearly stress-free swaged product. The difficulty in obtaining a completely formed rifled bore arises from the increasing tendency for galling as "fill", or the complete replication of the mandrel form, is approached. Over a wide range of conventional process design practices either complete fill is difficult to achieve before galling or a product of high residual stress is produced. Nearly stress-free barrels were produced with this process, but process design parameters for low values of residual stress were not entirely consistent with conditions necessary to achieve a completely formed bore. Test firing results show that barrels made under optimized process conditions were of sniper quality.

FOREWORD

This report was prepared by Dr. A. L. Hoffmanner* of TRW, Inc., Cleveland, Ohio in compliance with Contract DAAF03-73-C-0005 and by Dr. K. R. Iyer of the Research Directorate, GEN Thomas J. Rodman Laboratory, Rock Island Arsenal, Rock Island IL.

* Dr. A. L. Hoffmanner is currently with Battelle Memorial Institute, Columbus, Ohio.

CONTENTS

	<u>Page No.</u>
DD Form 1473 Report Documentation Page - R&D	i
Foreword	iii
Contents	iv
List of Figures	vi
List of Tables	viii
1.0 INTRODUCTION	1
1.10 Background	2
1.20 Program Plan	3
2.0 PROCEDURE	7
2.10 Tube Preparation	7
2.11 Material	7
2.12 Material Preparation	7
2.13 Gun Drilling	8
2.14 Tube Finishing	8
2.20 Swage Tooling Design	9
2.21 Die Design	12
2.22 Mandrel Design	13
2.23 Bushing Design	20
2.30 Swage Instrumentation	23
2.40 Inspection Procedures	27
2.50 Residual Stress Measurements	28

CONTENTS (Continued)

	<u>Page No.</u>
3.0 RESULTS	32
3.10 Machine Measurements	32
3.20 Dimensional Measurements	38
3.30 Bore Surface Quality	38
3.40 Residual Stress	46
4.0 ANALYSIS OF RESULTS	66
5.0 PROCESS OPTIMIZATION	81
6.0 BARREL FABRICATION AND EVALUATION	86
7.0 CONCLUSION	89
8.0 REFERENCES	90
Appendix	91
Distribution List	96

LIST OF FIGURES

<u>Figure</u>		<u>Page No.</u>
1	Schematic illustrations of forms of defective rifling and associated borescope observations.	4
2	Flow chart to establish baseline data.	6
3	Schematic cross-section of the interior of the swage.	10
4	Die design features and nomenclature for double reduction and conventional dies.	15
5	Photographs of two die quarters from Set 3XX1 and Set 6XX1	16
6	Mandrel No. 1: Conventional design.	17
7	Mandrel No. 2: Mandrel with expanding taper.	18
8	Mandrel No. 3: Mandrel with decreasing taper.	19
9	Profilometer trace of Mandrel Number 1-2.	22
10	Schematic illustration of swage showing location of instrumentation.	24
11	Section of chart from Blank No. 8K2S2.	26
12	ECM fixture for residual stress determinations.	29
13	ECM residual stress determination fixture installed in an ANOCUT machine.	30
14	Photographs of barrel cross section at the land area.	39
15	Mandrel showing galling and resulting tearing.	40
16	Inner diameter dependence on machining time of rifling and the dependence of the outer diameter and gage length on the inner diameter during boring out using ECM.	47
17	Residual stress determination for Blank No. 63S1.	49
18	Residual stress determination for Blank No. 8K2S1.	50
19	The dependence of strain energy density on overgrind.	57
20	Diametral and length changes as a function of strain energy density.	60
21	The dependence of diametral expansion on overgrind.	61

LIST OF FIGURES (Continued)

<u>Figure</u>		<u>Page No.</u>
22	The dependence of axial expansion on overgrind.	62
23	Push rod force dependence on reduction.	72
24	The reduction-overgrind relations for producing a 0.3002 inch land diameter and corresponding mandrel forces.	74
25	The dependence of the Quality Factor on reduction and overgrind.	75
26	The dependence of strain energy density on process parameters.	77
27	The dependence on overgrind and reduction of the significant processing parameters required to produce a land diameter of 0.3002 inch with minimum distortion and a Quality Factor value of 0.	80
28	The dependence of tube diameter, die angle and strain energy density on reduction and overgrind for defining optimum process design conditions.	83

LIST OF TABLES

<u>Table No.</u>		<u>Page No.</u>
I	Description of Swaging Dies	14
II	Mandrel Dimensions	21
III	Measurements on Swaged Barrel Blanks	33
IV	Process Design Parameters and Quality Measurements for Swaged Blanks	42
V	Residual Stress Measurements	52
VI	Total Diameter and Length Changes	59
VII	Dimensional Measurements after Machining of Six Inch Barrel Lengths	64
VIII	Process Variables and Responses	67
IX	Predicting Equations and Statistics	68
X	Qualitative Review of the Predicting Equations	70
XI	Measurements on Swaged Blanks and the Corresponding Fabricated Barrels	87

1.0 INTRODUCTION

1.10 Background

Precision cold forging of barrels by either rotary swaging or radial forging is the most recent trend in barrel manufacturing procedures in the United States and has been adopted in other nations. The utility of this barrel fabrication technique has been amply demonstrated for conventional weapons in terms of precision and cost, but there are inherent problems with this procedure which could affect the quality and stability of barrels required for accurate performance. Because these problems are common to other well developed technologies, information is available for defining an effort for solution of these problems which arise mainly from residual stress gradients and process design parameters affecting complete fill of the mandrel form. Understanding of the source of these problems and how they are affected by tool design and fabrication procedures would provide a quantitative basis for process design for improved quality and accuracy and a significant advancement in barrel technology.

A brief review is provided in the following to describe the problems associated with the manufacture of precision barrels to justify the approach taken in this program. In this context, conventional fabrication implies the use of either broaching or button rifling, recognizing that broaching is becoming less significant. Furthermore, button rifling is becoming secondary to cold forging for commercial and military barrel manufacture. However, relatively little is currently known about the effects of processing variables on the quality of the cold forged product and what alternatives in the fabrication sequence exist to improve and insure quality features when a particular requirement exists.

The fabrication sequences for manufacturing conventional barrels by either broaching or button rifling are similar. Rifling is one of the last steps and is usually preceded by machining the O.D. Therefore, when required, bore straightness is inspected and corrected before rifling. During broaching, the cutters can run out or float inconsistently, and button rifling will produce an undesirable bore taper. The difficulties and inaccuracies in the fabrication of barrels by button rifling and broaching increase as the blank hardness increases, particularly above about Rc 25. At hardnesses above about Rc 35, these techniques are extremely expensive and button rifling becomes nearly impossible to perform. These problems have probably resulted in the recent fabrication of sniper barrels by button rifling from material at Rc 24 as massive tubes without any O.D. contouring (1).

- (1) Rock Island Arsenal personnel, private communication (February 1972).

Precision rotary swaging of barrels utilizes a tubular blank which is usually cold forged between four reciprocating dies over a mandrel to impart the rifling. The blank is fully plastic during swaging and, as a result of inhomogeneous plastic deformation, residual stresses exist throughout the thickness of the blank. Typically, area reductions in the range of 15 to 25 percent are used. The larger reductions provide definite economic advantages in terms of reduced blank preparation costs, but must be selected based on considerations of structural integrity at the bore surface. Excessive reductions can produce galling and large localized shear strains about and beneath the lands which can lead to fine cracks. In general, large reductions produce considerable work hardening, sometimes preceded by work softening at low reductions (2), and promote localized shear about the lands (3). The residual stress appears to be tensile at the I.D. and compressive at the O.D. because machining of swaged barrels usually results in bore contractions. Typically, this contraction is greatest at the muzzle (4).

The dimensional precision provided by precision swaging depends on the precision of the starting blank and the alignment of guide bushings and dies. Typically, some manufacturers of these barrel fabrication machines will guarantee ± 0.0002 inch on bore dimensions with straightness equal to or better than the straightness of the starting blank for production fabrication. No similar claims can be made with other types of production equipment and, with special care, significantly greater precision can be obtained (3) because swaging tends to improve the concentricity and straightness of the starting blank and almost exactly reproduces the mandrel surface finish and contour. It is not unusual to achieve surface finishes in the range of 8 to 12 microinch AA* with blanks originally prepared with 100 microinch AA finishes.

The major advantages of precision rotary swaging over broaching and button rifling are fabrication economy, precision, surface finish and relative ease in producing the rifling in materials of high hardness. However, a major disadvantage is the severe magnitude and gradients of residual stress which exist throughout a swaged barrel. This condition results in a straightness dependence on asymmetry of the O.D. contour, an unknown response of the system to pressure during firing, and a general instability of the rifled blank during final machining. These problems have been observed (4) during commercial barrel manufacture where bore contractions as large as 0.0013 inch were observed in the finished product.

* Arithmetic Average

- (2) R.L. Suffredini, "How Swaging Affects Mechanical Properties of Steel," Metal Progress, ASM (Aug. 1963) 109.
- (3) A.L. Hoffmann, "Rotary Swaging of Precision Barrels," First Quarterly Report on U.S. Army Contract No. DAAF03-73-C-0005 (December 1972).
- (4) TRW Inc., Manufacturing Data on M14 (January 1963).

Galling of the workpiece to the mandrel and residual stress are two major problems with swaged barrels which have significantly affected fabrication costs. Both of these problems have not been well publicized. Galling results from process design parameters which produce a large length of contact of the die and workpiece and may precede complete fill of the mandrel form to produce good rifling. Galling occurs predominantly in the steps or sides of the lands and occasionally in the very center of the land and results in serious degradation of the land form. Since galling will result in destruction of the mandrel, its occurrence must be avoided. Attempts to avoid this problem have resulted in swaged barrels with "rounded" corners from using a maximum reduction sufficient to avoid galling while still producing a nearly complete rifling form. The appearance of rounded corners in swaged barrels is shown schematically in Figure 1. For a right hand twist galling will occur first on the left side of the rifling (viewed from the breech) where the amount of fill will be greater than the right side. Figures 1c and 1d show the land forms for complete fill with galling. Air gage measurements will not distinguish the two forms in Figures 1c and 1d from perfect rifling and it is not uncommon to find excellent dimensional precision with the incompletely filled form such as 1b. Because the corners of the incompletely formed land are free formed, control of their height and width is difficult. This condition can usually be observed with a borescope and usually results in a jerky motion when pushing a plug gage through the bore. The lack of control over the precise dimensions of rounded corners is a serious quality feature which causes impaired accuracy and reduced barrel life.

Residual stress originates from inhomogeneous deformation during metalworking and can be a significant factor in the dimensional stability of swaged barrels. The major problem with residual stresses occurs during finishing of the barrels. Highly stressed barrels can yield at very low lateral forces of the same magnitude of cutting forces to impair straightness and, because metal removal results in stress relaxation, the bore dimensions will either expand or contract depending on the sign (compressive or tensile) of the residual stress. The amount of expansion or contraction will also depend on the amount of material removed at a particular section. Current swaging practice usually results in bore contractions during finishing which are indicative of tensile stresses at the bore. The amount of contraction is usually greater at the muzzle because in this region more material is machined from the outer diameter. Conventional thermal stress relief treatments of swaged barrels can be used to reduce residual stresses if the resulting surface contamination and distortion of the barrels can be tolerated.

1.20 Program Plan

The objective of this program was to optimize the relevant process variables and heat treatments for fabrication of Cr-Mo-V (MIL-5-11595) 7.62mm M21 rifle barrels by rotary swaging and apply these conditions for fabrication of 6 barrels for demonstration of the procedures and for subsequent evaluation of the product.

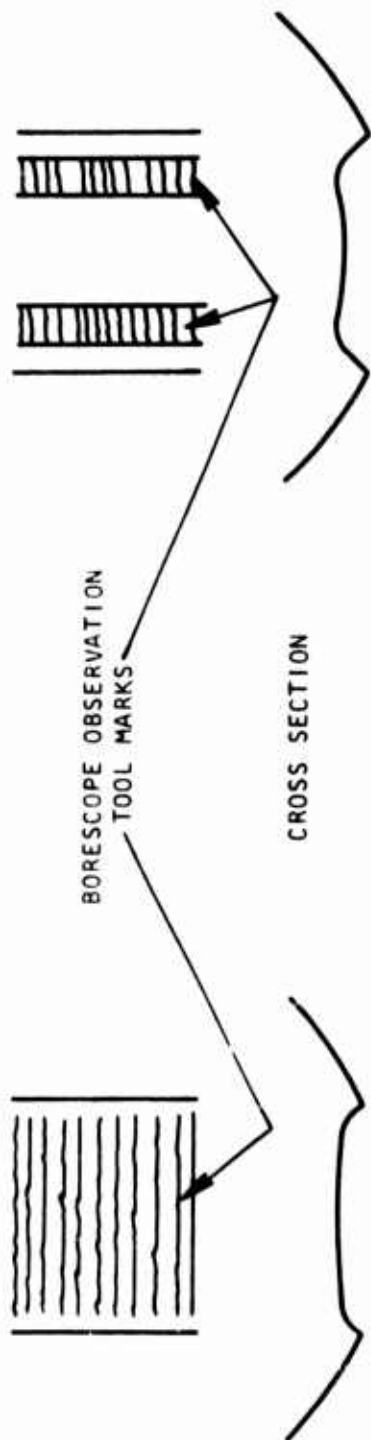


Figure 1a. Incomplete fill

Figure 1b. Partial fill

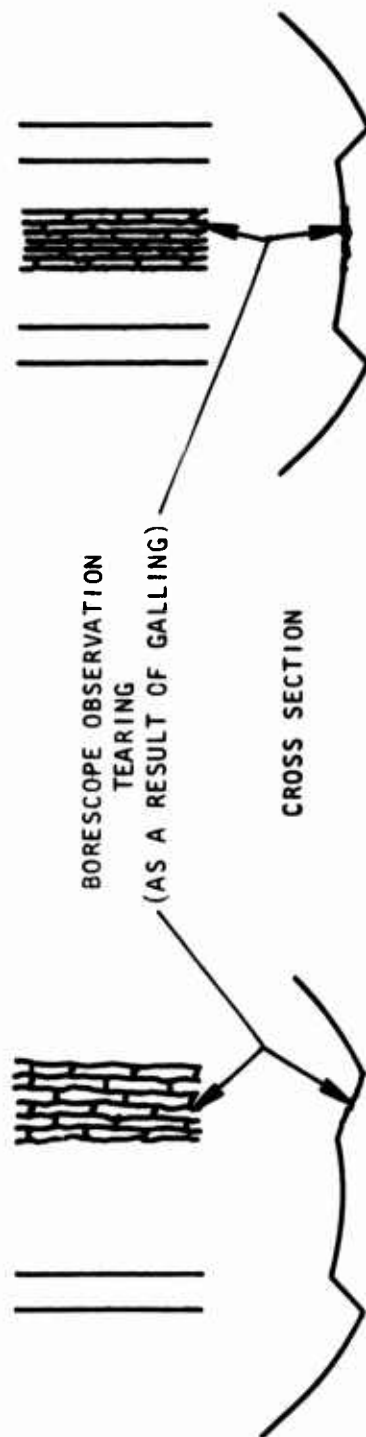


Figure 1c. Galling at land edge

Figure 1d. Galling at land center

Figure 1. Schematic illustration of forms of defective rifling and associated borescope observations.

The original plan for achieving this optimization is described by the flow chart in Figure 2. This flow chart describes the experimental design and evaluation procedures to establish base-line data for subsequent process design and optimization. The experimental plan was based on a sequence of factorial designs at predominantly two levels of the major process design parameters to determine their effects on barrel quality and residual stress. The major process design parameters are the following:

1. Mandrel design
2. Die design
 - a) die angle
 - b) overgrind
 - c) land length
 - d) land design
 - e) die radii
 - f) die exit design
3. Reduction
4. Machine parameters
 - a) feed rate
 - b) machine rpm
 - c) back pressure

Various combinations and permutations of these process design parameters were used to determine their effects on machine performance, product quality, and residual stress. Machine performance was determined by instrumenting the swage and recording the measurements on an oscillograph. The product quality was evaluated using conventional techniques (e.g., air gauges, borescope evaluation, straightness determinations, etc.). Residual stress was determined by using the Sach's "Boring Out" (5) technique. The results from these measurements with the process design parameters were entered into a digital computer to determine the optimum fabrication conditions using contemporary statistical-analytical techniques (6). The procedures used to obtain these measurements, the analytical techniques and the results will be discussed in the following.

- (5) A.A. Denton, "Measurement of Residual Stresses, Techniques of Metals Research, Vol. V, Part 2, "Measurement of Mechanical Properties," R.F. Bunshah, Editor, Interscience (1971) 234
- (6) N.R. Draper and H. Smith, Applied Regression Analysis, John Wiley and Sons, Inc., New York, N.Y. (1963)

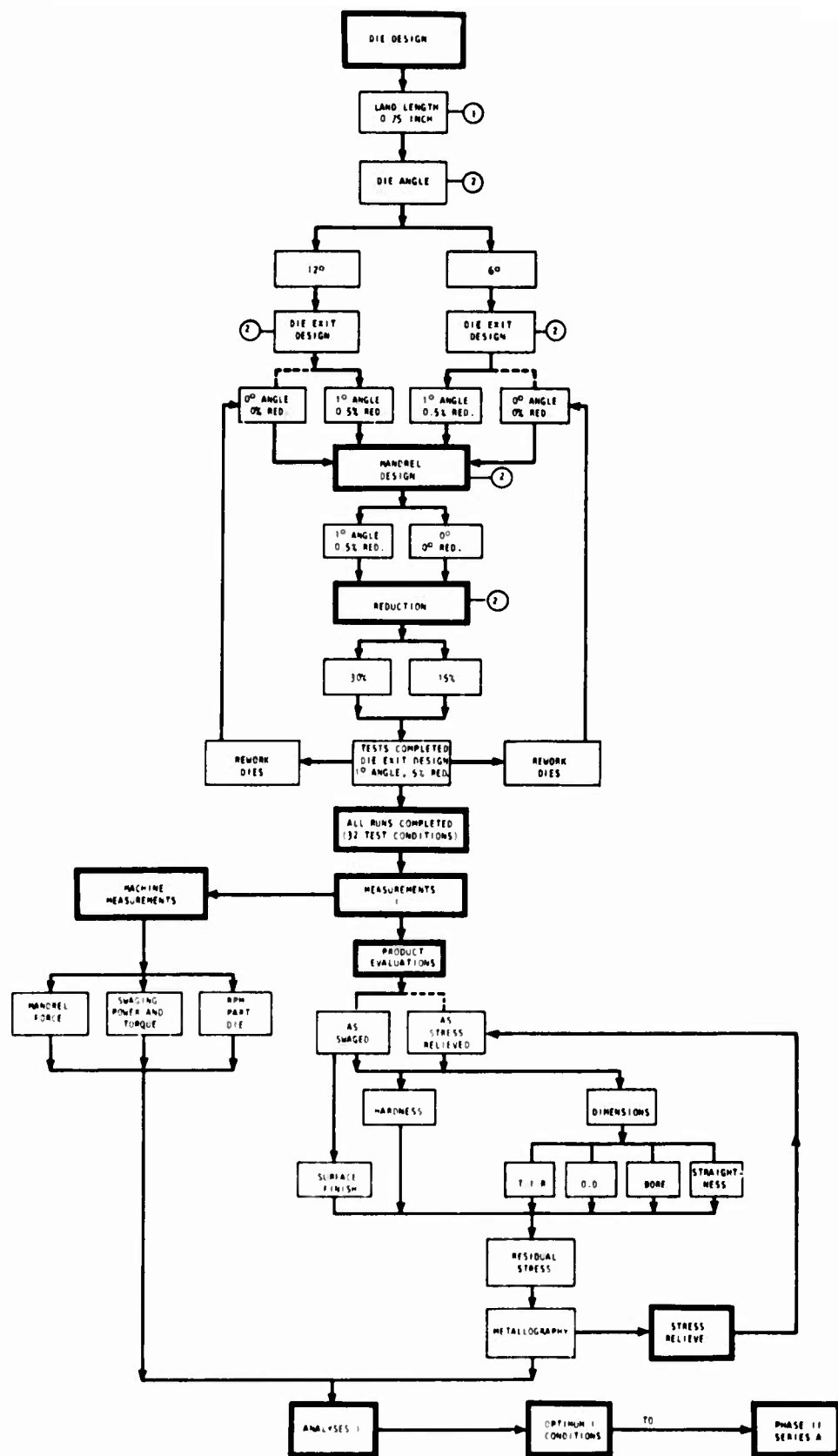


Figure 2. Flow chart to establish baseline data.

2.0 PROCEDURE

Standard preparation, fabrication and test procedures were established for all blanks. The following discussion will describe the preparation procedures, the swage tooling designs, machine instrumentation and inspection and measurement techniques.

2.10 Tube Preparation

2.11 Material

The material provided by the Rock Island Arsenal was Cr-Mo-V (MIL-S-11595) hot rolled bar of nominally 1-3/8 inch diameter and 47 inch length.

2.12 Material Preparation

All material was prepared in the same manner using the following procedures:

1. Centerless grinding was performed on the 47 inch long bars to remove the hot rolled surface and to provide diameters to within ± 0.001 inch, 0.030 inch larger than the final tube blank diameter for swaging.
2. Each bar was subsequently cut into 2 equal 23 inch lengths.
3. Heat treatment
 - a) The bars were racked vertically by standing them on a wire screen and supporting them vertically in loose fitting collars spaced vertically 10 inches apart and 10 inches above the screen.
 - b) Austenitizing was performed in molten salt at 1600°F for 45 minutes followed by a quench into circulating oil.
 - c) Tempering was performed in an endothermic gas atmosphere at 1210°F for 1-1/2 hours at temperature which was followed by a forced atmosphere cool to room temperature. This provided an as-tempered hardness of Rc 32 to 33. Other tempering temperatures produced Rc 36 at 1200°F and Rc 28 at 1225°F on test pieces.

- d) Cleaning, measurement and facing of the bars were performed after heat treatment. Measurement of the total runout of the bars after heat treatment was performed to obtain data for stock removal to permit grinding after gun drilling to provide concentric tubes of the proper dimensions in preparation for swaging. Subsequently, the ends were faced in preparation for gun drilling. The total runout from center after heat treatment was $0.0170 \pm .0085$ inch determined from measurements on 12 bars.

2.13 Gun Drilling

Gun drilling was performed at 200 surface feet per minute with a feed of 1.0 inch per minute using 0.3125 inch diameter Eldorado gun drills with an N-8 nose grind.

2.14 Tube Finishing

Tube finishing consisted of the following steps with the resulting dimensional and surface measurements:

- a) Measurements were made of the runout of the inner diameter from the outer diameter and the longitudinal surface finish after gun drilling to determine the necessary stock removal in preparation for swaging and to quantitatively describe the surface finish. These measurements provided the following:

1. Runout of O.D. from I.D. 0.023 ± 0.008 inch, and

2. I.D. surface finish:

	<u>Average</u>	<u>Maximum</u>
Roughness (inch x 10^6 AA*)	27	32**
Waviness (inch x 10^6) (2 x amplitude)	300	360**

- b) All tubes were finish ground to produce the O.D. concentric with the I.D. to within 0.005 inch T.I.R.

* Arithmetic Average

** Value below which 97.5% of the measurements occurred.

2.20 Swage Design

The basic elements of the swage (a 100 ton Intraform) which affect its performance and product quality are shown schematically in Figure 3. These elements are located at the front (i.e., at the entrance-guide bushing) and rearward within the swage-die enclosure and the remaining enclosure of the moving components of the machine. The swaging cycle is initiated when the push rod, under a controlled feed rate, feeds the workpiece through the front guide bushing and into the rotating and reciprocating swaging dies. The push rod is a hollow, replaceable extension of the feed mechanism with an outer diameter slightly smaller than the product diameter to permit free passage between the dies to complete swaging of the workpiece. The push rod is located concentrically with the workpiece by a slip-fit collar which slides over the push rod as the push rod enters the front bushing. The inner diameter of the push rod is selected to permit free passage of the mandrel and mandrel rod. Both the mandrel rod and push rod are connected to larger elements of the feed mechanism assembly, the mandrel rod extension and tail stock, respectively, which contain thrust bearings to permit nearly free rotation of these machine components in contact with the workpiece. The location of the mandrel relative to the dies is controlled by the mandrel positioning nut to permit positioning of the mandrel to approximately $1/8 \pm 1/16$ inch beyond the termination of the die land.

The counterholder or back pressure rod is attached to a hydraulic cylinder to provide a constant back pressure to the product exiting from the dies. This rod, which has nearly the same diameter as the product, enters the rear guide bushings and dies at initiation of the swaging cycle. During this portion of the cycle, the spring-loaded dowel pin on the end of the counterholder is depressed by the mandrel until the workpiece is fed through the dies during the swaging cycle. This procedure provides accurate concentric alignment of the counterholder, mandrel, workpiece and guide bushings. Once swaging begins, the dowel pin enters the swaged blank to maintain concentricity of the counterholder and swaged product.

The die closure is determined by the motion of the drivers which contain a sinusoidal form in contact with the rollers. This sinusoidal form is reputed to be the most desirable for barrel fabrication because it provides the most continuous type of "squeezing" action to promote a more uniform bore.

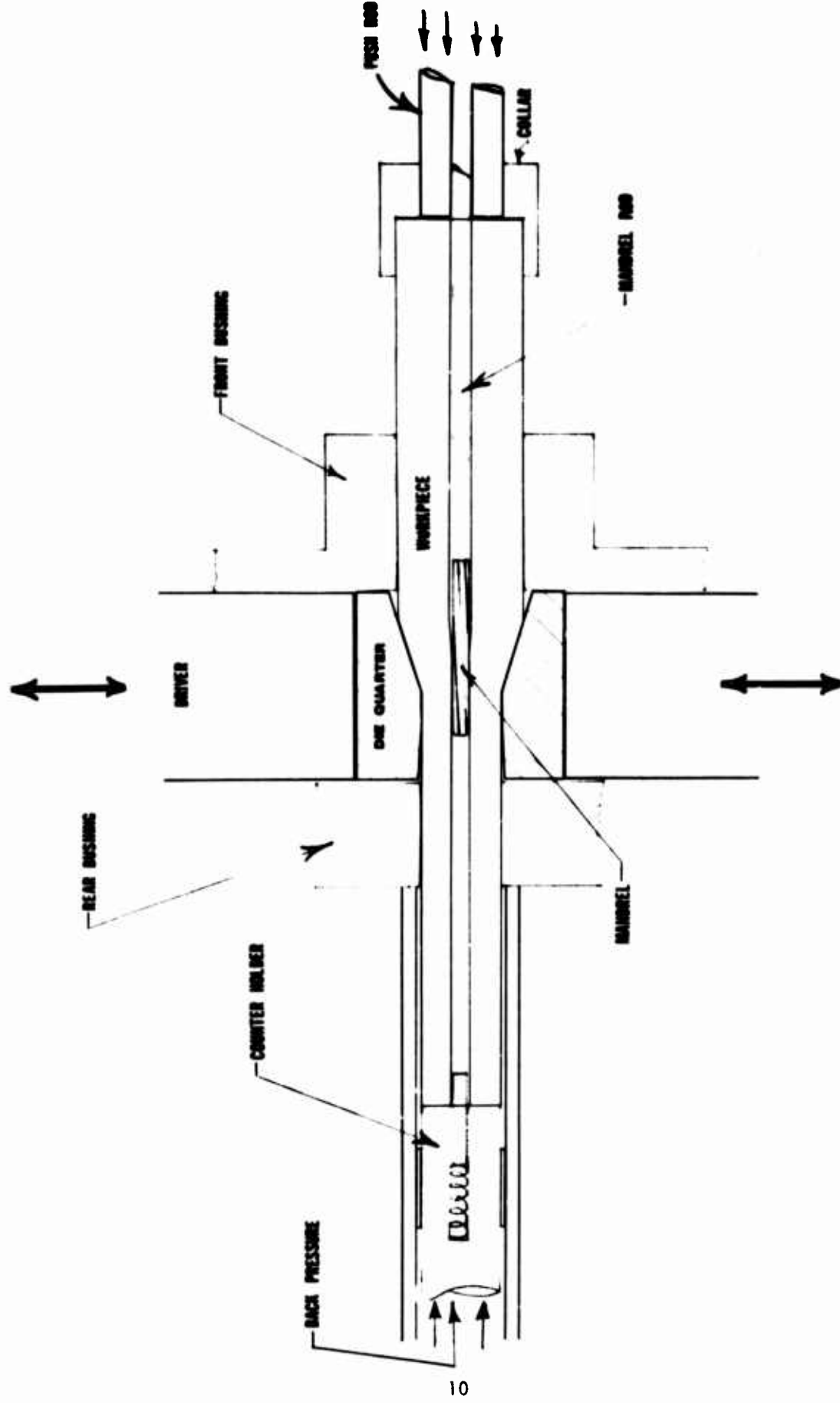


Figure 3. Schematic cross-section of the interior of the swage during a swaging cycle.

The specific swaging cycle used for this program consisted of the following steps:

1. Cleaning of the gun-drilled tube with felt patches and isopropyl alcohol;
2. Lubricating the tube blank with Wynn's Multipurpose Concentrate (a product of Autodynamics Inc.) with 10 volume percent molybdenum disulfide using a chamois patch;
3. Moving the counterholder to its forward position between the dies;
4. Insertion of the mandrel rod into the tube blank and subsequently inserting the tube blank into the entrance guide bushing until it contacted the counterholder;
5. Rapid traverse of the push-rod assembly with the attached collar to the feed position (in contact with the workpiece);
6. Sliding the mandrel rod assembly into the locked position;
7. Engaging the feed gears to initiate swaging until after the completion of the swage cycle;
8. Stopping the dies in the open position and rapidly reversing the push rod - feed assembly while ejecting the product with the counterholder;
9. Unlocking and retracting the mandrel rod assembly and removal of the swaged product.

No special precautions were taken to lubricate the outer diameter of the workpiece with the exception that it was always wiped with a clean rag. Consistent lubrication was provided by oil circulating within the roll cage and about the dies, a characteristic of the Intraform.

All swaging was performed on the 100 ton prototype Intraform at Cincinnati Swaging and all tooling was designed specifically for this machine. Different swaging mandrels and dies were constructed with both conventional designs and unconventional design features to provide mechanical stress relief and improved barrel quality. These designs were combined and permuted to provide quantitative evaluations of the effects and interactions of these specific designs using the statistically designed experimental plan. In order to provide an unambiguous record of the conditions used in producing a barrel blank a simple but complete coding or blank specification system was developed. This system is described with the following examples:

Initial tube diameter (L = 1.300 inch)
 ↑
 Die angle (semi-angle) → 6|L2 ← Number of times the die had been ground
 ↓
 Mandrel number (No. 1 is a conventional design)

The die described in this example had a 6° die angle (12° included angle) and possessed other internal features introduced by the second grinding of this die. This die is referred to as 6XX2; however, other numbers or letters may occur with the die angle to appropriately describe the die. The dies which were used in the program are described in Table 1.

The second number in the blank specification number refers to the mandrel design. These designs, shown as prints in a later section, were as follows:

<u>Mandrel No.</u>	<u>Mandrel Description</u>
1	Conventional design
2	Increasing (expanding) taper
3	Decreasing (contracting) taper

The outer diameter of the tube before swaging is described by the letters L (1.300 inch), S (1.200 inch) and M (1.235 inch). Most of the bars were swaged to an outer diameter of nominally 1.120 inch. Variations of this swaged diameter occurred before the proper amount of die shimming was established.

The last number in the blank specification refers to the number of times the die was ground and, since the die was ground to a particular geometry, this corresponds to the particular geometry of the die used to fabricate the blank.

2.21 Die Design

The swaging dies were fabricated from M-2 high speed steel double tempered to Rc 61/63 with a ground surface finish less than 15 microinch AA. All dies were designed with a side clearance or gap between die quarters of 0.060 inch.

The prominent die design features are listed in Table 1 with the die specification number. These features consist of the entrance angle, the die land length and the exit angle between which there is a transition or blending region produced by a radius of 3.0 inch and the die overgrind. The percent overgrind determines the

ovality of the swaging die and is determined by the percent difference between the die diameter and the diameter of the part. Different overgrinds can exist in the entrance and die bore areas.

The general features of the die designs shown in Figure 4 correspond to the double reduction die and the conventional die. The major distinctions between the two designs are the abrupt relief after the primary land, and the secondary land producing a nominal 0.5 percent additional reduction possessed by the double reduction die. In both cases the reduced bar diameter $2R_b$ is defined by the distance of closest approach of the dies and is smaller than the actual ground-in or bore diameter $2R_g$ of the dies by an amount determined by the overgrind. Photographs of two die quarters from 3XXI and 6XXI are shown in Figure 5.

The critical features of the double reduction die are the relief between the primary and secondary lands, the length and depth of this relief region, and the secondary reduction and land length. The purpose of the secondary relief was to allow the reduced blank to relax to an equilibrium condition after removal of the working stresses imposed by the primary land. This equilibrium condition would necessitate expanding with yielding to establish a residually stressed blank. The subsequent secondary reduction will produce yielding according to the magnitude of the imposed applied stress field and the residual stress existing after the secondary relief. In this manner mechanical stress relief can be achieved to a degree determined by the magnitudes of the stresses imposed by the secondary land and the residual stresses existing in the reduced blank after the secondary relief. For these reasons, the secondary reduction must be tuned to provide mechanical stress relief in accordance with the existing residual stresses in the partially swaged blank, but cannot be too large to impose its own characteristic residual stress. The secondary reduction of 0.5 percent was designed to produce an O.D. displacement equal to 3 times the displacement necessary for yielding at the I.D. and one-half the displacement necessary for yielding at the O.D. for an otherwise stress-free tube surrounding a mandrel. This reduction is empirical, but can be justified on past experience with double reduction dies for extrusion (7) and drawing (8).

2.22 Mandrel Design

Mandrel design is known to be a significant factor affecting dimensional stability, precision and surface finish during the fabrication of tubular products. Therefore, mandrel design was also included as a design factor in the process evaluation. The designs

- (7) R.J. Fiorentino, et al., "Development of the Manufacturing Capabilities of the Hydrostatic Extrusion Process, "Interim Engineering Progress Report No. IR-8-19S(1x), Battelle Memorial Institute, Columbus Laboratories. March 1967.
- (8) J.K. Misra and N.H. Polakowski, "In-Process Control of Residual Stress in Drawn Tubing," TASME, J. of Basic Engineering (Dec. 1969) 810.

TABLE I
Description of Swaging Dies

Die Specification Number	Die Angle		Primary Land Length (inch)	Secondary Land Length (inch)	2x(Die Radius) (inch)	Overgrind(%) Based on 1.120 inch Blank Dia.
	Entrance	Exit				
3XX1	3°	1.5°	0.50	0.10	1.155	3.0
3XX2	3°	1.5°	0.50	0	1.155	3.0
3CXX1	3°	1.5°	0.125	0	1.245	10.0
3KRXX2	3°	1.5°	0.50	0	1.280	12.5
41S1	4°	1.5°	0.1	0	1.240	10.0
6XX1	6°	1.5°	0.50	0.10	1.155	3.0
6XX2 (6XX4)	6°	1.5°	0.50	0	1.155(1.160)	3.0
6XX3	6°	1.5°	0.50	0	1.318	15.0
6XX30	6°	1.5°	0.50	0	1.155	15.0/3.0*
8KXX1	8°	1.5°	1.00	0	1.280	12.5

* The die entrance was overground 15% and the die bore or land area was overground 3%.

Double Reduction Die

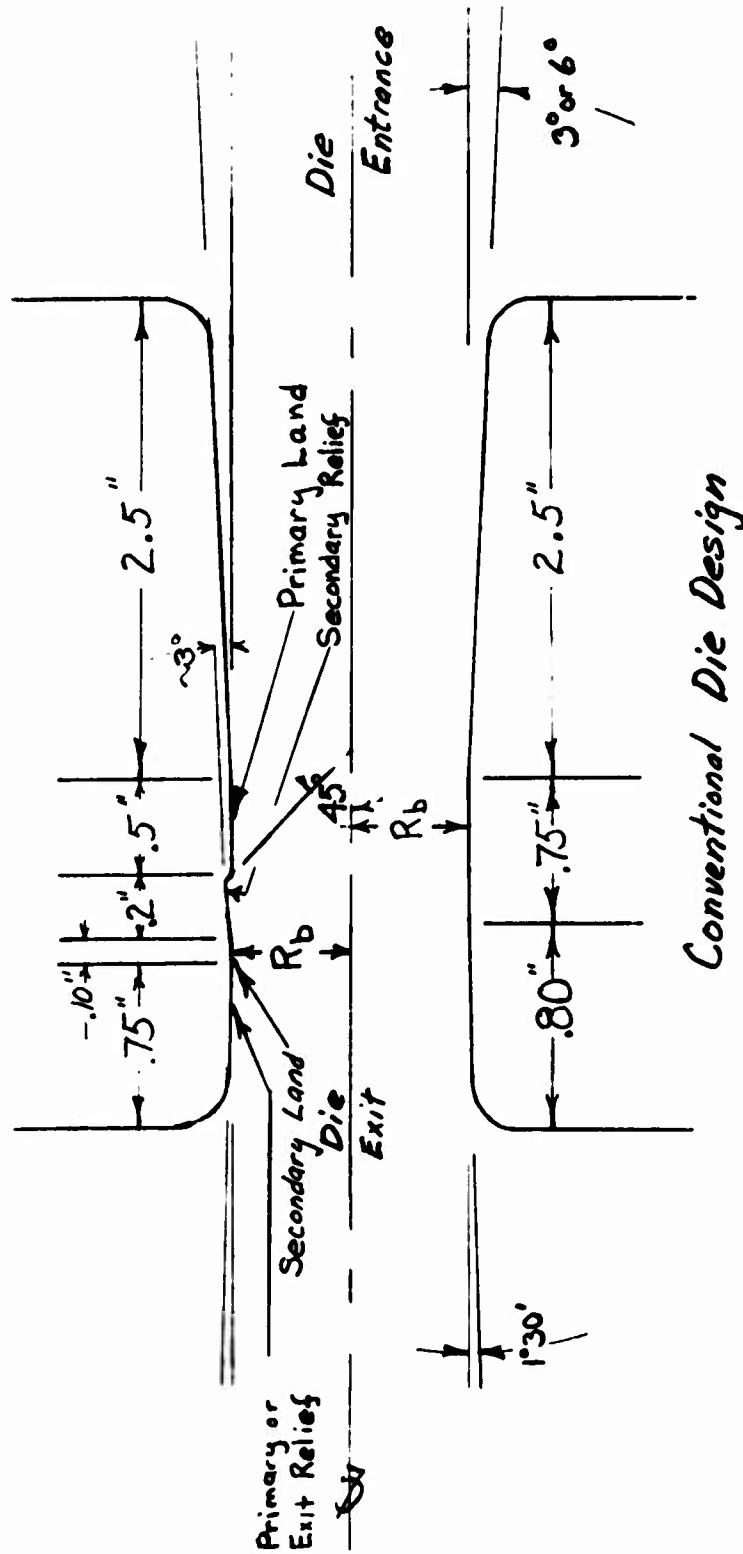


Figure 4. Die design features and nomenclature for double reduction and die design.

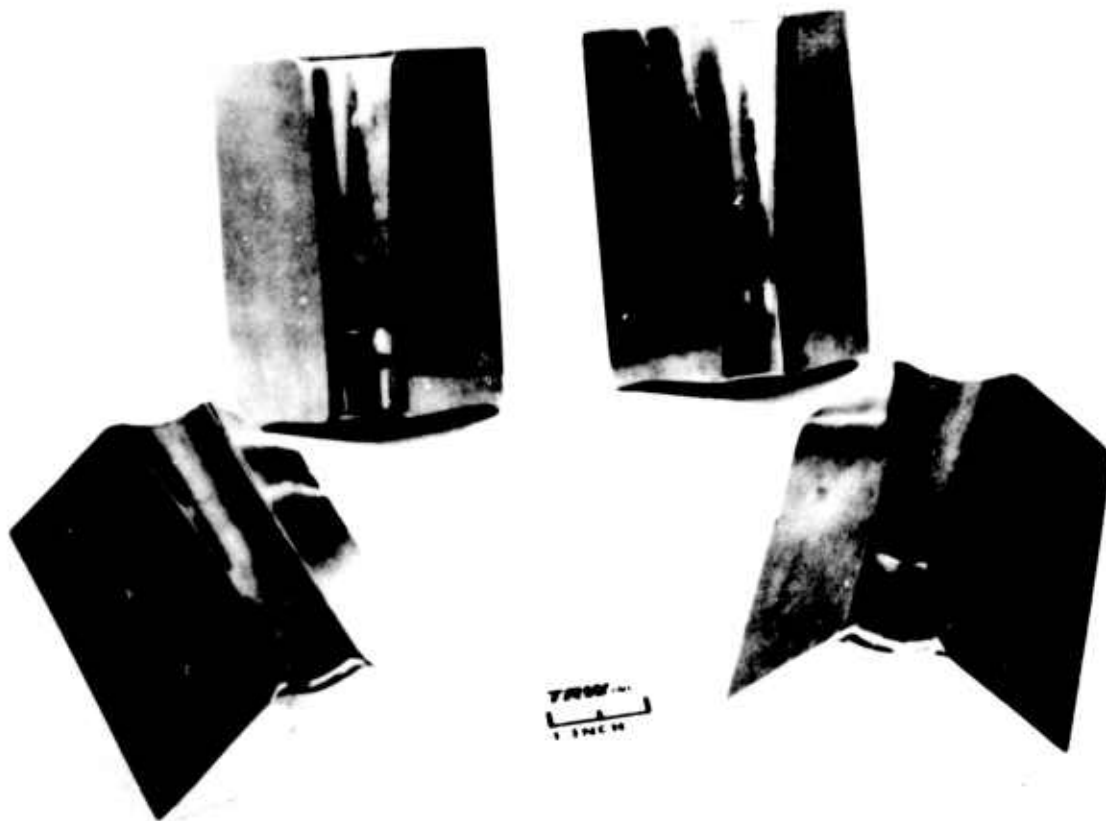


Figure 5. Photographs of two die quarters from the Set 3XXI and Set 6XXI dies.

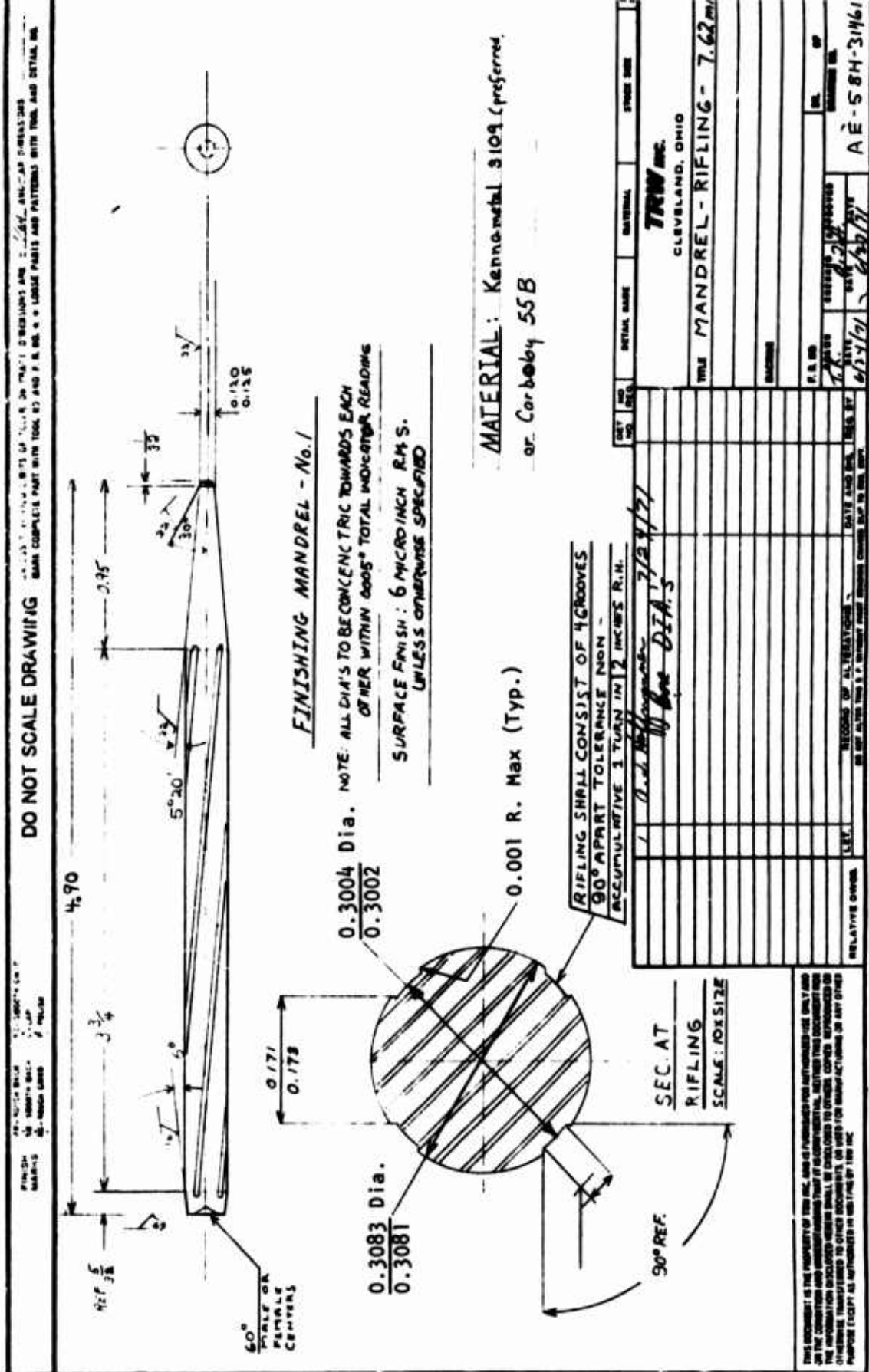
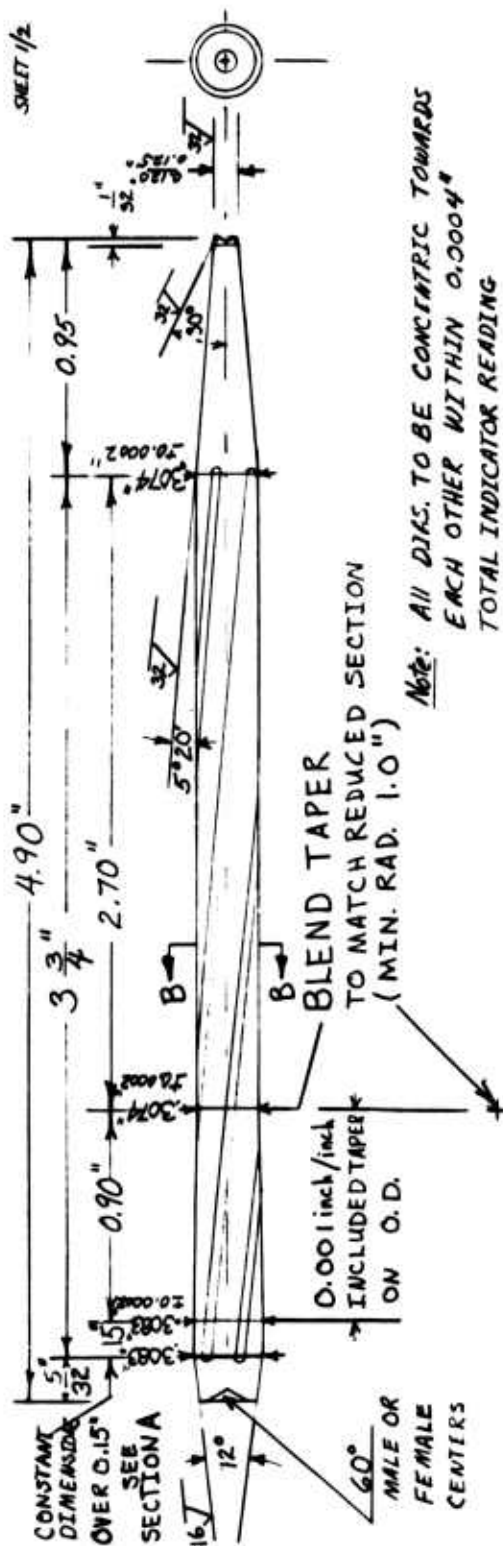


Figure 6. Mandrel No. 1: Conventional design finishing mandrel.



SURFACE FINISH:

6 MICROINCH RMS
UNLESS OTHERWISE
SPECIFIED

MATERIAL: KENAMETAL 3109 (preferred)
or CARBOLLOY 55B

FINISHING MANDREL

NO. 2A
7.62 mm
AE-50H-319CNA-2A

A. L. Hoffmann
TRW Inc.
Cleveland, Ohio
10/10/72

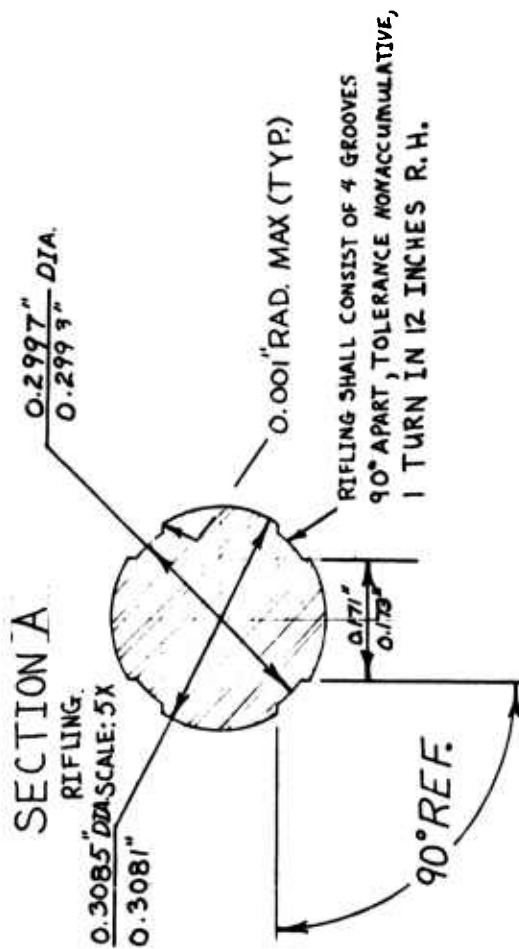


Figure 7. Mandrel No. 2: Mandrel with expanding taper.

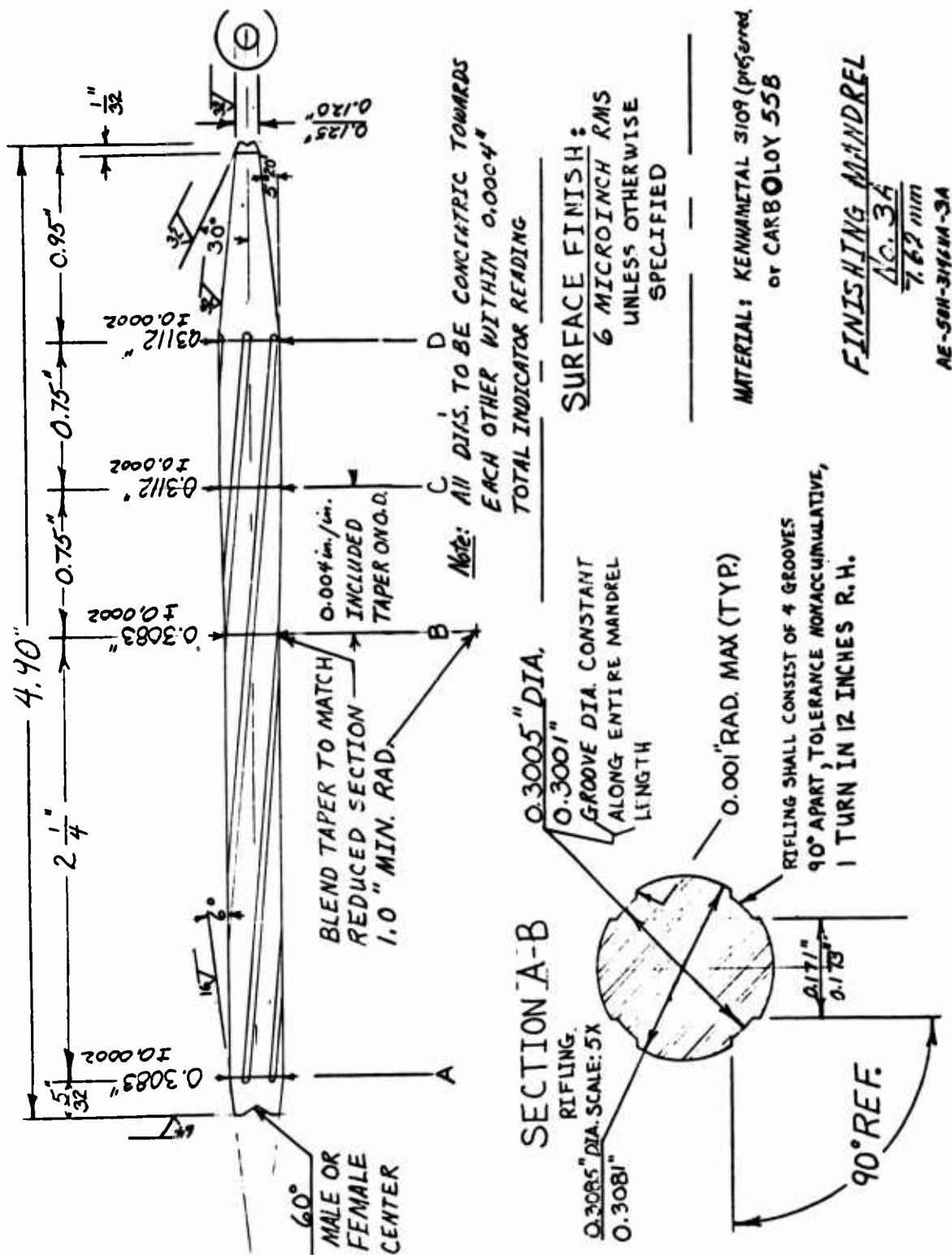


Figure 8. Mandrel No. 3: Mandrel with decreasing taper.

which were selected are shown in Figures 6, 7 and 8 and correspond to the conventional design, conventional design plus a positive or expanding taper, and a negative taper leading to the conventional design, respectively. The potential advantages of the expanding and decreasing tapers are improved dimensional stability, and improved surface finish and concentricity, respectively. The expanding taper was designed to produce twice the bore displacement required for yielding at the bore, which is approximately equal to the bore displacement for initiation of yielding in the blank free of residual stress. The mandrel with the decreasing taper was designed with a maximum diameter and taper to provide nearly complete contact of the bore and mandrel during the entire time when the blank is between the dies. For a particular reduction, this mandrel should improve the surface finish of the bore and provide better radial alignment and concentricity than the conventional design.

Dimensional inspection of the mandrels was performed using a vernier micrometer standardized by measurements on a 0.3000 inch gage block. These measurements of the land and groove diameters were taken at 90° to each other at the back, middle and front of the mandrels, where the front refers to the mandrel end in last contact with the rifled blank. The average and range of the measurements at the back and front positions are shown in Table II. The results show a few disparities with print specifications (particularly numbers 2-1 and 1-1), the most serious being Mandrel No. 1-1 which was 0.0005 inch oversize on the land dimension. Because of the long delivery time for mandrels, all of these mandrels were accepted; however, only specifically selected mandrels were used for final production of barrels. Mandrel Nos. 2-1 and 1-1 were used only for specimen preparation where the major concern was dimensional precision relative to the dimensions of the front portion of the mandrel and not strict adherence to the barrel print dimensions.

The profilometer trace of Mandrel No. 1-2 in Figure 9 shows that the land region exhibits greater roughness than the groove and the land-groove radii appear extremely sharp in accordance with the print specifications.

2.23 Bushing Design

A 5.5 inch entrance bushing, a 2.0 inch exit bushing, and a stepped collar to concentrically locate the tube and push rod were used to maintain straightness. Both bushings were indicated to be concentric with the machine centerline. Initially, the entrance bushing was constructed by shimming an existing bushing. Although this arrangement appeared satisfactory, it was questionable and all subsequent bushings were bored 0.002 inch over nominal stock dimensions. This procedure resulted in a marked improvement and consistency of straightness and was subsequently used as the standard practice unless noted otherwise in the presentation of results.

TABLE II

Mandrel Specification	<u>Measured Mandrel Dimensions</u>			
	<u>Measurement Position</u>			
	<u>Back</u>		<u>Front</u>	
	<u>Diameter (inch)</u>		<u>Diameter (inch)</u>	
	<u>Land</u>	<u>Groove</u>	<u>Land</u>	<u>Groove</u>
No. 1-1	.3000 \pm 0.001	.3081*	.3009 \pm 0.0001	.3081
No. 1-2	.3002 \pm 0.0001	.3083 \pm 0.0001	.3003 \pm 0.0001	.3083
No. 1-3	.3003 \pm 0.0001	.3082 \pm 0.0001	.3003 \pm 0.0001	.3082
No. 2-1	.3001 \pm 0.0008	.3073	.2998 \pm 0.0001	.3083
No. 2-2	.3001 \pm 0.0001	.3073	.2998 \pm 0.0001	.3083
No. 3-1	.3005	.3115 \pm 0.0001	.3004 \pm 0.0002	.3082
No. 3-2	.3004 \pm 0.0001	.3115 \pm 0.0001	.3005 \pm 0.0001	.3084

* Tolerances not specified indicate that the dimension repeated to better than 0.0001 total band about the mandrel.

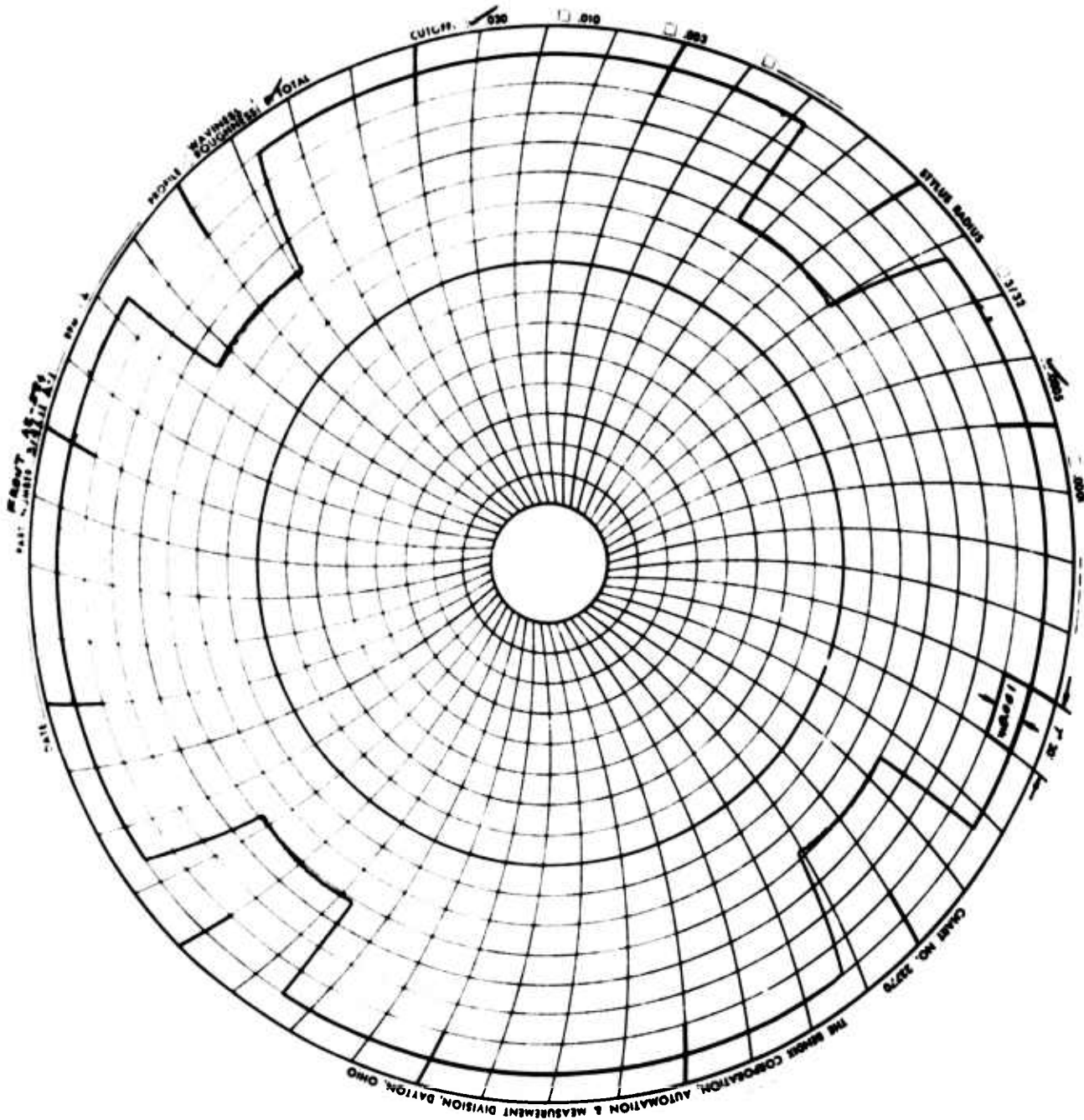


Figure 9. Profilometer trace of Mandrel Number 1-2.

2.30 Swage Instrumentation

Instrumentation of the swage consisted of the following gauges and measurements:

1. Strain gauge load cells with slip ring contacts for measurements on the following machine components:
 - a) torque and horsepower measurements on the main drive shaft; and
 - b) push-rod load directly off of the push rod.
2. Mandrel rod force from strain gauges mounted on the mandrel rod support fixture.
3. Workpiece angular velocity from a rotational-linear potentiometer driven by friction of a rubber wheel spring loaded against the workpiece.
4. Die angular velocity determined by a tachometer generator connected directly to the drive shaft-die housing assembly.

The location of these gauges are shown schematically in Figure 10.

A Visicorder (Model No. 906C) light beam oscillograph was used to record the output of the instrumentation on the swage. Before installation, the load cells (torque, push rod and mandrel) were calibrated on a previously calibrated and certified Instron Universal Testing Machine using a half-bridge strain gage indicator. Three calibration resistors were used for each load cell to correlate the mechanical load with the appropriate electrical response for transfer of the calibration to the Visicorder and for in-process calibration. The calibration of the load cells installed on the swage was also checked using a calibrated proving ring after initial installation and after running 20 barrel blanks. Perfect agreement was maintained between the calibrated response of the gauges and the calibration resistors and load measurements. After initial calibration, the calibration of the torque and push rod cells with external resistors was transferred to the internal calibration circuit of the Visicorder carrier amplifiers for ease of operation. Because of the required sensitivity, the push rod cell was calibrated with external resistors only.

The machine and piece rpm-measuring circuits were calibrated on the machine by appropriately adjusting their outputs through "trim pots" in the circuits to provide particular chart displacements corresponding to rates of flywheel rotation (measured with a mechanical tachometer) and piece rotation (measured optically) respectively.

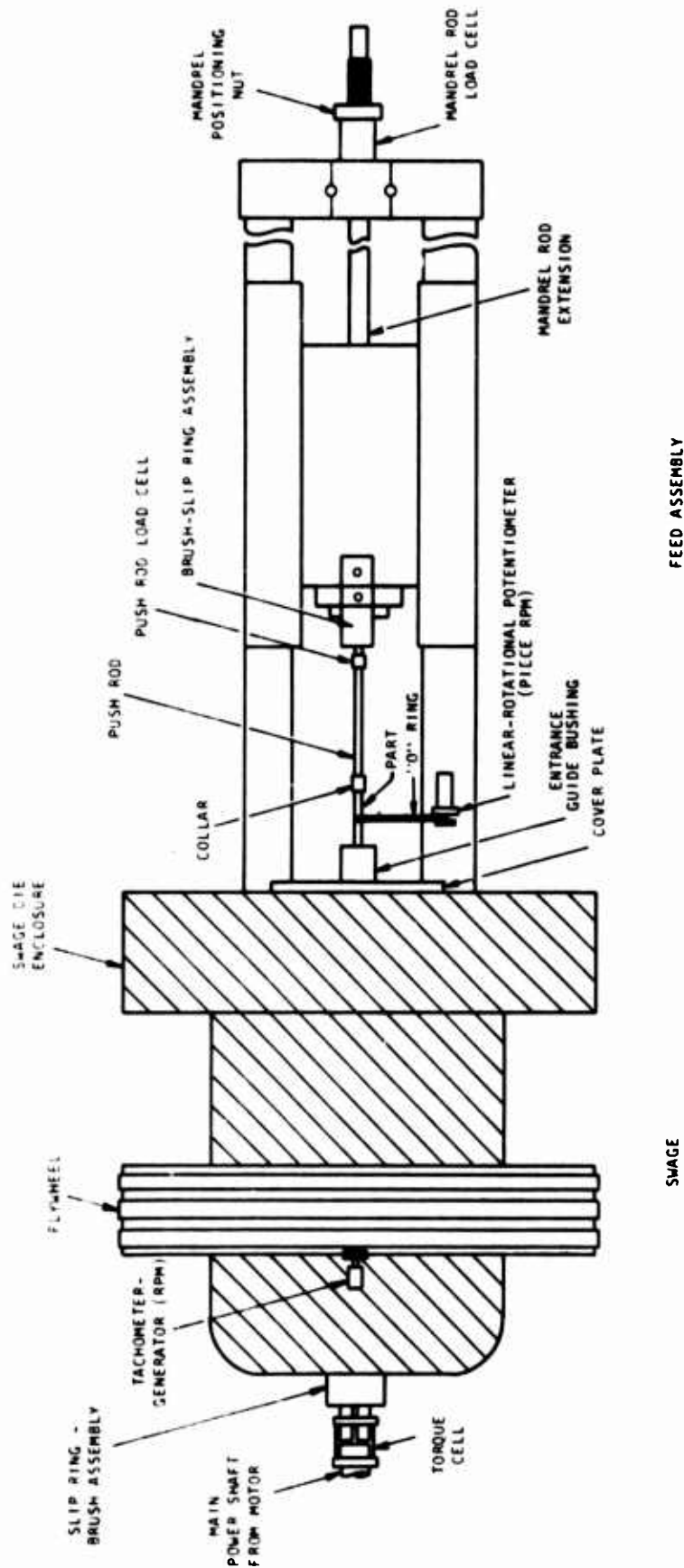


Figure 10. Schematic illustration of swage (top view) showing location of instrumentation.

The calibrations provided the following responses on the Visicorder chart:

<u>Gauge</u>	<u>Response</u>
Torque cell	250 ft.lb./inch
Push rod cell	2000 lb./inch
Mandrel rod cell	800 lb./inch
Machine RPM	200 rpm/inch
Piece RPM	1 line/1.58 piece revolutions (piece rpm determined by chart speed in inches/minute and the number of lines per minute)

Initially, calibrations were performed before each run; however, this procedure showed that the calibration was stable and this condition was relaxed. Subsequent calibration checks were made and recorded after every third blank and at the start and finish of each day of swage operation.

The Visicorder recordings were made at a chart speed of 0.2 inch/sec. (12 inches/minute). Therefore, one complete run required a chart length in excess of 2 feet. A segment of a run for Blank No. 8K2S2 is shown in Figure 11 in which the recordings are appropriately labeled. The salient features of this chart are the extreme oscillations of the push rod load. This could have been anticipated from the fact that the rack and pinion drive for the tailstock on which the push rod is mounted is driven by a gear drive connected directly to the main power shaft. For the chart shown, the drive provided an average 1/16 inch feed per machine revolution independent of whether the dies were opened or closed. Apparently during die closure, a very high compressive push rod force is developed because of the restricted feed travel. When the dies open, the elastic energy stored in the machine is rapidly released and essentially ejects the piece into the dies resulting in a temporary tensile load on the push rod. This behavior is typical of most swages and is usually overcome by using a back pressure on the part through the ejector or counter holder mechanism. This procedure was employed by applying a constant back pressure (usually 2100 pounds) through a hydraulic cylinder connected to the ejection mechanism. The purpose of this back pressure was to reduce the amplitude of oscillation and the noise level during operation of the machine.

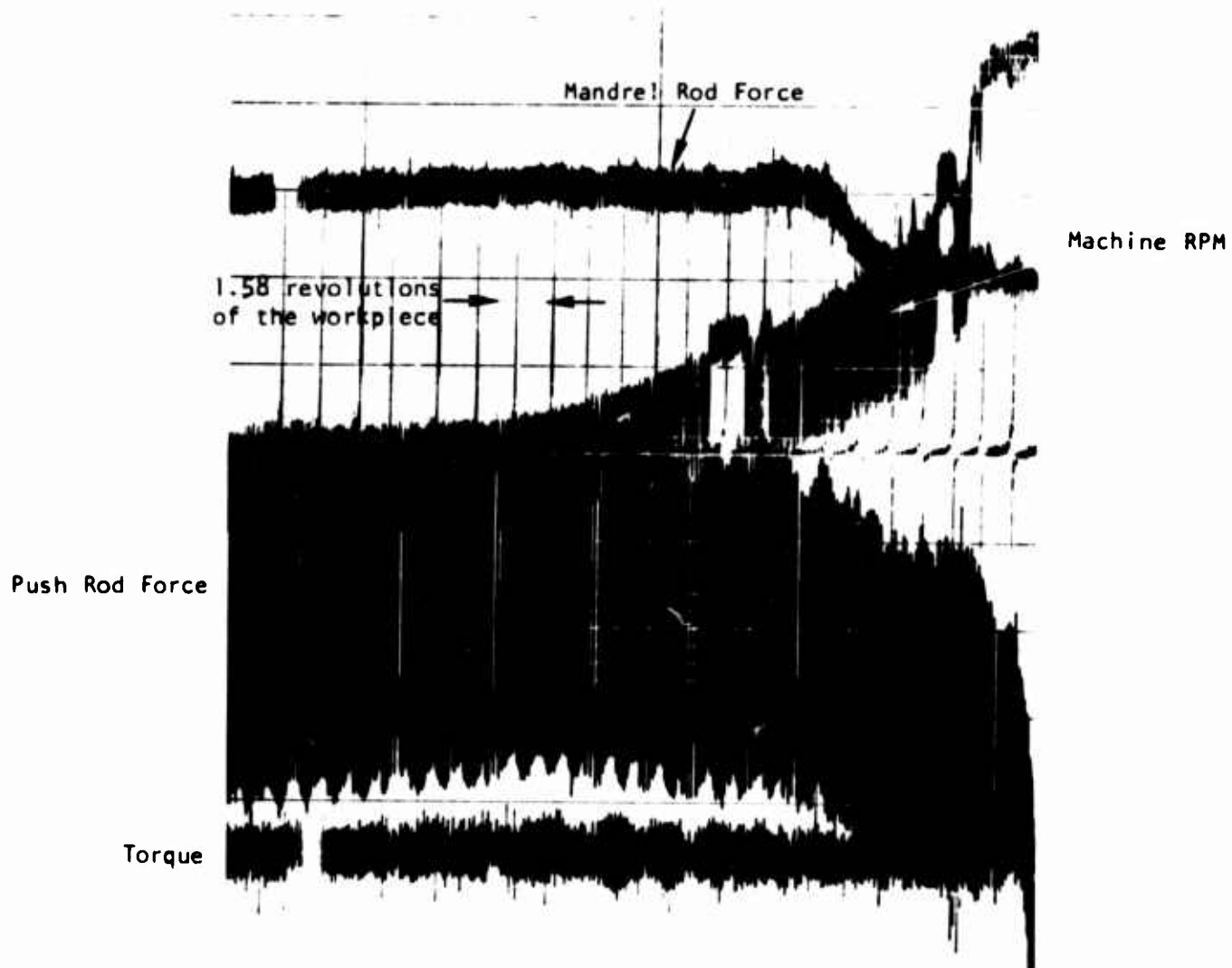


Figure 11. Section of chart from Blank No. 8K2S2 (chart width is 6.0 inch).

The oscillations of the machine rpm were proportional to the amplitude of oscillation of the push-rod force. Because the average rpm recordings also did not agree with the time for the total feed cycle, it appears that the tachometer-generator was periodically bouncing off the flywheel from the force of the push rod impact. In fact, during one run (63L1) the tachometer lost all contact with the flywheel and provided no response. Because of this problem, values for the machine rpm were determined from the time of the total feeding cycle, the length of the tube (23 inches) and the feed-drive setting (either 1/16 or 1/32 inch per machine revolution). At an average machine setting of 250 rpm, the feed rate would be 15.5 inch/min.

2.40 Inspection Procedures

Conventional inspection procedures were used to evaluate each swaged barrel blank (unless otherwise specified) in the following order:

1. Borescope Observations

Borescope observations were made on setup pieces to establish the necessary reduction for each die. Once this reduction was established borescope observations were made on each forged piece according to the schedule. Micro-meter measurements of the swaged blank diameter were also made at this time on every piece.

2. O. D. Straightness Measurements

O. D. straightness was determined by measuring the total indicated runout (T.I.R.) of the barrels turned on balancing wheels separated by 16.125 inch. The readings were subsequently transformed to a straightness measure defined as T.I.R. per foot.

3. Bore Dimensions

Calibrated air gauges were used to determine the land and groove diameters along the entire barrel length.

4. Drop Plug Measurements of Bore Straightness

Hardened steel plug gauges of two different lengths (0.5 and 4.0 inch) were used to determine bore straightness. The plug sizes were as follows:

0.5 inch length - 0.3004 to 0.2994 inch range in 0.0001 inch increments, and

4.0 inch length - 0.3000 to 0.2968 inch range in 0.0004 inch increments.

The tolerance on the diameter of the plugs was 0.000040 inch split about the specified diameter. The maximum diameter gauges of 0.5 inch and 4.0 inch lengths which would pass through each barrel blank were determined. A stringent measure of straightness was then provided by the difference between the 2 diameters divided by 3.5 inch to provide straightness per inch.

2.50 Residual Stress Measurements

The measurement of residual stress in the barrels was performed after dimensional inspection of each part. The Sachs (5) boring out technique was used with the boring being performed on a 3000 Ampere ANOCUT ECM machine. A schematic diagram of the ECM fixture and LVDT displacement transducers is presented in Figure 12. This fixture, shown in Figure 13, consists of two accurately aligned holding blocks which contain chambers and ports for introducing the electrolyte to the part and accurately machined 1.110 inch diameter holes to accept the part. One of the blocks is stationary and is an insulator (epoxy laminate). The other block is movable on a slide to provide for insertion and removal of the part from the fixture and is also conducting (70/30 brass) to provide ground contact for the specimen. A slip fit of the specimen in the blocks was used to permit free linear expansion of the part while still maintaining a good seal to contain the electrolyte under pressure. This slip fit was achieved by machining 1.5 inch lengths of the diameter at each end of the specimen (6.25 ± 0.1 inch long) to 1.1085 ± 0.001 inch. The electrode (0.25 inch diameter) is inserted through a reamed hole in the epoxy-laminate block, through the specimen and into an epoxy-laminate plug in the brass block. The holes in the blocks for the electrode were accurately machined to be on the same center as the holes for holding the specimens to achieve proper alignment of the bore and the electrode. Before inserting the barrel segment in the fixture, 10 inch x 10 inch x 0.125 inch thick Neoprene sheets were slipped over the ends of the specimen to avoid any splashing of the NaCl (1 lb./gal.) electrolyte onto the gages. Subsequently, the gages were placed on the segment for measurement of incremental axial extension (ΔL) and diametral change (ΔD). Both gages were calibrated for three attenuation settings on a Visicorder to provide nominal sensitivities of 0.0001 inch for chart displacements of 2 inches, 1 inch and 0.20 inch. The gage length for axial extension was nominally 2.50 inch and for diametral measurements was nominally 1.12 inch or the full blank diameter.

A typical run consisted of placement of the specimen and gages in the fixture; equilibration of the entrance and exit temperatures of the electrolyte to $80^\circ\text{F} \pm 0.1^\circ\text{F}$ using manual controls for electrolyte heating and cooling; disconnection of the LVDT's from the recorder to avoid conducting power outside of the ECM machine; initiation of the power cycle for a specific time; reconnection of the LVDT's;

- (5) A.A. Denton, "Measurement of Residual Stresses," Techniques of Metals Research, Vol. V, Part 2, "Measurement of Mechanical Properties," R.F. Bunshah, Editor, Interscience (1971) 234

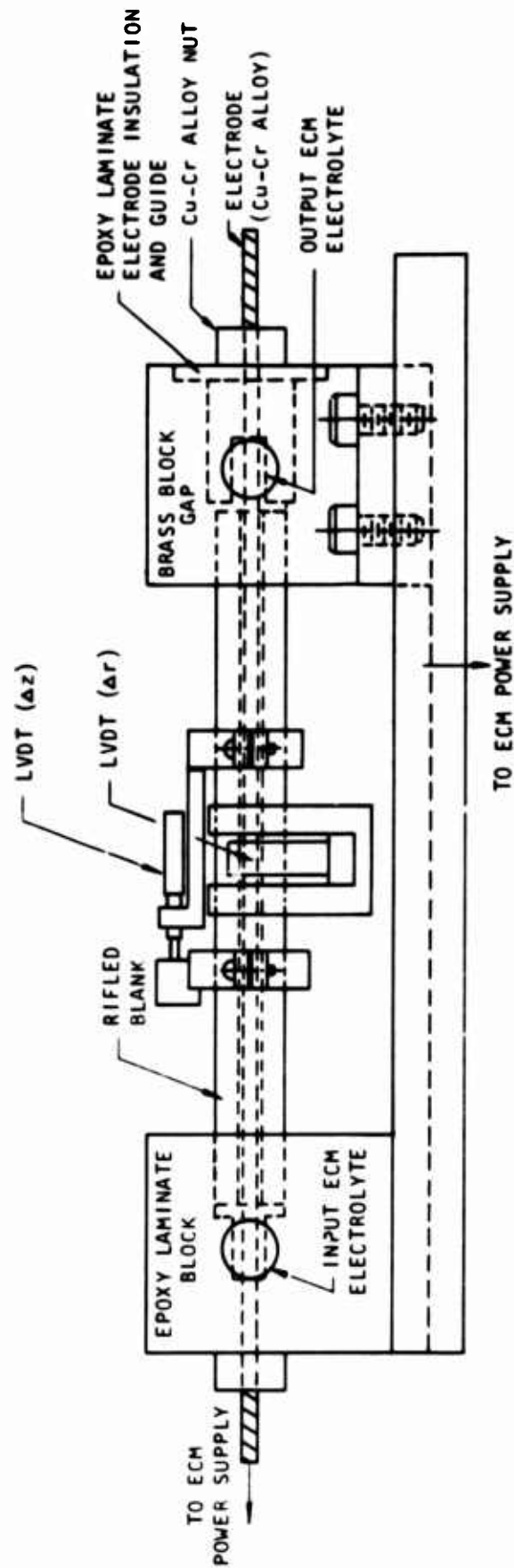


Figure 12. ECM fixture for residual stress determinations.

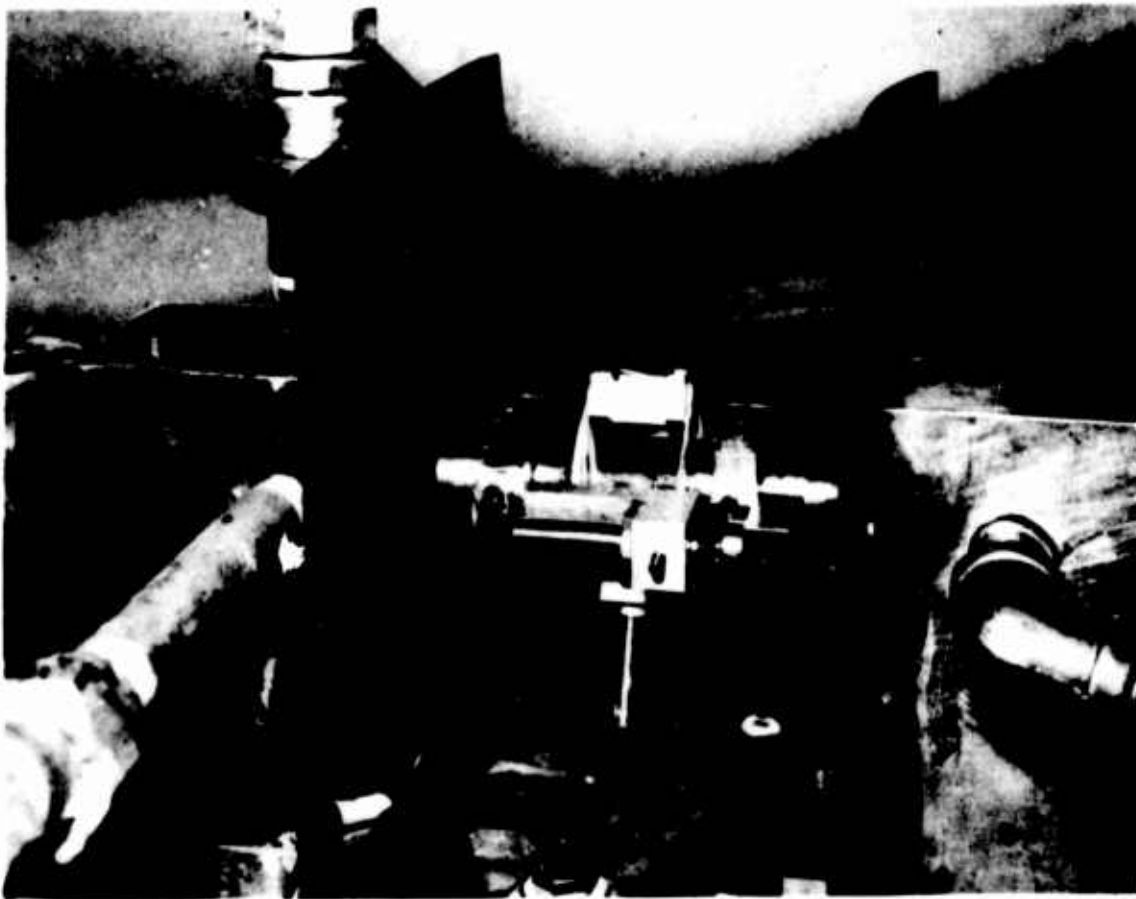


Figure 13. ECM residual stress determination fixture installed in an ANOCUT machine with the specimen and gauges in position for testing.

reequilibration of temperature; and measurement of the incremental displacements ΔL_j and ΔD_j . After this incremental measurement, the LVDT's were returned to their null positions, the temperature was equilibrated and the next run initiated. Initially, measurements were made of the bore diameter by removing the specimen from the fixture after each run. This procedure was found to be unnecessary because machining time could be related directly to bore diameter with an accuracy of better than ± 0.001 inch. This relation was established by plotting the incremental inner diameters as a function of time without changing the initial machine settings, which were the following: voltage, 15.9 volts (a constant); electrolyte pressure 115 psi (which continually decreased to about 60 psi depending on the inner diameter); and current (initially 1200 amps which decreased continually to about 230 amps).

3.0 RESULTS

The experimental results consist of four distinct types of measurements: machine measurements, dimensional measurements, surface quality and residual stress. These results will be presented in the following with discussions of significant observations involved with obtaining the measurements.

3.10 Machine Measurements

The machine and dimensional measurements for each barrel are presented in Table III listed in the sequence they were swaged. All data, unless otherwise specified, were obtained at a feed rate of 1/16 inch per machine revolution (each machine revolution corresponded to 7 die closures) and a back pressure of 2100 pounds. Other conditions evaluated included a feed rate of 1/32 inch/revolution and a back pressure of 500 pounds as noted in Table III.

Wherever two values of machine measurement separated by a diagonal line (such as push rod force) are presented in Table III, the high and low values represent the corresponding average values at the extremities of a band. For the same type of presentation under dimensional measurements, the high and low values correspond to the actual maximum and minimum measurements. The push rod force was recorded as positive when compressive and negative when tensile. During some tests at high die angles the push rod force went off scale in both the positive and negative directions (+12000 and -1400 pounds respectively). This condition resulted in severe hammering which was primarily from the feed mechanism and not from the dies. The major source of this hammering appears to be the lack of some effective energy absorbing device between the feed drive and the dies. Because the main driveshaft is geared directly to the hammers and the feed mechanism, the feed drive is continuous except for the buildup and release of elastic strain energy in the drive train during die opening and closure. The negative push rod force measurements indicated that the workpiece must have separated momentarily from the push rod after being propelled forward by the release of elastic strain energy in the feed drive train upon opening of the dies. The purpose of the back pressure rod is to provide a counter pressure to reduce the hammering in the feed system and is quite effective as noted by the results for the amplitude of the push rod force in Table III.

The measured mandrel rod force ranged from 60 to over 3000 pounds, but appeared to decrease with increasing overgrind and die angle. The data show that both increasing overgrind and die angle reduced the contact length with the mandrel (i.e., caused the bore to move inward at a slower rate relative to the outer diameter), and, therefore, larger reductions were required to achieve form as the overgrind and die angle increased. There appears to be a relatively abrupt increase in the mandrel force as the mandrel form approaches complete fill. This abrupt change was often associated with galling before the mandrel form had been filled. The mandrel force from run No. 34 on was not recorded

TABLE III
Measurements on Swaged Barrel Blanks

Blank Specification	Run No.	Machine Measurements			Diameter Initial/Final (inch/inch)	Dimensional Measurements			Remarks
		Push Rod Force (lbs)	Mandrel Rod Force (lbs)	Torque (lb-ft)		Straightness T.I.R. (in/ft)	Bore Dia. (in.) Land	Drop Plug Measurements Groove (in/in)	
31M1	1		3220+390 Mandrel broke		1.235/1.108				Torn rifling & broken mandrel rod
63M1	2	8100/1900	1270+240	243	1.235/1.121	0.0014 in/ft			
63S1	3	5240/1240	284	255	1.200/1.118	0.0041 in/ft	.30022 .30011	.30830 0.3001/.3002	
63L1	4	1200+ -1000	Mandrel rod broke	247	1.300/1.107				Torn rifling & broken mandrel rod (mandrel destroyed)
62S1A	5	5400/-600	316	104+42	240	70.3	1.200/1.121	0.0020 in/ft	.30027 .30011
8K2S1	6	9200/-1400	182	110+45	262	42.5	1.200/1.116	0.0054 in/ft	.30137 .30093
32S1	7	6200/-600	380	100+52	232		1.200/1.118	0.0057 in/ft	.29983 .29978
62S1B	8	5000/-800	310	254	254	57	1.200/1.120	0.0028 in/ft	.30022 .30010
61S1	9	4600/-1000	190	294	294	66	1.200/1.121	0.0041 in/ft	.30016 .30008
31S1	10	5600/1200	315	108+74	242	59	1.200/1.118	0.0060 in/ft	.29982 .29973
33S1	11	6600/-400	414+20	113 +58	248		1.200/1.119	0.0012 in/ft	.30009 .29989
8K1S1A	12	8600/0	63	129+64	230		1.200/1.120	0.00037 in/ft	.3016 .3012

* Guide bushings listed only after a change has been made.

New front & rear bushings (1.202 & 1.122 inch inner dia. respectively)

TABLE III (Continued)

TABLE 111 (Continued)											
Blank Specification	Run No.	Machine Measurements					Dimensional Measurements				
		Push Rod Force (lbs)	Force (lbs)	(lb-ft)	Machine RPM	Piece RPM	Diameter Initial/Final (inch/inch)	Straightness T.I.R. (in/ft)	Bore Diameter (In) Land Groove	Drop Plug Measurements (In/in)	Remarks
8K1S1B	13	8600/-600	60	110±58	237		1.200/1.119	0.00075 in/ft	.30197 .30163	.30840	
8K3S1	14	7200/-600	158	132±68	258		1.200/1.119	0.00015 in/ft	.3051 .3021	.30862	
3KR1S2-1A	15	4200/800	102	152±64	185 258		1.200/1.124	0.00052 in/ft	.30008 .30003	.03768	
3K41S2-1B	16	3900/-200	102	129±64	195 260		1.200/1.125	0.00034 in/ft	.30001 .29956	.30770	.2992/.2988
3C1S1	17	4540/1140	118	129±64	274		1.200/1.0961	0.0029 in/ft	.29984 .29977	.30792	
61S2-1A	18	9800/200	740±90	145±48	281	67	1.200/1.110	0.00090 in/ft		.30740	
61S2-1B	19	9540/200	720±80	168±62	277	64	1.200/1.119	0.00067 in/ft	.29984 .29972	.30740	.2994/.2992
31S2-1	20	7660/1860	1260±200	126±64	251	52	1.200/1.107	0.00216 in/ft	.29972 .29956	.30780	
32S2	21	7060/1660	790±120	120±61	272	100	1.200/1.117	0.00140 in/ft	.29970 .29964	.30755	.2992/.2992
62S2	22	8240/1560	925±190	139±58	262	83	1.200/1.121	0.00142 in/ft	.29973 .29963	.30732	.2993/.2992
3C2S1	23	3800/1040	142±40	142±55	268	78	1.200/1.122	0.00241 in/ft	.29997 .29988	.30793	.2995/.2992
3K 2S2	24	5260/1460	417±79	129±58	242	89	1.200/1.118	0.00135 in/ft	.29985 .29994	.3076	.2993/.2992
62S30	25	6400/800	204±118	123±52	255	67	1.200/1.119	0.00053 in/ft	.30020 .30010	.30756	.2997/.2996
61S30	26	4660/460	134±102	126±42	290	64	1.200/1.119	0.00210	.30084 .30077	.30828	.3003/.3000

TABLE III (Continued)

Blank Specification	Machine Measurements					Dimensional Measurements					Remarks
	Run No.	Push Rod Force (lbs)	Mandrel Rod Force (lbs)	Torque (lb-ft)	Machine RPM	Piece RPM	Diameter Initial/Final (inch/inch)	Straightness T.I.R.	Pore Diameter (in) Land Groove	Prop Plug Measurements (in/in)	
61L30	27	13000/-600	1260±1100	178±84	274	85	1.300/1.196	0.0033 in/ft	.30028 .29946	.30799 .2991/.2988	Front bushing: 1.302 in. inner dia.
61L3-1	28	10520/1920	1570±690	120±55	240		1.300/1.177	0.00352	.30016 .30002	.30822 .30815	Torn rifling and broken mandrel rod
62L3-1	29	9360/360	472±181	126±61	278		1.300/1.176	0.0156	.29966 .29946	.3077 .3073	1.220 inch inner dia. rear guide bushing
62L3-2	30	7140/740	276±254	123±55	242		1.300/1.218	0.00180	.30074 .30049	.30750 .30747	500 lbs. back pressure
62L3PA	31	6800/-200	300±196	132±55			1.300/1.218	0.00187	.30100 .30070	.30750 .30746	500 lbs. back pressure
8K2L1	32	11300/-700		187±71	240	65	1.300/1.193	0.0167	.29993 .29981	.30782 .30758	Mandrel force load cell did not record properly
8K1L1	33	12000+ -1400+ off scale	228±39	155±48	268		1.300/1.194	0.0054	.30061 .30044	.30810 .30797	
61L3-2	34	8460/1060	**	113±32	283		1.300/1.219	0.0045	.30087 .30048	.30803 .30786	
61L3PA	35	5520/-1340		136±29	272		1.300/1.218	0.0022	.3012 .30104	.30802	500 lbs. back pressure
61X3	36	3440/740		126±23	264		1.180/1.118	0.00825	.3035 .3033	.30834	
61S3	37	5350/0		126±23	241		1.200/1.120	0.0015	.30050 .30040	.30826 .30824	
61S3F	38	4800/200		149±23	244		1.200/1.117	0.0028	.30155 .30151	.30824 .30822	.040 in/rev. feed rate

** Mandrel force load cell did not operate properly.

TABLE III (Continued)

Blank Specification	Run No.	Machine Measurements			Machine RPM	Piece RPM	Diameter Initial/Final (inch/inch)	Straightness T.I.R. (in/ft)	Dimensional Measurements			Remarks
		Push Rod Force (lbs)	Handrel Rod Force (lbs)	Torque (lb-ft)					Land	Bore Diameter (in)	Groove (in/in)	
31X2	39	5160/960		120-45	255		1.180/1.114	0.0044	.30048 .30042		.30832	
8K1M1	40	11360/-640		171-52	252		1.220/1.118	0.0023	.30052 .30048		.30816 .30814	
61S4-1	41				250		1.220/1.152	0.0034	.30218 .30211		.30842	.040 in/rev feed rate 1.200 inch rear guide bushing
61S4-2	42				250		1.220/1.122	0.0043	.30009 .30007		.30802	.040 in/rev feed rate slight galling
61S4-R1	43				250		1.187/1.107	0.00042	.30021 .30020		.30817	1.120 inch rear guide bushing, 2400 lbs. back pressure
61S4-R2	44				250		1.187/1.106	0.00083	.30038 .30042		.30834	500 lbs. back pressure
61S4R9-1	45				250		1.187/1.106	0.00078	.30035 .30031			1000 lbs. back pressure
61S4R9-2	46				250		1.187/1.105	0.00072	.30025 .30022			2400 lbs. back pressure
61S4R9-3	47				250		1.187/1.104	0.00074	.30023 .30021			2000 lbs. back pressure
61S4R9-4	48				250		1.187/1.101	0.00122	.30022 .30020			2000 lbs. back pressure
61S4R9-5	49				250		1.187/1.098	0.00121	.30015 .30012			2000 lbs. back pressure slight galling
61S4R9-6	50				250		1.187/1.098	0.00047	.30015 .30012			2000 lbs. back pressure slight galling

because of malfunction of the load cell. Unfortunately, this problem was not observed because calibration runs indicated normal behavior during the sequence of tests.

The torque measurements obtained from the main drive shaft contain the effects of frictional losses in the machine, and the power to drive both the dies and the push rod. High torque was always associated with high push rod force. Both the machine and piece rpm showed some variation about an average setting; however, only the average was recorded. The machine rpm was set by observing a gage connected to the tachometer-generator at the same instant the run was initiated. It did not appear that the other process design parameters had a significant effect on machine rpm. The piece rpm was controlled by friction with the entrance and exit guide bushings and within the thrust bearings on the push rod and back pressure assemblies. This friction reduced the piece rotation during die opening. The fraction of the closing cycle in which the dies and workpiece were in contact was determined by the die design, feed rate and reduction, which consequently also affected the piece rpm. For these reasons, the piece rpm in the Intraform cannot be independently controlled, but usually ranged between 40 and 90 rpm.

The most significant general observations from the results of Table III are the following:

1. Push rod force (a compressive force) increases with increasing die angle, reduction and decreasing overgrind.
2. Mandrel rod force increases with reduction and decreasing overgrind.
3. The percent reduction required for achieving the mandrel dimensions increased with increasing die angle and increasing overgrind.
4. Torque does not show a strong correlation with any process design parameter. This observation is probably related to the fact that the torque measurement includes both the power for swaging and the power to drive the feed mechanism since both the swaging dies and feed mechanisms are driven by the main drive shaft of the machine. Approximately 20 ft-lb of drive shaft torque are required for each average 1000 pounds of push rod force at a nominal feed rate of 15 inch/min.
5. Severe impacting of the push rod can occur during swaging as shown by the high and low limits of the push rod force.

3.20 Dimensional Measurements

The dimensional measurements from the swaged barrels are presented in Table III with the machine measurements. The dimensional measurements include the initial tube and final blank outer diameter; the O.D. straightness presented as T.I.R./foot; the bore dimensions; and the largest "go" plug gages. The land and groove diameters of the bore are provided as the maximum and minimum measured values. When only one diameter is given, which corresponds to the majority of groove diameters, there was no discernible variation of the air gage during the measurement. The plug gage measurements are provided as the maximum diameter 0.5 inch long gage to go through the bore over the maximum diameter 4.0 inch long gage. The total difference between the two diameters of the plug gages cannot be attributed entirely to lack of straightness because the range of diameters of the 4.0 inch long gages decreased in increments of 0.0004 inch from 0.3000 inch, whereas the shorter gages were used in 0.0001 inch increments. Therefore, part of the difference between the two diameters was associated with the increments between gage diameters. A difference of 0.0001 inch between the two diameters corresponds to a bore straightness of 0.00034 inch/ft. In general, the plug gages indicated a better straightness than the measurements of T.I.R. of the outer diameter. For this reason, plug gages were not used for the later trials in this program and the single measure of straightness was the runout of the outer diameter. Many of the recorded land and groove diameters are smaller than the mandrel dimensions given in Table II. This observation may be associated with residual stress. The plug gage measurements average about 0.0004 inch smaller than the air gage measurements.

The guide-bushing design and alignment at entrance and exit from the dies appear to be the most significant factors affecting straightness. This is demonstrated by the results in Table III where guide bushings 0.002 inch larger than the nominal tube and swaged blank diameters were used unless otherwise noted. For the cases where oversized bushings were used, there was a noticeable decrease of straightness (i.e., increased runout). With large clearances between the swaged blank and the guide bushing, an obvious correlation existed between the magnitude of the push rod force and the runout.

3.30 Bore Surface Quality

Bore surface quality was empirically defined by borescope observations of the swaged barrels. Three general features, in addition to sharply-defined, well-formed rifling, were observed as discussed with Figure 1. Photographs of barrel cross sections demonstrating these defects are shown in Figure 14. These defects (incomplete fill, partial fill and tearing) may occur combined under certain circumstances as demonstrated by the bottom segment in Figure 14. The cause of tearing is galling or adhesion of steel to the mandrel which is shown in Figure 15.



a. Complete fill



b. Partial fill (rounded corners)



c. Partial fill with tearing at one land corner and at the land center.

Figure 14. Photographs of barrel cross section at the land area.



Mandrel-edge deterioration at land-groove junction.



Segment of the bore from Blank No. 63L1 showing deterioration of the rifling at the land-groove junction.

Figure 15. Mandrel showing galling and resulting tearing of the rifling (Specimen No. 63L1).

In order to optimize barrel quality, a quantitative rating was required. This rating was established by defining a rifling quality parameter of +1 for rifling without tearing, regardless of the degree of fill, and a rating of -1 for tearing or galling. This rating was based on the consideration that regardless of the amount of fill, galling or torn rifling produced a defective product. Fill was analyzed separately as the land diameter established by air gage measurements. Therefore, high quality rifling was defined by a borescope rating of +1 with rifling dimensions equal to or less than the dimensions of the mandrel. These ratings along with other relevant swaging parameters are described in Table IV.

A major discrepancy was soon found in this rating system because air gage measurements identical to the mandrel dimensions did not necessarily define complete fill at the corners of the lands (e.g., as described by the middle section in Figure 14). A more desirable measurement would be based on the actual height at the corners of the land. However, such measurements cannot be performed with current conventional gages.

The results in Table IV clearly show that the range of reductions for good quality rifling under the conditions evaluated is very narrow. A serious problem was encountered with the 61S4 dies in evaluating swaging conditions based essentially on obtaining good rifling form at lowest residual stress. In these trials (Sequence nos. 41 through 50) galling always preceded complete fill. Therefore, it was concluded that acceptable quality rifling could not be produced by these specific conditions. After these findings a major effort was devoted solely for defining the conditions for producing acceptable rifling and residual stress became secondary in relative significance.

The very strong dependence of quality on overgrind, die angle and percent reduction, the inability to achieve complete fill before galling, and, when acceptable rifling could be produced, the very narrow range of reduction separating the beginning of complete fill and galling required significant changes in the original program plan as described in Figure 2 and placed severe limitations on the subsequent effort and schedule. The major change in the program plan resulted from the condition where galling preceded fill. This necessitated evaluation of a large number of setup pieces before the effect of reduction on quality and fill could be defined. These setup or preliminary trials began to show that reduction was not truly an independent variable if complete fill were defined as the major quality criterion. This finding led to the formulation of the Quality Factor Q as a dependent process parameter to define conditions under which galling could be averted, although complete fill might not be achieved. Land diameter was then established as the quantitative measure of fill and the Quality Factor as the separate measure of quality. As will be shown, although land diameter does not insure fill, this parametric relation could be used to insure fill by setting the land diameter equal to 0.0001 inch smaller than the mandrel diameter and then determining the condition which would produce this bore at an acceptable level of quality.

TABLE IV

PROCESS DESIGN PARAMETERS AND QUALITY MEASUREMENTS FOR SMAGED BLANKS

Blank Specification	Sequence No.	Tube Dia. (in.)	Percent Reduction	Land Length (in.)	Percent Overgrind	Feed Rate (in/rev)	Back Pressure (ksi)	Rifling Quality	Strain Energy Density (psi)	Peak Stress, (ksi)	Remarks
31S1	10	1.200	13.14	.5+2nd	3.18	.064	2100	.2998	6.58	26.9/50.2	
32S1	7	1.200	13.14	.5+2nd	3.18	.064	2100	-1 .2998	10.7	133/83.9	
33S1	11	1.200	13.12	.5+2nd	3.80	.064	2100	-1 .3001	10.7	89.1/54.5	
31M1	1	1.235	19.52	.5+2nd	4.01	.064	2100	-1			
31X2	39	1.180	10.60	.50	3.90	.064	2100	+1 .3005	8.3	20.4/41.8	
31S2	20	1.200	14.92	.50	4.10	.064	2100	-1 .2997	10.3	23.1/43.8	
32S2-2	21	1.200	11.46	.50	3.27	.064	2100	-1 .2997	7.7	32.0/50.1	
3K1S2-1A	15	1.200	12.22	.1	9.39	.064	2100	-1 .3001	8.81	32.8/55.7	
3K1S2-1B	16	1.200	12.12	.1	9.30	.064	2100	+1 .3000			
3K2S2	24	1.200	13.13	.1	9.08	.064	2100	-1 .2999	8.79	46.5/50.2	
3C1S1	17	1.200	16.92	.50	13.98	.064	2100	-1 .2998			
3C2S1	23	1.200	12.52	.50	11.95	.064	2100	-1 .3000	2.03	57.0/74.1	

TABLE IV (Continued)

Blank Specification	Sequence No.	Tube Dia. (in.)	Percent Reduction	Land Length (in.)	Percent Overgrind	Feed Rate (in/rev)	Back Pressure (ksi)	Rifling Quality	Strain Energy Density (psi)	Peak Stress (ksi)	Remarks
61S1	9	1.200	12.68	.5+2nd	2.93	.064	2100	+1 .3002	20.8	73.8/80.7	
62S1A	5	1.200	12.68	.5+2nd	2.93	.064	2100	+1 .3003			
62S1B	8	1.200	12.83	.5+2nd	3.00	.064	2100	+1 .3002	11.3	26.0/44.7	
63S1	3	1.200	13.13	.5+2nd	3.18	.064	2100	+1 .3002	22.0	82.3/92.1	
63M1	2	1.235	17.56	.5+2nd	2.93	.064	2100	-1			
63L1	4	1.300	27.49	.5+2nd	4.10	.064	2100	-1			
61S2-1A	18	1.200	12.99	.5	3.10		2100	-1 .2998	3.7	-30.0/-49.7	
61S2-1B	19	1.200	12.99	.5	3.10	.064	2100	-1 .2998	1.4	-11.5/-15.0	
62S2	22	1.200	12.68	.5	2.93	.064	2100	-1 .2997	2.90	-74.0/-77.2	
61S30	25	1.200	12.99	.5	15.08/3.10*	.064	2100	+1 .3008	11.8	38.7/42.5	Multiple over-grind bend overground smaller than entrance
62S30	26	1.200	12.99	.5	15.08/3.10*	.064	2100	+1 .3002			
61L30	27	1.300	15.38	.5	9.27/-3.26*	.064	2100	-1 .3003			
61X3	36	1.180	10.23	.5	15.18	.064	2100	+1 .3035			
61S3	37	1.200	12.83	.5	15.0	.064	2100	+1 .3005	35.4	110/117	

TABLE IV (Continued)

Blank Specification	Sequence No.	Tube Dia. (in.)	Percent Reduction	Land Length (in.)	Percent Overgrind	Feed Rate (in/rev)	Back Pressure (ksi)	Rifling Quality	Strain Energy Density (psi)	Peak Stress (ksi)	Remarks
6133F	38	1.200	13.30	.5	15.23	.032	2100	+	.3016	13.5	36.3/45.3
61L3-1	28	1.300	14.03	.5	10.72	.064	2100	+	.3002	16.3	35.9/48.6
61L3-2	34	1.300	12.08	.5	7.52	.064	2100	+	1.97	17.2/-17.4	
61L3PA	35	1.300	12.22	.5	7.60	.064	500	+	.3009		
62L3-1	29	1.300	18.17	.5	10.80	.064	2100	-	.3012		
62L3-2	30	1.300	12.08	.5	7.52	.064	2100	+	.2997	16.2	26.3/49.1
62L3PA	31	1.300	12.22	.5	7.60	.064	500	+	.3007	11.9	36.5/24.4
61S4-1	41	1.220	13.03	.5	4.10	.032	1000	+	.3010	3.24	22.3/-24.9
61S4-2	42	1.220		.5	4.10	.032	500	.3022			
61S4-R1	43	1.187		.5	3.00	.040	2400	.3001			
61S4-R2	44	1.187	13.18	.5	4.10	.040	500	.3002			
61S4R9-1	45	1.187	13.18	.5	4.18	.040	1000	+	.3004		
61S4R9-2	46	1.182	13.34	.5	4.27	.040	2000	.3003			
61S4R9-3	47	1.187	13.50	.5	4.34	.040	2000	+	.3002		
61S4R9-4	48	1.187	13.97	.5	4.59	.040	2000	+	.3002		
61S4R9-5	49	1.187	14.43	.5	4.82	.040	2000	-	.3001		
61S4R9-6	50	1.187	14.43	.5	4.82	.040	2000	.3001			

TABLE IV (Continued)

Blank Specification	Sequence No.	Tube Dia. (in.)	Percent Reduction	Land Length (in.)	Percent Overgrind	Feed Rate (in/rev)	Back Pressure (ksi)	Rifling Quality	Strain Energy Density (psi)	Peak Stress (ksi)	Remarks
8K1S1A	12	1.200	12.88	1.0	12.11	.064	2100	+1 .3016			
8K1S1B	13	1.200	12.99	1.0	12.18	.064	2100	+1 .3070			
8K2S1	6	1.200	12.47	1.0	12.42	.064	2100	+1 .3014	43.4	71.7/83.8	
8K1L1	32	1.300	15.66	1.0	6.32	.064	2100	+1 .3006	14.0	23.7/35.0	
8K2L1	33	1.300	15.80	1.0	6.40	.064	2100	-1 .2999	12.9	46.7/24.2	
8K1M1	40	1.220	16.02	1.0	12.26	.064	2100	+1 .3005			

3.40 Residual Stress Measurements

The dimensional changes during enlargement (boring out) of the specimen inner diameter were recorded as a function of ECM-machine time. These measurements include the cumulative changes of the tube length ΔL , the change of the tube diameter ΔD and the machine on time from which the specimen I.D. was determined. Examples of these measurements are shown in Figure 16 for specimens sectioned from blanks 8K2S1 and 63S1. These data were used in the Sachs' analysis using the following procedure. After each time interval Δt_j , measurements of the length and diameter changes ΔL_j and ΔD_j respectively were made. These changes were summed to provide the following cumulative quantities:

$$L_i = \sum_{j=1}^{j=i} \Delta L_j, \text{ and}$$

$$D_i = \sum_{j=1}^{j=i} \Delta D_j$$

at the end of the time interval

$$t_i = \sum_{j=1}^{j=i} \Delta t_j.$$

Since t_i was directly related to the inner diameter ($2r_i$), these three quantities provide a relation between L_i , D_i and $2r_i$.

These data were incorporated into the Sachs' analysis in the following manner:

$$\epsilon_{zi} = \text{axial strain} = L_i/L_o$$

$$\epsilon_{\theta i} = \text{circumferential strain} = D_i/D_o$$

where L_o is the original axial gage length (nominally 2.50 inch) and D_o is the original blank diameter. It is conventional to specify the following strain parameters:

$$\Lambda_i = \epsilon_{zi} + \nu \epsilon_{\theta i}, \text{ and}$$

$$\theta_i = \epsilon_{\theta i} + \nu \epsilon_{zi},$$

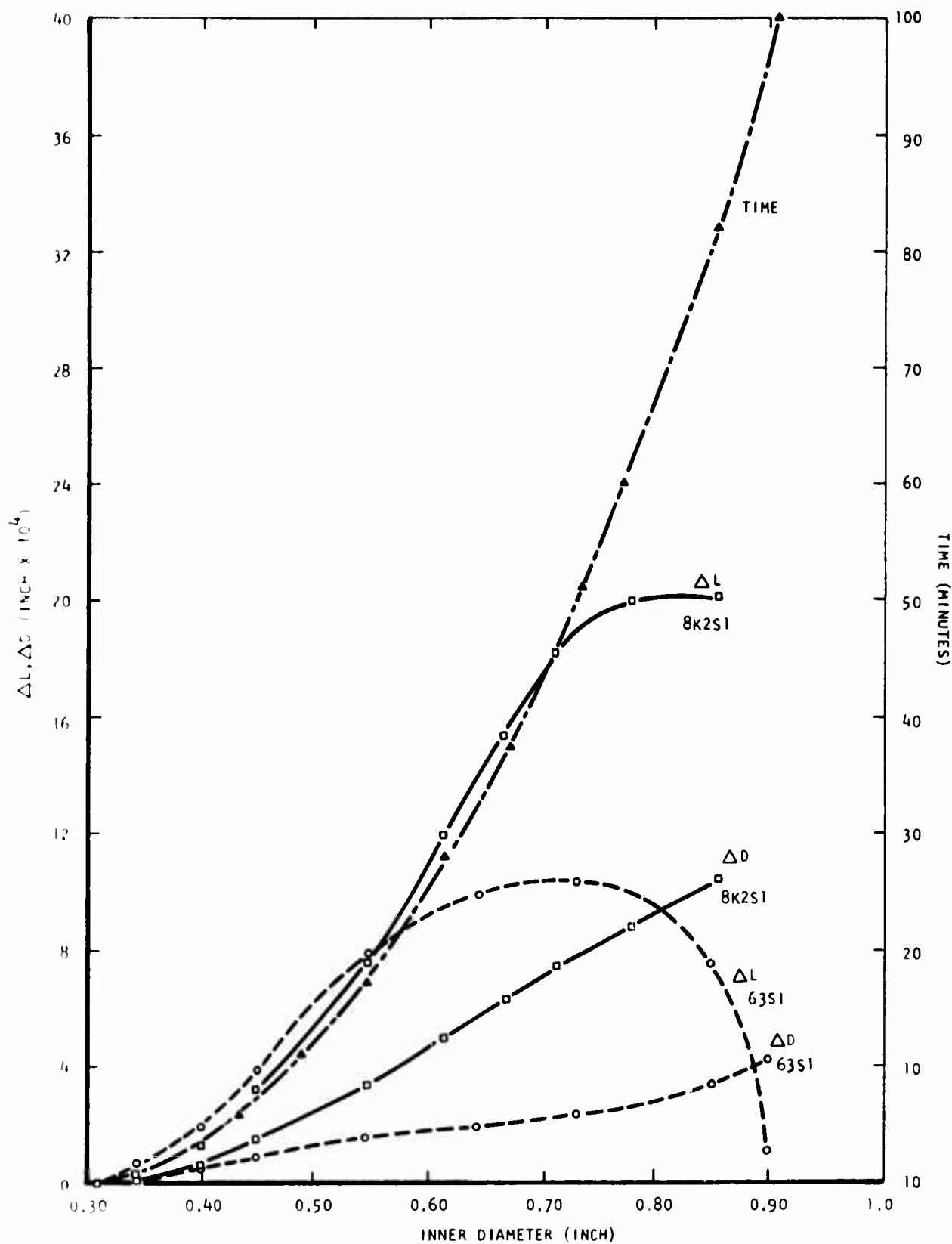


Figure 16. Inner diameter dependence on machining time and the dependence of the outer diameter and gage length on the inner diameter during boring out using ECM.

where ν is Poisson's ratio (0.293). With E = Young's modulus (30×10^6 psi) and the following defined parameters:

$$A_i = \pi r_i^2$$

$$A_o = (\pi/4) D_o^2$$

$$B = E/(1-\nu^2)$$

the axial stress $\sigma_{zi}(r_i)$, the circumferential stress $\sigma_{\theta i}(r_i)$ and radial stress $\sigma_{ri}(r_i)$ can be written as follows:

$$\sigma_{zi} = B[(A_o - A_i) \frac{d\Lambda_i}{dA_i} - \Lambda_i]$$

$$\sigma_{\theta i} = B[(A_o - A_i) \frac{d\theta_i}{dA_i} - \frac{(A_o + A_i)}{2A_i} \theta_i]$$

$$\sigma_{ri} = B[\frac{A - A_i}{2A_i}] \theta_i$$

These expressions must naturally satisfy boundary conditions based on equilibrium of the tube which are also a basis for their derivation (5). However, the boundary conditions also provide an additional check on the accuracy of the data.

A computer program was written to use the raw data as input and generate the strain parameters Λ_i and θ_i . These data are used as input to a four-point interpolation routine (Aitken's Method (9)) to generate functions $\Lambda(A)$ and $\theta(A)$ based on an exact fit of a curve to the data within the framework of the analysis. These functions were used for numerical differentiation of Λ and θ over increments of $\Delta A = \Delta A_i = 0.02$ inch² which is a smoothing procedure not necessarily arbitrary for a numerical method. The derivatives were defined as existing at A_i corresponding to the center of the increment, where Λ_i and θ_i were also evaluated and inserted into the stress equations to provide $\sigma_z(A_i)$, $\sigma_\theta(A_i)$ and $\sigma_r(A_i)$ which were subsequently transformed to their dependence on r_i and printed. The results of such analyses are shown in Figures 17 and 18 for the data in Figure 16.

(9) System 360, Scientific Subroutine Package 360-A-CM-03X Version 2, IBM Corp., White Plains, N.Y. (1971).

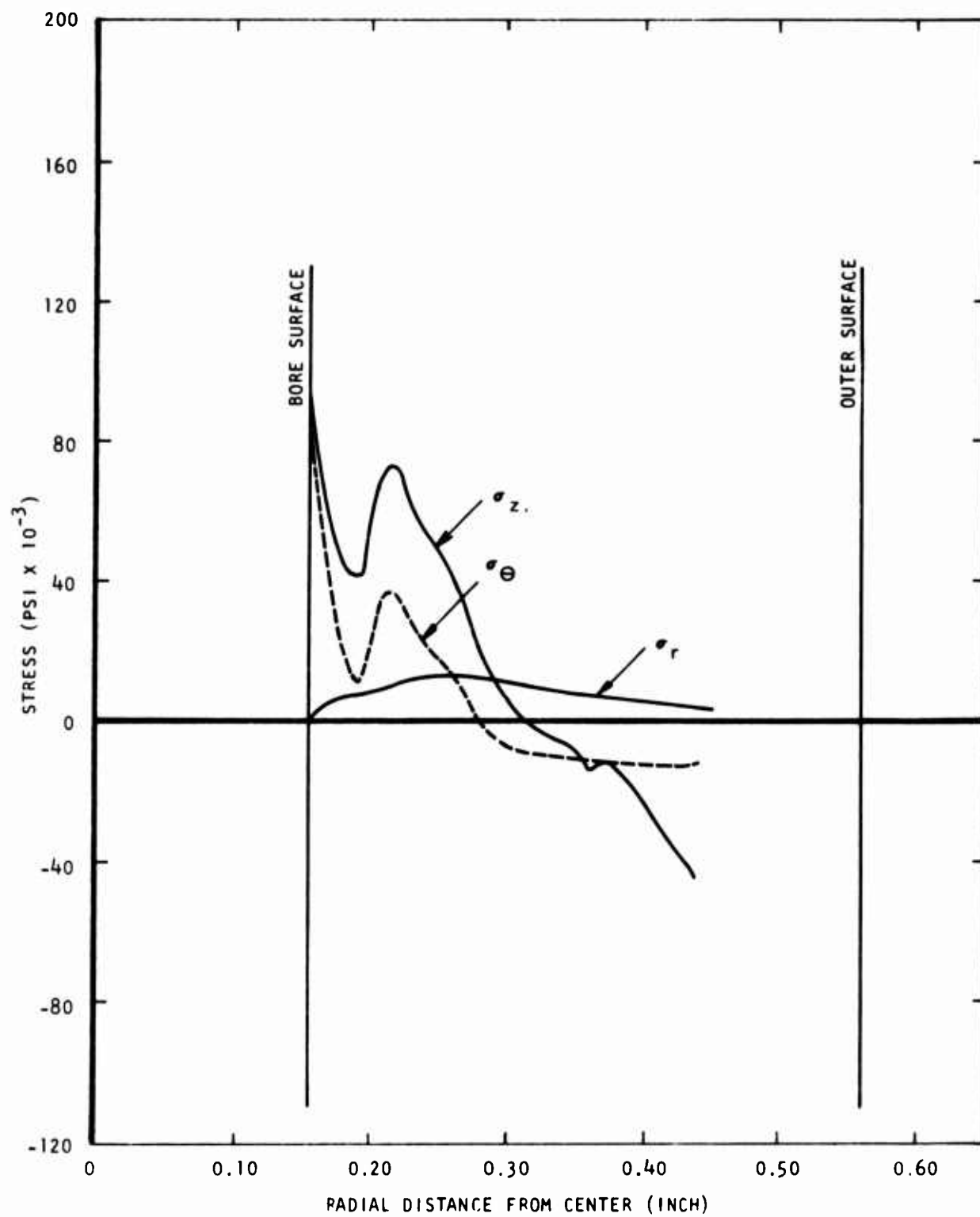


Figure 17. Residual stress determination for Blank No. 63S1.

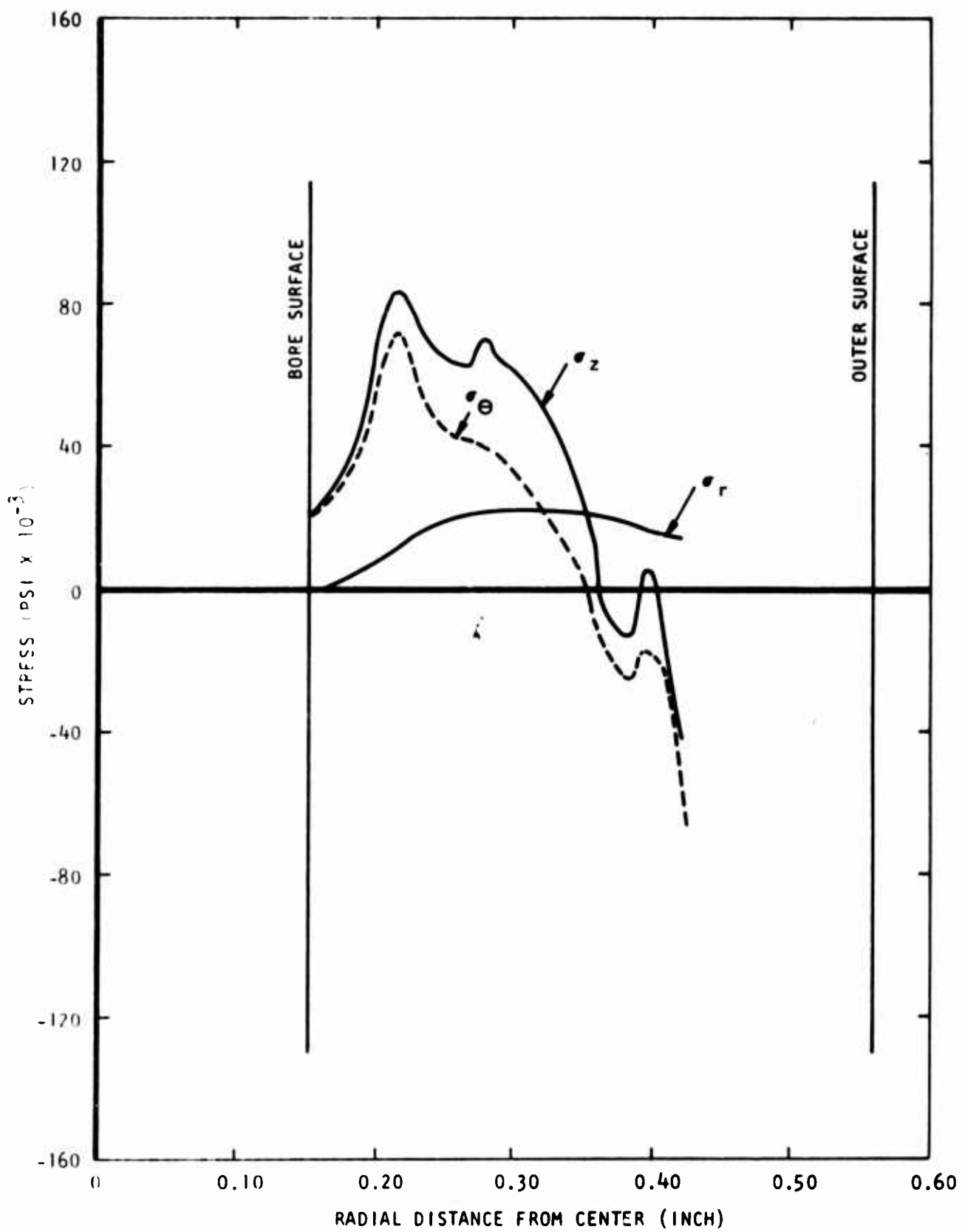


Figure 18. Residual stress determinations for Blank No. 8K2S1.

Residual stress measurements were made on a variety of barrel blank specimens to determine the effects of process design on residual stress. These results are presented in Table V as the values of the circumferential and axial (σ_θ and σ_z) stress components at the bore surface (radial position of 0.154 inch from the blank centerline) the radial location and magnitudes of the peak values of the stress components σ_r (the radial stress, which is zero at the bore and outer diameter), σ_θ and σ_z , and these stress components at radial distances from the blank centerline of 0.200, 0.275 and 0.35 inch, unless otherwise specified in the remarks column. In general, σ_θ and σ_z changed sign at a radial position of approximately 0.35 inch. The initial bore diameter was taken as the groove diameter, nominally 0.308 inch, which was assumed to introduce an insignificant error. After boring out to a diameter of 0.342 inch, all remnants of the lands had been removed.

The duplicate measurements on both the same bar (using two specimens) and specimens from different bars swaged under the same conditions show good agreement. In general, the greatest discrepancy between replicate measurements occurred at the bore surface; however, elsewhere the average stress measurements were very similar. The major source of error in the measurements appeared to be temperature control which was manually maintained at $\pm 0.1^\circ\text{F}$ during a displacement measurement. Although the instrumentation was very stable and a sensitivity of 10^{-6} inch was used, typical repeatability was found to be less than $\pm 2 \times 10^{-6}$ inch. In general, experimental error would be most significant at low displacements, which is typical of the measurements nearest the bore.

The stress values in Table V are presented for general information to show the magnitudes and distribution of the stresses. Measurements in most cases were not made much beyond half the wall thickness (radial position of 0.35 inch) because the stress components must obey the equilibrium relations which place some symmetry in the stress distribution. These relations and boundary conditions provide information on the average stresses in the remainder of a tube without the additional time involved in testing. Because peak stress is not necessarily indicative of residual stress or the possibility of distortion under load, the stress distributions were used to determine the strain energy density U to define a single parameter characterizing residual stress and its relation to process design. This parameter was defined by the following relation:

$$U = \frac{1}{V} \int_0^{D_o/2} \int_{r_i}^r \left[\frac{1}{2E} (\sigma_r^2 + \sigma_\theta^2 + \sigma_z^2) - \frac{\nu}{E} (\sigma_r \sigma_\theta + \sigma_\theta \sigma_z + \sigma_z \sigma_r) \right] 2\pi r dr dz,$$

$$= \frac{1}{\pi (D_o^2/4 - r_i^2)} \int_{r_i}^{D_o/2} \left[\frac{1}{2E} (\sigma_r^2 + \sigma_\theta^2 + \sigma_z^2) - \frac{\nu}{E} (\sigma_r \sigma_\theta + \sigma_\theta \sigma_z + \sigma_z \sigma_r) \right] 2\pi r dr,$$

Where V is the volume of the part.

TABLE V
Residual Stress Measurements

Specimen No.	Bore		Peak σ/a (ksi/in)		$a = 0.20$ Inch			$a = 0.275$ Inch			$a = 0.350$ Inch			Strain Energy Density (psi)	Remarks
	σ_θ	σ_z	σ_r/a_r	σ_θ/a_θ	σ_r/a_r	σ_θ/a_θ	σ_z/a_z	σ_r/a_r	σ_θ/a_θ	σ_z/a_z	σ_r/a_r	σ_θ/a_θ	σ_z/a_z		
31S1	26.9	50.2	10.4 .267	26.9 .154	50.2 .154	7.30	26.8	40.1	10.3	8.6	20.7	8.0	-12.3	-7.1	6.58
32S1	133.4	83.9	13.6 .267	133.4 .154	83.9 .154	10.2	14.9	30.8	13.5	10.2	33.1	9.5	-16.8	-11.7	10.65
33S1	89.1	54.5	12.2 .255	89.1 .154	54.5 .154	10.6	16.3	34.5	12.0	5.6	19.1	10.6*	-11.4*	2.62*	* $a=0.306$
31S2	-20.5	27.9	6.2 .301	23.1 .199	43.8 .199	1.3	23.0	43.6	5.8	12.8	20.6	6.1*	3.7*	-1.8*	* $a=0.306$
31X2	2.0	26.8	5.1 .199	20.4 .199	41.8 .199	3.4	19.8	41.4	4.5	8.7	15.2	5.1*	12.7*	-1.7*	* $a=0.306$
32S2-1	-10.6	9.2	6.0 .255	27.8 .207	56.1 .207	2.6	27.0	51.2	5.9	7.9	18.7	3.8	-6.6	-6.8	7.56
32S-2	-19.2	15.7	7.2 .311	32.0 .199	50.1 .199	2.5	31.7	49.7	6.8	13.1	19.3	7.2*	6.2*	0 *	* $a=0.316$
3K1S2-1A	28.6	55.7	13.2 .326	32.8 .207	55.7 .154	7.1	32.7	49.6	12.4	19.7	20.2	13.1	10.5	-15.3	8.81
3K2S2	-28.9	12.1	11.8 .296	46.5 .199	50.2 .199	3.5	46.3	49.7	11.2	21.3	12.1	11.5*	2.7*	-7.9*	* $a=0.316$
3C2S1	12.8	58.7	17.2 .306	57.0 .215	74.1 .200	8.3	52.6	74.1	17.0	21.1	29.4	16.4	2.5	8.3	20.26
61S1	73.8	80.7	14.1 .242	73.8 .154	80.7 .154	12.0	32.5	55.3	13.2	0	21.5	10.1	-21.1	-5	20.77
62S1B	11.0	23.4	9.6 .279	26.0 .342	44.7 .199	4.9	29.4	44.5	9.6	11.4	20.8	9.2*	3.8*	17.2*	* $a=0.316$
63S1	82.3	92.1	12.5 .270	82.3 .154	92.1 .154	8.2	24.7	57.3	12.3	4.2	27.3	7.9	-10.4	-8.1	22.03
61S2-1A	-30.0	-49.7	-3.43 .311	-30.0 .154	-49.7 .154	-3.3	-5.4	-10.0	-3.3	-4.3	-13.1	-3.3	-5	-18.9	3.74

TABLE V (Continued)

Specimen No.	Bore			Peak σ/a (ksi/in)			$a=0.20$ Inch			$a=0.275$ Inch			$a=0.350$ Inch			Strain Energy Density (psi)	Remarks
	σ_θ	σ_z	σ_r	σ_θ/a	σ_z/a	σ_r/a	σ_θ	σ_z	σ_r	σ_θ	σ_z	σ_r	σ_θ	σ_z	σ_r		
6152-1B	2.5	1.7	-2.85	-11.5	-15.0	-1.0	-9.9	-11.1	-2.8	-1.2	-9.6	-2.1	-7	-14.1		1.39	
			.261	.207	.341												
6252	-74.0	-77.2	-6.5	-74.0	-77.2	-6.1	+8	-6.2	-4.3	3.0	-10.1	-2.5	4.5	-7.9		2.88	
			.191	.154	.154												
6153BS9	20.0	8.2	4.4	20.1	13.0	3.5	10.8	12.5	4.4	4.2	7.6	3.3	-6.4	-11.3		0.884	
			.273	.154	.222												
6153AS011	3.1	-10.2	-3.3	-2.8	-13.5	.23	-7	-4.3	-.04	.39	-1.5		-1.9	-9.8		0.405	**Max. range of measurement
			.376	.376	.376												
6251B	11.0	23.4	9.6	26.0	44.7	4.9	29.4	44.5	9.6	11.4	20.8	9.2	3.8	17.2		11.25	*a=0.316
			.279	.242	.199												
6351	82.3	92.1	12.5	82.3	92.1	8.2	24.7	57.3	12.3	4.2	27.3	7.9	-10.4	-8.1		22.03	
			.270	.154	.154												
6152-1A	-30.0	-49.7	-3.43	-30.0	-49.7	-3.3	-5.4	-10.0	-3.3	-4.3	-13.1	-3.3	-5	-18.9		3.74	
			.311	.154	.154												
6152-1B	2.5	1.7	-2.85	-11.5	-15.0	-1.0	-9.9	-11.1	-2.8	-2.8	-9.6	-2.1	-7	-14.1		1.39	
			.261	.207	.341												
6252	-74.0	-70.2	-6.5	-74.0	-77.2	-6.1	+8	-6.2	-4.3	3.0	-10.1	-2.5	4.5	-7.9		2.88	
			.191	.154	.154												
6153	-2.6	10.8	13.61	36.8	46.3	3.43	28.8	34.9	11.4	28.9	36.9	13.7	21.9	31.1		16.5	*a=0.326
			.346	.229	.229												
6153F	3.4	4.4	13.1	36.3	45.3	4.2	29.7	35.2	11.4	23.4	36.4	13.1	15.6	23.1		13.46	
			.35	.229	.2361												
61L3-2	19.8	44.5	14.7	35.9	48.6	6.4	33.6	48.6	13.5	24.5	33.1	14.5	9.7	15.3		16.30	
			.331	.229	.207												
61L3-1	- .4	-17.4	16.2	17.2	-17.4	1.1	9.8	1.5	4.8	16.9	12.0	6.1	1.0	9.6		1.97	
			.331	.261	.154												
62L3-1	15.9	21.9	12.4	26.3	49.1	4.5	23.2	43.4	10.2	25.0	38.2	12.4	14.8	19.5		16.24	
			.350	.236	.236												
62L3-2	-58.6	-53.8	-8.8	36.5	24.4	-3.8	16.7	7.5	3.9	20.3	17.6	8.8	32.0	24.4		11.90	
			.350	.239	.350												

TABLE V (Continued)

Specimen No.	Bore		Peak σ/a (ksi/in)			a=0.20 inch			a=0.275 inch			a=0.350 inch			Strain Energy Density (psi)	Remarks
	σ_θ	σ_z	σ_r/a	σ_θ/a	σ_z/a	σ_r	σ_θ	σ_z	σ_r	σ_θ	σ_z	σ_r	σ_θ	σ_z		
61L3PA	-16.8	-24.9	$\frac{7.92}{.316}$	$\frac{22.9}{.261}$	$\frac{18.2}{.261}$	1.93	11.6	12.5	6.3	22.5	17.6	7.8*	15.8*	14.1*	4.37	*a=0.311
62L3PA	4.9	6.0	$\frac{6.72}{.316}$	$\frac{22.3}{.267}$	$\frac{-24.2}{.154}$	0	8.9	2.1	4.8	21.9	16.3	6.6*	16.8*	14.6*	3.24	*a=0.311
8K2S1	20.6	21.2	$\frac{21.6}{.312}$	$\frac{71.7}{.214}$	$\frac{83.8}{.214}$	8.0	69.3	70.8	20.8	40.7	68.8	21.4	3.7	23.9	43.40	
8K1L1	41.2	25.5	$\frac{23.7}{.291}$	$\frac{35.0}{.261}$	$\frac{35.0}{.261}$	6.8	20.8	30.0	10.4	23.4	34.5	12.7*	20.6*	22.4*	13.96	*a=0.336
8K2L1	-14.7	-25.2	$\frac{14.4}{.321}$	$\frac{53.1}{.261}$	$\frac{46.7}{.342}$.44	18.2	22.7	10.9	51.2	45.8	13.8	-16.2	24.2	12.87	
8K1M1	4.4	14.9	$\frac{12.4}{.316}$	$\frac{33.2}{.236}$	$\frac{52.8}{.23.6}$	3.8	26.6	43.9	11.2	27.6	43.2	12.4*	12.3*	26.0*	20.24	*a=0.316

The strain energy density U is also presented in Table V with units of inch-pounds/cubic inch or pounds per square inch. This quantity was used to rate the magnitude of the residual stress in the barrel, rather than peak stress, because the strain energy is most indicative of the average absolute magnitude of the residual stress. The average stress, because of equilibrium requirements, would be very small.

All of the measurements recorded in Table V were obtained from cold-swaged barrel segments with the exceptions of 61S3ASR11 and 61S3BSR9 which were obtained from two segments of Blank No. 61S3 after thermal stress relief treatments. The measurements on 61S3ASR11 and 61S3BSR9 were obtained after 1.5 hour stress relief treatments at 1100°F and 900°F respectively, which were followed by furnace cooling at 100°F/hour to 500°F, and then air cooling. These thermal treatments resulted in a reduction of the residual stress from a value of $U = 16.5$ psi for 61S3 to 0.405 for 61S3ASR11 and 0.884 for 61S3BSR9. Although these treatments produced the lowest values of strain energy density, the peak stresses in specimen 61S2-1B are lower than 61S3BSR9 and are nearly equal to 61S3ASR11. The results for specimens 61S3 and 61S30 should be noted because they were produced under nearly identical conditions except for the overgrind in the land area of the dies. Specimen No. 61S3 was produced from a die with a 15 percent overgrind whereas 61S30 was overground to only 3 percent in the land area. This small overgrind in the land area will affect metal flow over a small region within the transition area of the two overgrinds at the entrance-land junction of the die. The smaller overgrind of the land resulted in a strain-energy density of 11.8 psi or approximately 30 percent less than the value obtained with the large constant overgrind of 61S3.

The following trends are apparent from a careful review of the results in Table V:

1. Swaging can produce bars with either tensile or compressive stresses at the bore, although the results indicate a predominance of tensile bore stresses.
2. Increased overgrind increases the strain energy density.
3. Strain energy density appears to be proportional to the feed rate.
4. Overgrind of the land area appears to be a significant factor in affecting residual stress as shown by specimens 61S3 and 61S30.
5. Percent reduction when fill has been achieved does not appear to be a significant factor affecting residual stress.
6. The residual stress appears to increase with increasing die angle.

The most apparent factor affecting residual stress is overgrind as shown in Figure 19 where U is plotted as a function of overgrind for three die angles and two mandrel designs. This plot shows a general trend of increasing strain energy density with increasing percent overgrind. The lowest values were obtained from blank numbers 61S2, 61L3 and 62S2 and the highest value from 8K2S1. The apparent spread of the data was anticipated because for each data point process design variables, in addition to overgrind, differed. In general, nine process design variables were required to specify the conditions used to produce a rifle blank. For this reason, any trends or correlations shown on a two-dimensional graph are indicative of a strong dependence of the quality parameter on a process design variable. However, a significant spread of the data points would be anticipated unless the other eight process variables had no effect on the quality parameter. This fact necessitated the use of statistical procedures to determine parametric relations between quality and machine performance parameters and the nine process design variables.

The major problems with residual stress in swaged barrels arise from the partially finished condition of the swaged product which requires that distortion and stress relaxation as a result of further finishing be minimized to satisfactorily meet the print specifications. Distortion of swaged barrels, due to their axial symmetry, is primarily from bending under the load applied by the machine tool during finishing the outer diameter and is promoted by both the magnitude and the form of the distribution of residual stress in the swaged product. For example, as the axial component of the residual stress increases, the possibility for distortion or bending under the load from the cutting tool would be expected to increase. Stress relaxation in a residually stressed part occurs during machining as the residual stress adjusts to a new equilibrium condition after each machining pass. This stress relaxation produces axial and diametral changes dependent on the amount of material which was removed and the original distribution of residual stress. Therefore, the bore dimensions would reflect the amount of material removed from the outer diameter. With this reasoning, it follows that strain energy density has two components: distortion (i.e., bending) and bore contraction (stress relaxation). These components should be proportional to the amount of expansion in the axial (bending) and radial directions which occurs upon stock removal if no additional stresses are produced. Ideally, if a negligible strain energy could be achieved, neither of these components would exist. Since the uniform strain energy density for yielding of Cr-Mo-V at Rc 32 is approximately 600 psi, it was originally thought that U values of 10 or less were for all practical purposes equivalent to zero. However, this condition was found to be false and significant stress relaxation occurred for strain energy densities as low as 2 psi as shown in the subsequent results. In order to evaluate these effects of residual stress, the diametral expansion and axial extensions (in a 2.520 inch gage length) at the outer diameter were measured after the bore of the barrel blanks had been enlarged by ECM

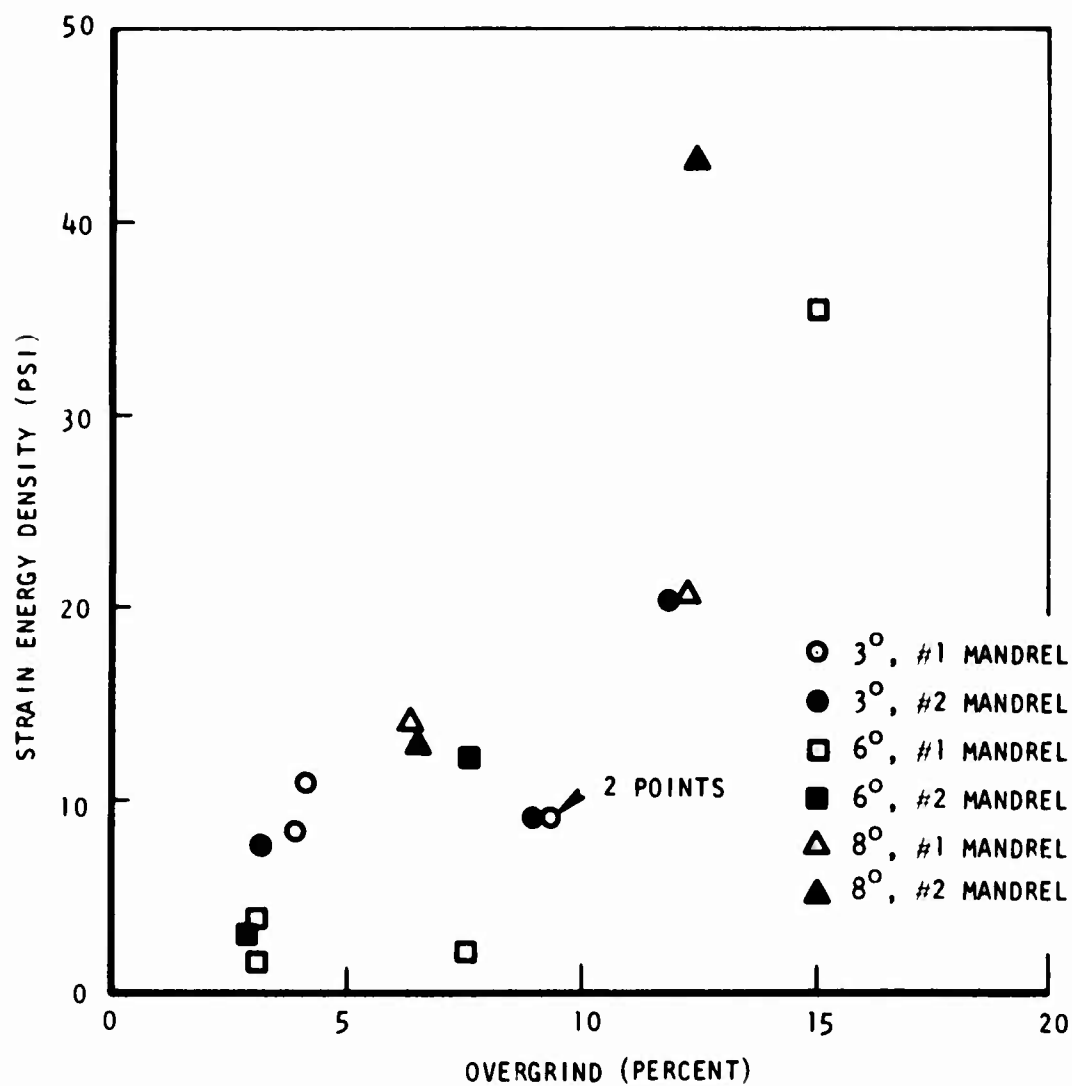


Figure 19. The dependence of strain energy density on overgrind.

to one-half the outer diameter or to typically 0.560 inch. The observed effect would be similar to the inverse effect after reducing the outer diameter to one-half its original value, roughly the minimum outer diameter of the M21 barrel. The results of this evaluation are shown in Table VI and plotted in Figure 20 as diametral and length expansions as a function of the strain energy density. The results show that diametral changes of significant magnitudes, when compared with the tolerance band of 0.0001 inch on the M21 barrel, can occur for all values of strain energy density greater than 0.8 psi. For values of strain energy density greater than 10 psi, it is possible that the required barrel taper would be sufficient to produce a variation of the bore contraction in excess of 0.0001 inch. The axial expansion shows a better dependence on strain energy density than the diametral expansion, and indicates that extensions in excess of 10^{-4} in./in. can occur for U values in excess of 5. Although the expansion in the axial direction is not objectionable, this expansion is indicative of a distortion potential under the load applied by the cutting tool during finishing. Because the diametral expansion did not correlate well with strain energy density, an additional attempt for a better correlation was made by plotting the diametral and axial expansions as functions of overgrind for three die angles and two mandrel designs at constant back pressure and feed rate. These results are shown in Figures 21 and 22. The correlation of expansion with overgrind is improved for diametral expansion. The results indicate that diametral expansion of less than 0.0001 inch will occur for overgrinds less than 5 percent.

The question naturally arises concerning the practical limit on the strain energy density, i.e., what is a tolerable level of bore contraction without producing a strong potential for distortion? To evaluate the correlation between axial extension and distortion potential, and diametral expansion and stock removal, a series of tests were performed on selected blanks under the following conditions:

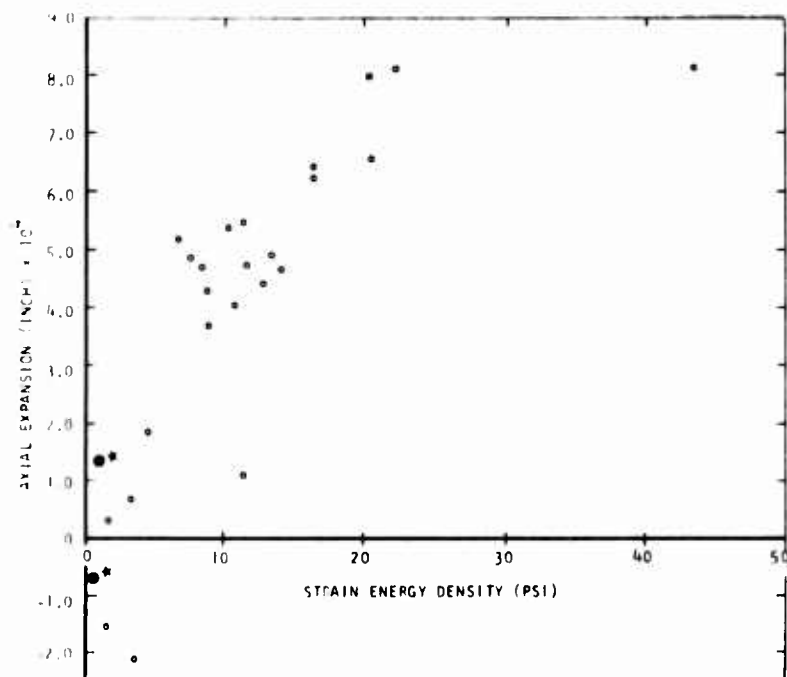
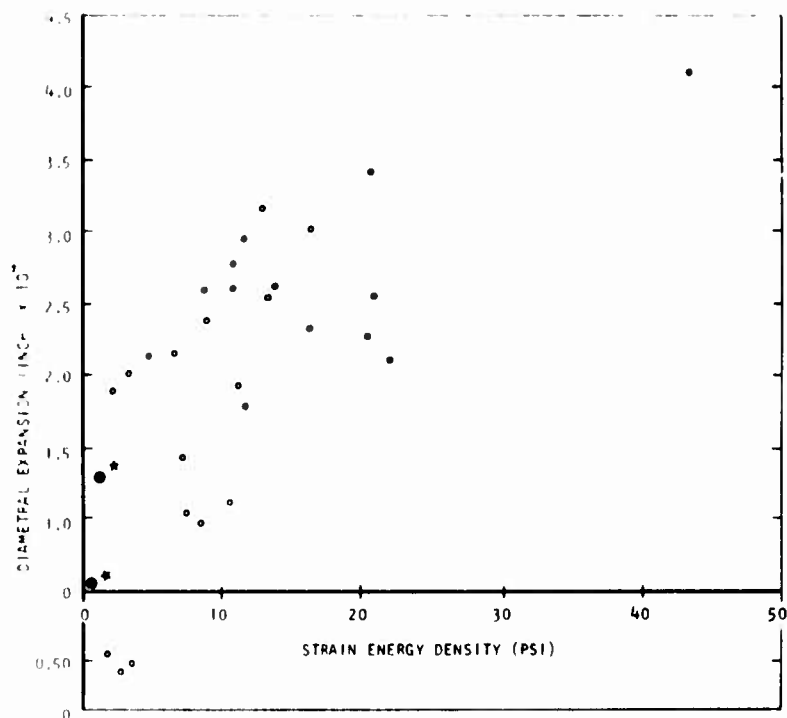
1. Each barrel segment was chamfered on one end with a piloted center drill.
2. Each barrel segment was placed in a four-jaw chuck (soft jaws) with 7.0 inch extending beyond the chuck.
3. Each barrel segment was centered to provide a maximum runout at the chuck of 0.001 inch T.I.R. and on the chamfer (i.e., 7.0 inches from the chuck) of 0.001 inch T.I.R.
4. A center on the tailstock was placed in the chamfer and machining passes over a 6.0 inch length were performed under the following conditions:*

* These machining conditions were selected for demonstration purposes only and do not represent optimum conditions.

TABLE VI

Total Diameter and Length Changes
After Removal of One-Half the Inner Diameter by ECM

<u>Specimen No.</u>	<u>Dia. Change (in x 10⁴)</u>	<u>Length Change (in x 10⁴)</u>	<u>Strain Energy Density(psi)</u>
31S1	1.651	5.223	6.58
32S1	2.27	6.08	10.7
33S1	2.073	4.103	10.7
31S2	0.611	5.403	10.3
31X2	0.507	4.662	8.3
32S2-1	0.9424	4.843	7.56
32S2-2	0.650	5.15	9.82
3K1S2	1.882	4.281	8.81
3K2S2	2.120	3.6624	8.79
3C2S1	2.885	8.007	20.3
61S1	2.03	7.02	20.8
61S3BSR9	0.806	1.356	0.884
61S3ASR11	0.0868	.722	0.405
62S1	1.42	5.53	11.3
63S1	1.60	8.20	22.0
61S2-1A	-0.490	-2.10	3.70
61S2-1B	-0.430	-1.505	1.40
62S2	-0.565	-2.25	2.90
61S30	2.452	4.738	11.7
61S3	2.060	5.40	16.5
61S3F	2.063	4.927	13.5
61L3-1	1.4042	.3316	1.97
61L3-2	2.559	6.331	16.3
62L3-1	1.310	1.119	11.9
62L3-2	1.818	6.410	16.2
61L3PA	1.656	1.840	4.37
62L3PA	1.504	.7206	3.24
8K2S1	3.60	8.20	43.4
8K1L1	2.133	4.698	14.0
8K2L1	2.617	4.430	12.9
8K1M1	1.774	6.552	20.2



CIRCLED DATA POINTS OBTAINED FROM THERMALLY STRESS RELIEVED SPECIMENS.

Figure 20. Diametral and length changes as a function of strain energy density.

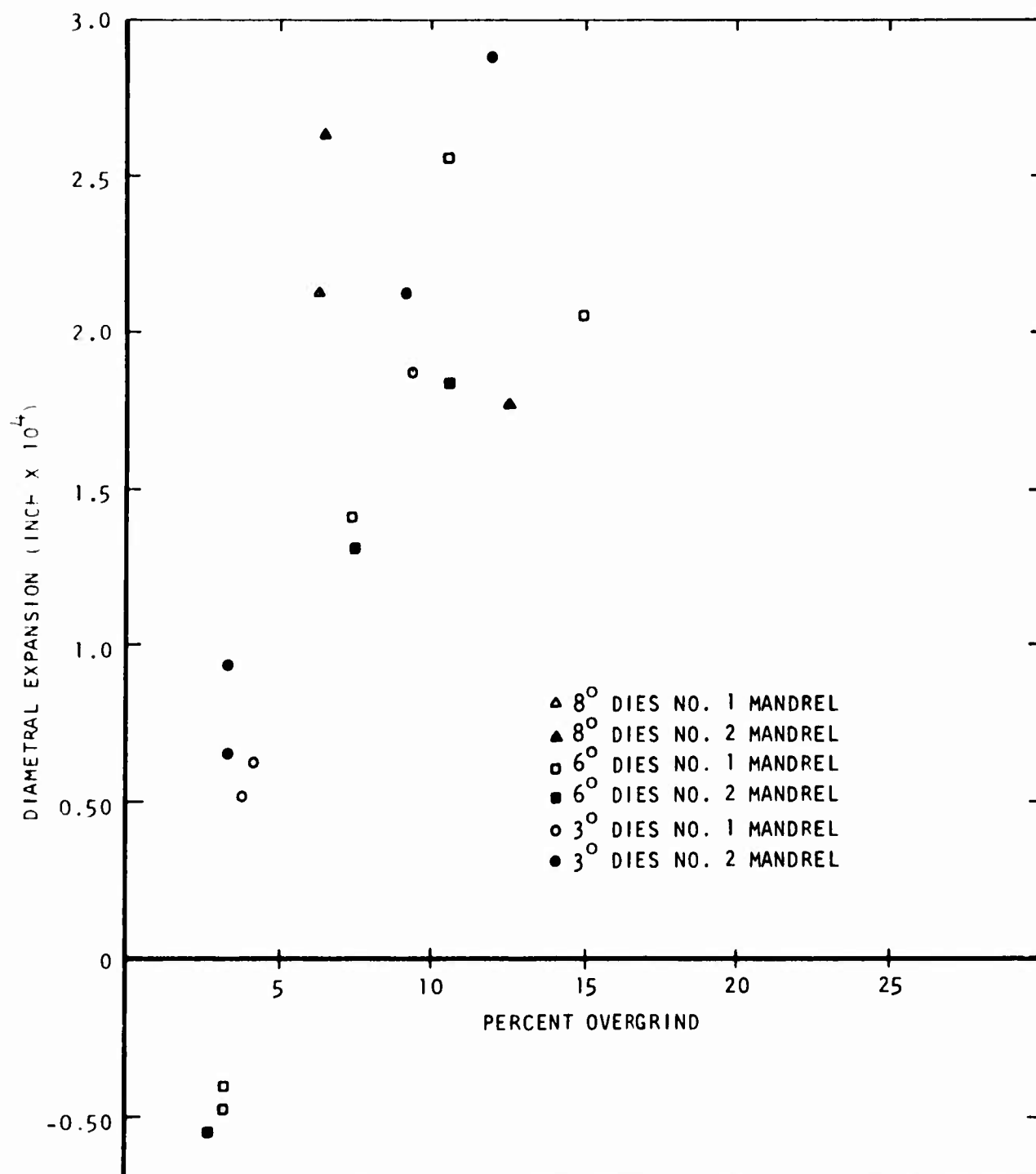


Figure 21. The dependence of diametral expansion on overgrind.

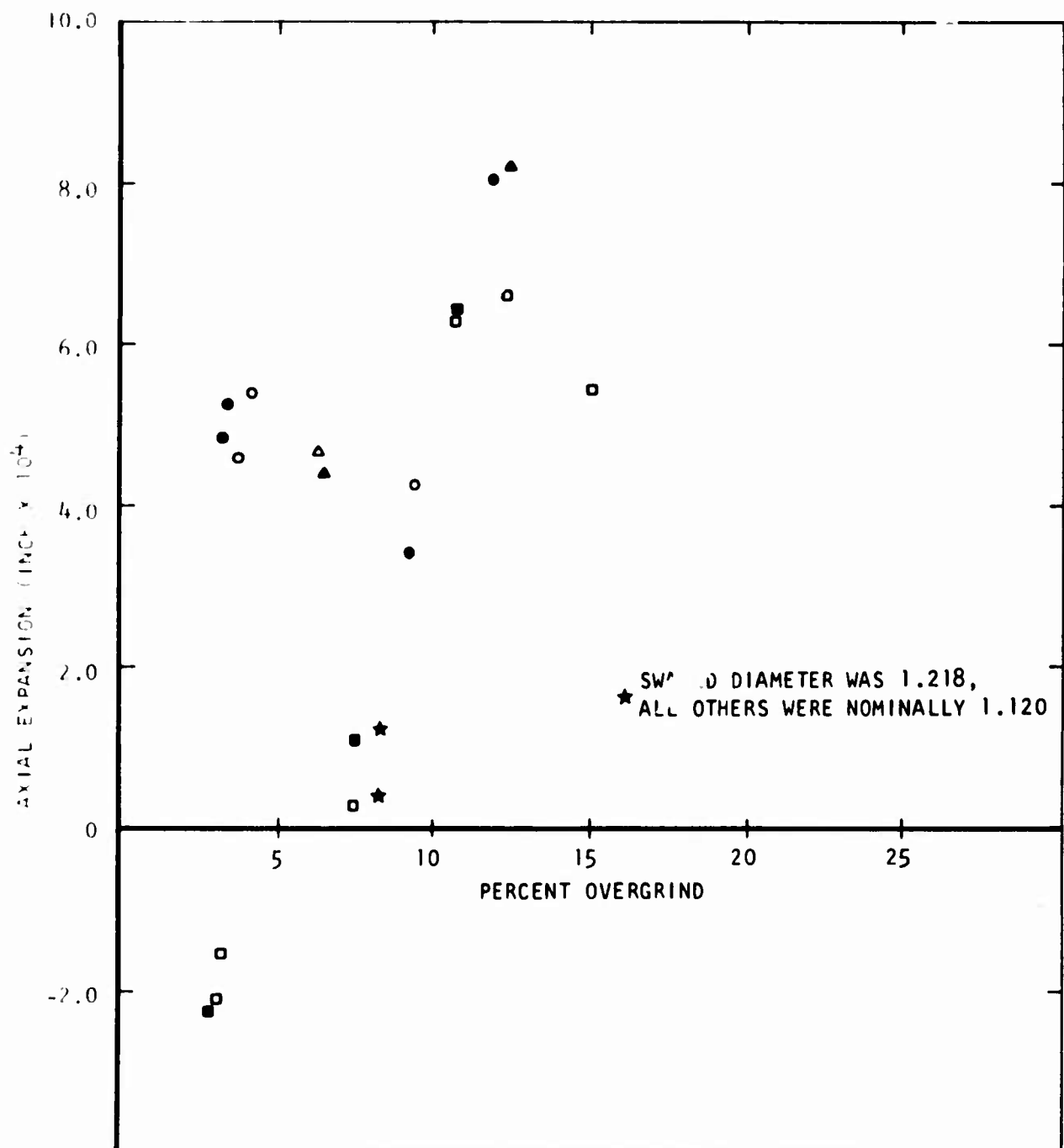


Figure 22. The dependence of axial expansion on overgrind.

<u>Pass No.</u>	<u>Part Speed (rpm)</u>	<u>Feed Rate (in./rev.)</u>	<u>Depth of Cut (in.)</u>
1	539	.01	.05
2	539	.01	.05
3	539	.01	.05
4	539	.005	.03
5	539	.005	.02
6	539	.005	.01
7	539	.005	.01
8	539	.005	.01

5. Measurements of diameter and runout were taken after completion of the third and final machining passes near the chuck, at the center of the cut length and at the end before and after removal of the centers.
6. A carbide insert (C-2 grade) of suitable geometry with coolant was used and a new insert surface was used for each blank. The tool holder was initially aligned, then maintained in this position for machining of all the blanks.
7. After removal of the blank from the machine, the land diameters at the machined and as-swaged areas were measured for comparison.

The measurements of the runout of the inner diameter after the third pass and the change of the bore diameter after the final pass are shown in Table VII. In all cases the runout after the third pass was equal to or slightly larger than the runout after the final pass. Because some of the blanks were nearly stress free, a significant portion of this runout must be attributed to the high tool forces generated during the heavy roughing passes. The larger runout produced during the roughing pass would be expected for tubes with residual stress because machining modifies the residual stresses and causes stress relief. Therefore, as the diameter is reduced, the strain energy will also decrease. For this reason, the roughing passes are critical. With the exception of 62S1, the runout after roughing correlated very well with the absolute

TABLE VII

Dimensional Measurements After Machining
of Six Inch Barrel Lengths

<u>Specimen Number</u>	<u>Change of Land Dia. (in$\times 10^4$)</u>	<u>Diametral Expansion (in$\times 10^4$)*</u>	<u>Runout After 3rd Pass (in)</u>	<u>Axial Expansion (in$\times 10^4$)*</u>	<u>Strain Energy Density</u>	<u>Final Machined Outer Dia. (in.)</u>
61S2-1B	0.2	-0.430	0.009	-1.505	1.40	0.656
61L3-2	-1.2	1.404	0.004	0.332	1.97	0.757
31X2	-0.4	0.507	0.014	4.662	8.30	0.642
62S1	-1.1	1.42	0.003	5.53	11.3	0.651
8K2S1	-1.4	3.60	0.025	8.20	43.4	0.661

* From Table VI

magnitude of the axial expansion indicating that residual stress was also a factor contributing to runout. Because of the apparently negligible increase of runout observed after the finishing passes, a subsequent trial was performed with 61S2-1A with roughing at a feed of 0.005 inch/rev. and a depth of cut 0.03 inch. Five passes were taken under conditions which otherwise were identical to the preceding. After this five-pass roughing operation the runout was measured to be negligible (e.g., equal to or less than 0.001 inch), and was similar to the final runout after the finishing passes. This observation indicates that the tool forces during heavy roughing can interact with the residually stressed blank to produce bending approximately proportional to the strain energy density or axial expansion. However, based on the magnitude of the residual stress there appears to be a maximum or threshold tool force determined by the machining conditions.

The change of the land diameter after machining is shown in Table VII to correlate with the diametral expansions experienced after ECM bore expansion. The diametral expansion which occurred at the outer diameter should be approximately proportional to the negative value of the change of the land diameter. This relation is shown for 61S2-1B which exhibited a bore expansion after machining and the other specimens which contracted.

The diametral and axial expansions can be considered as components of the total strain energy or strain energy density, U . Both quantities appear to become negligible as U becomes zero. The diametral expansion, as would be expected, correlates very well with the bore contraction after machining and the axial expansion appears to be proportional to the distortion tendency of the swaged blank. The dependence on strain energy of the diametral expansion is not obvious as shown by the results in Figure 20. The results in Figures 20 and 21 indicate that distortion and contraction would be minimized at values of strain energy density below 10 psi with overgrinds below about 5 percent. These relations will be developed further in the following section on Analysis of Results.

4.0 Analysis of Results

Each blank was produced under a set of conditions which required specification of a minimum of nine independent process variables. These variables are listed in Table VIII with the corresponding coded symbols to be used in the analysis of results. Several additional process parameters would have required definition if they had not been held constant or were controllable. The process responses (push rod force, mandrel rod force, land diameter, quality and strain energy density) were selected as being most significant in terms of machine performance and product quality. Torque and horsepower were not found to be limiting factors, but were found to be related to push rod force. Push rod force was indicative of the magnitude of hammering in the feed mechanism and, in one case of high push rod force, resulted in failure of an alignment-support fixture attaching the feed mechanism to the swage. The mandrel rod force was selected as a significant process response because it became very large (over 1500 pounds) under conditions of galling and incipient galling and it might be indicative of mandrel life in a large production run. The other quantities, land diameter, quality and strain energy density, are definitely product quality features. Straightness was not considered as a process response once it was found that proper bushing design produced a significant improvement of straightness well within the requirements of the M21 barrel specification. However, high push rod force was found to impair straightness and increased land length appeared to improve straightness when oversize bushings were used.

The value of proper bushing design should not be underestimated because it represents a relatively small, fixed cost which insures straightness. In addition to producing a high quality product, straightness obtained through bushing design permits greater flexibility in optimizing other process parameters and reduces barrel finishing costs by eliminating the need for barrel straightening and by making the swaged product more amenable to automated finishing. Furthermore, once a blank is mechanically straightened, asymmetric residual stresses are introduced which require continued straightening as the blank is being finished.

Parametric relations were determined for the responses to the process variables using multiple regression analysis (6). These predicting equations are presented in Table IX with the corresponding statistics describing the standard error and fit. The predicting equations were determined by standard and stepwise regression analysis of the linear relations and linear relations plus interactions corresponding to second and third order effects. The two most significant predicting equations based on the smallest standard error are given in Table IX and, in some cases, a third is provided to show the response to a particular set of process variables. Table X provides a qualitative review of the effects of the process variables based on the desired change in a particular response. In these illustrations + corresponds to a positive increase and - to a decrease to achieve a desired response in the machine performance and in product quality.

- (6) N.R. Draper and H. Smith, Applied Regression Analysis, John Wiley and Sons, Inc., New York, N.Y. (1963).

TABLE VIII

Process Variables and Responses

Variable Designation	Process Variables
x_1	Percent overgrind
x_2	Die land length (inch)
x_3	Feed rate (inch/revolution)
x_4	Back pressure (pounds force $\times 10^{-3}$)
x_5	Tube diameter (inch)
x_6	Percent reduction
x_7	Die entrance angle (degrees)
x_8	Percent mandrel reduction achieved by special mandrel design
x_9	Secondary reduction (percent) achieved by die land design
<u>Process Responses</u>	
P	Push rod force (pounds $\times 10^{-3}$)
M	Mandrel rod force (pounds $\times 10^{-3}$)
L	Barrel land diameter (either as inch or inch $\times 10^{-3}$)
Q	Rifling quality (dimensionless quantity)
U	Strain energy density (psi or in-lb./in. ³)
D	Diametral expansion (inch $\times 10^4$)

TABLE IX

Predicting Equations and Statistics

Dependent Variable	Regression Equations	Standard Error of Measurement	F .95 Ratio
Push Rod Force $P(\text{lbs.} \times 10^{-3})$	$P = -17.0 - .310X_1 + 4.35X_2 + 13.76X_3$ $+ 1.22X_4 + 11.54X_5 + .426X_6$ $+ .316X_7 - 1.971X_8 - .6496X_9$ $P = -1.33 - .328X_1 + 4.40X_2 + .533X_6$ $+ .370X_7 - .701X_9$	1.0158	10.29
Handrel Force	$M = 12.94 - 1.820X_6 + .0677(X_6)^2$ $- 0.00531X_1X_6$ $M = 2.19 + .362X_1 - .0862X_6X_7$ $- .00646(X_1)^2 - 5160X_6 + .801X_7 + .0400(X_6)^2$ $+ .0257(X_7)^2 - .0452X_1X_6 - .0749X_1X_7 + .00685X_1X_6X_7$ $M = -1.94 - .0758X_1 + .219X_6$.3504	7.41
		.3585	2.27
Land Diameter	$LX10^3 = 311 + .701X_1 + .83061X_2 - 25.62781X_3 - .13778X_6X_7$ $- .00605X_1^2 - 2.00214X_6 + 1.34441X_7 + .09431X_6 + .05514X_7$ $- .04151X_1X_7 + .00409X_1X_6X_7$ $LX10^3 = 299.63 + .0765X_1X_7 - .00421X_1X_6X_7$ $L = .30186 + 0.00010X_1 - .00025X_6 + .00020X_7$.457	5.18
		.310	6.25
		.3846	15.11
		0.00045	7.18

TABLE IX (Continued)

Dependent Variable	Regression Equations	Standard Error of Measurement	F .95 Ratio
Quality Factor Q	$Q = -6.19 + .092X_1 + 6.21X_5 - .25X_6 + .279X_7 - 3.299X_8 + .1543X_9$ $Q = -5.63 + .093X_1 - .133X_2 - 9.37X_3 - .0957X_4 + 6.35X_5 - .250X_6 + .280X_7 - 2.99X_8 + .165X_9$.745	6.32
Strain Energy Density U (psi)	$U = 58.4 + 2.04X_1 + 12.5X_2 + 549.7X_3 - 90.1X_5 + 1.39X_7 + 1.58X_9$ $U = 36.0 + 2.12X_1 + 12.4X_2 + 548.0X_3 + 3.15X_4 - 72.9X_5 - .435X_6 + 1.38X_7 + 8.46X_8 + 1.65X_9$	5.19 5.34	4.70 3.18
Diametral Expansion $\Delta D (\text{inch} \times 10^{-4})$	$\Delta D = -10.0 + 0.222X_1 + 2.56X_2 + 7.87X_5 - 0.269X_7 + .327X_9$	0.496	9.42

TABLE X

Qualitative Review of the Predicting Equations

<u>Desired Response</u>	<u>X_i Overgrind</u>	<u>X₂ Land Length</u>	<u>X₃ Feed Rate</u>	<u>X₄ Back Press.</u>	<u>X₅ Tube Dia.</u>	<u>X₆ Reduction</u>	<u>X₇ Die Angle</u>	<u>X₈ Mandrel Reduction</u>	<u>X₉ 2nd Die Reduction</u>
P -	+	-	-	-		-	-		+
M -	+					-			
L -	-					+	-		
Q+	+				+	-	+	-	+
U -	-	-	-	-	+		-		-
Net Desired Combination of Process Variables	?	-	-	-	+	?	?	-	?

The quantitative and qualitative relations described in Tables IX and X respectively describe the results within the range of swaging conditions evaluated with the precision described in Table IX. In general, increased back pressure produced smaller bore dimensions with a slightly increased finished O.D. (see 61L3, 61L3PA, 62L3 and 62L3PA in Table III) provided other parameters were held constant, and reduced the amplitude of the push rod force oscillations. The apparent lack of these predictions in the equations in Table IX could have resulted from the relative significance of the effect of back pressure compared with the effects of the other parameters, the lack of a full evaluation of back pressure within the experimental design, and the use of peak push rod force rather than amplitude in the evaluation. The effect of back pressure on bore dimensions was small when complete fill of the mandrel form was being approached and, therefore, the small change which was observed in two cases was within the range of error of the predicting equations.

The use of peak or maximum push rod force, rather than push rod force amplitude, was arbitrary. However, the results in Table III indicate that the amplitude and the maximum values were proportional. Although decreased back pressure will lower the push rod force, some back pressure is required to insure a compressive push rod force and reduce the degree of hammering.

The dependence of the push rod force (compressive extremity of the force amplitude) on percent reduction is presented in Figure 23 for dies of 0.1 inch land length and three die angles. The 0.1 inch land length was selected because the analysis demonstrates that this is a good upper limit on land length. Other conditions are provided as labeled on the dashed curves in each of the three sets of curves for different die angles. These curves were obtained from the second regression equation for push rod force in Table IX. The agreement between the prediction and observation is good as shown by the standard error. Therefore, only a few specific points were shown on the curves to demonstrate the agreement. These results show that push rod force increases with increasing reduction, die angle, land length and decreasing overgrind. Also the regression results indicate that increasing secondary die reduction reduces this force.

The results in Table IX indicate that mandrel force increases most significantly with increasing reduction and decreasing overgrind, although land length and die angle are also significant. However, compared with the mandrel force, the standard error of a prediction is large. This error is probably associated with the positioning of the mandrel (after the early trials, attempts were made to maintain the end of the mandrel to within 0.1 to 0.2 inch beyond end of the die land), the assumed form of the predicting equation, and the failure of the load cell in the later tests which restricted the range of processing conditions where valid data were obtained. The actual range of test conditions will affect the accuracy and precision of the predicting equation by not providing sufficient data to develop the full response of mandrel force to all of the possible changes in processing parameters.

A critical factor affecting the mandrel force prediction is the effect of reduction. Since proper die fill was obtained over a small range of reduction, which appeared to be on the order of 0.02 percent, low mandrel

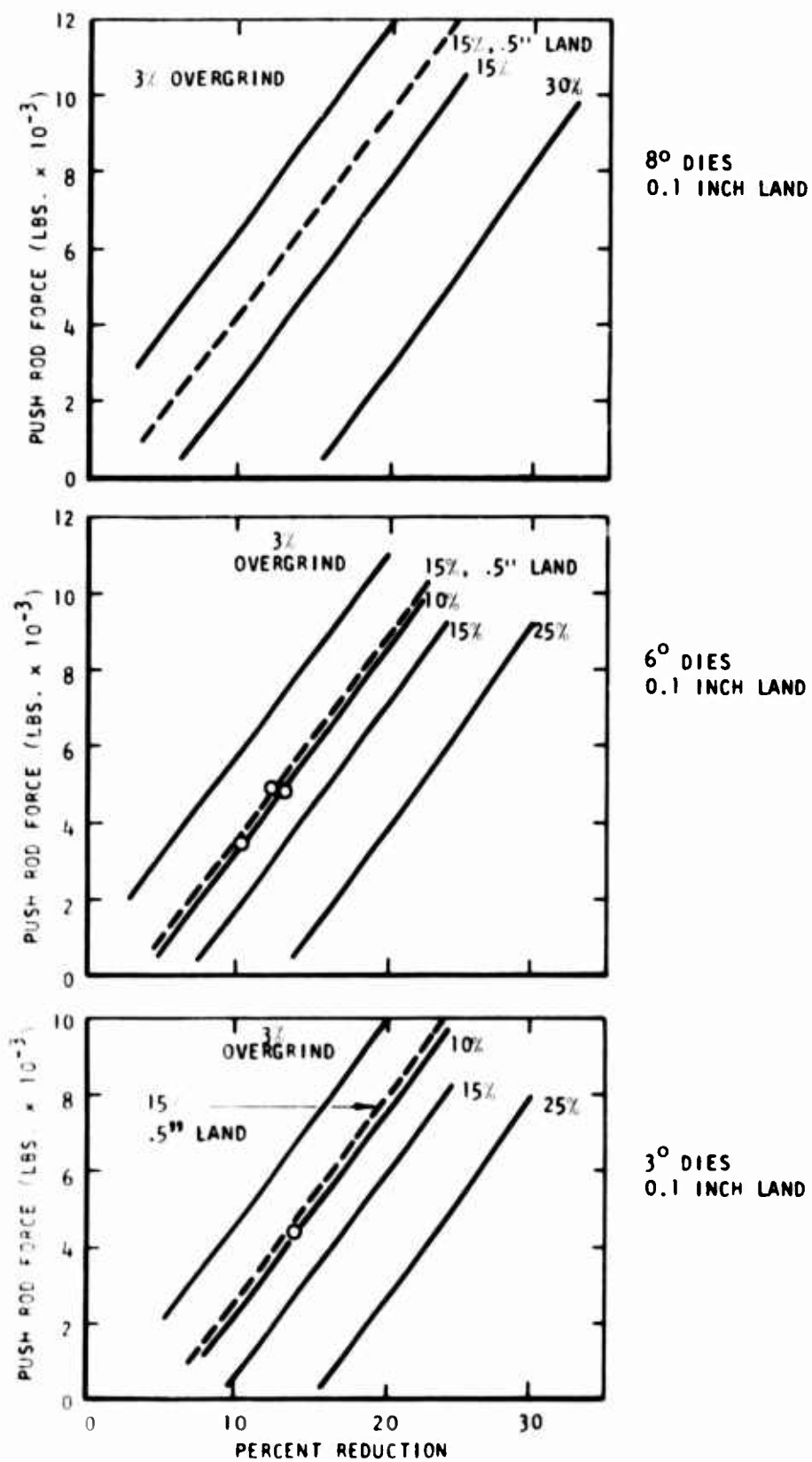


Figure 23. Push rod force dependence on reduction.

forces, below about 150 pounds, were observed over a large range of reductions up to the point of die fill where the force increased rapidly with increasing reduction. Any attempt at larger reductions resulted in galling and mandrelrod breakage. These latter measurements were excluded from the analysis. Therefore, the equations do not exactly reflect mandrel force at complete fill, but mandrel forces within the range of 0.0000 inch to 0.0015 inch above the completely filled bore dimensions. For nearly identical swaging conditions the mandrel force measurements exhibited a negligible dependence on bore dimensions within the range of 0.0000 to 0.0015 inch oversize. Therefore, the equations in Table IX represent the mandrel force dependence on process design within the specified ranges of the standard error when galling did not occur. Although the error is relatively large, the equations are useful for design to avoid exceptionally high forces (in excess of 1500 pounds) which are typical of galling.

The effect of reduction and overgrind on mandrel force is shown in Figure 24 as contours of constant force superimposed on the reduction-overgrind relation to achieve a 0.3002 inch diameter land (obtained from the predicting equation for land diameter in Table IX) for 3°, 6°, and 8° entrance angles. The results indicate a minimum mandrel force at intermediate reductions and overgrinds. The minimum occurs at lower overgrinds as the die angle is increased. This observation appears intuitively correct for the conditions of complete or consistent amount of fill because at low overgrinds the lack of ovality or increased die closure places very high pressure on the mandrel, and at higher overgrinds which require greater reductions to achieve fill, the contact length of the mandrel and workpiece under pressure is higher. Therefore, under intermediate values of reduction and overgrind one would expect that the combined effects of closure and contact length might be optimized to provide low mandrel forces. These results indicate that low mandrel force is favored by selecting a die angle-percent overgrind product equal to 55 ± 15 .

The relation between overgrind and reduction to achieve a 0.3002 inch land diameter from a 0.3002 inch mandrel is shown in Figure 25 for three die angles. Although the F-ratio test indicated that significant relations existed between L and the process parameters, comparatively large standard error resulted from swaged land diameters smaller than the mandrel dimensions which appear indicative of residual stress. No satisfactory procedure was found to avert or eliminate this error.

The quality factor Q was developed to establish some quantitative basis to avert galling. Since it was impossible to accurately define the degree of galling or the degree of tearing, the quality parameter Q was set equal to -1 when borescope observations indicated tears and +1 when no tears were observed. However, this parameter provided no assurance that fill would be achieved. An attempt to provide this assurance involved the use of the third equation for L in Table IX. This relation was set equal to 0.3002 and the relation between overgrind, reduction and die angle meeting this condition was substituted in the first equation for Q. The resulting expression for Q with a die angle of 6°, tube diameter of 1.200 inch, 0.5 inch die land and zero mandrel and secondary die reduction was evaluated in terms of reduction and overgrind for Q = 0 and 1 as shown in Figure 25. Data points corresponding to borescope observations of galling or no galling are superimposed on these

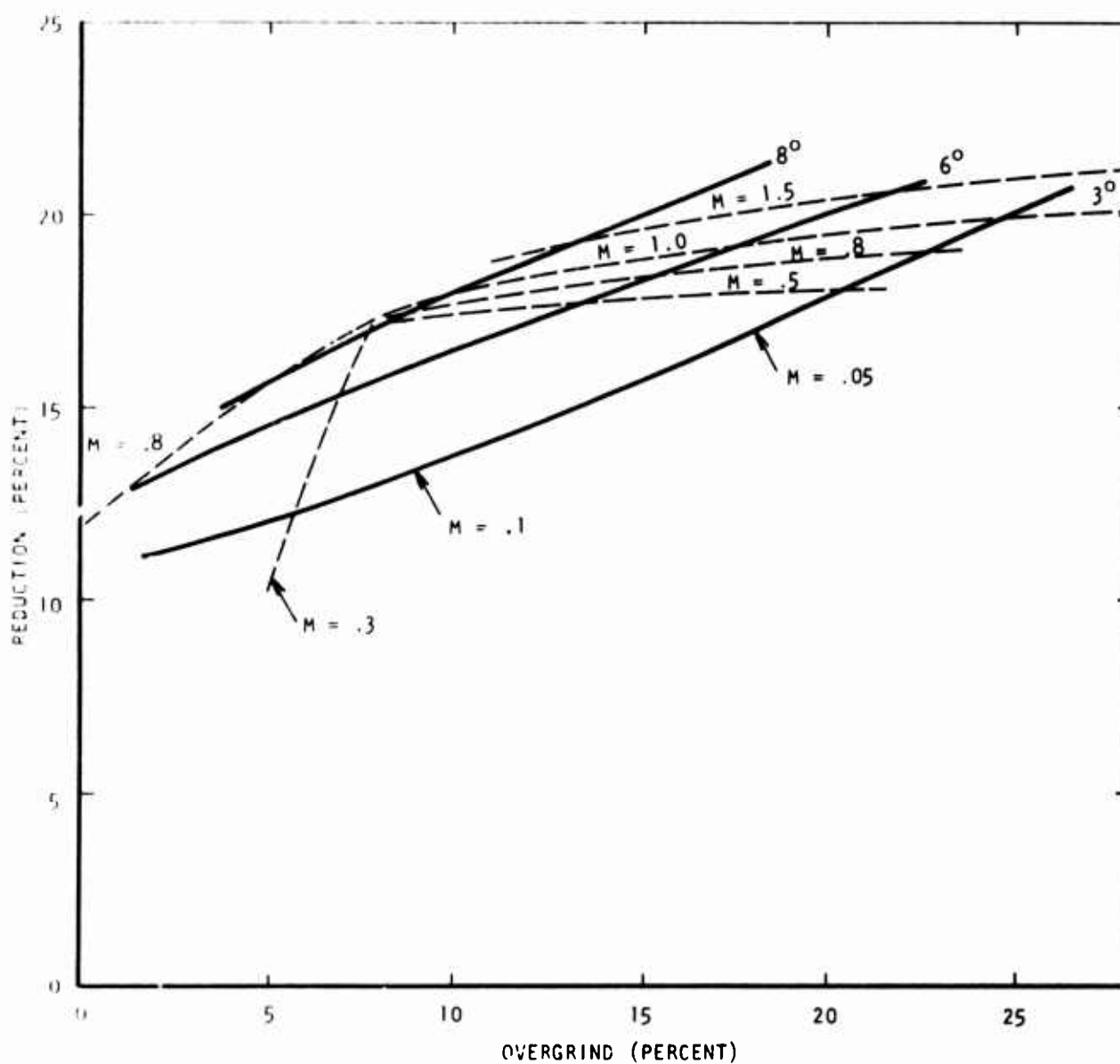


Figure 24. The reduction-overgrind relations for producing a 0.3002 inch land diameter and corresponding mandrel forces.

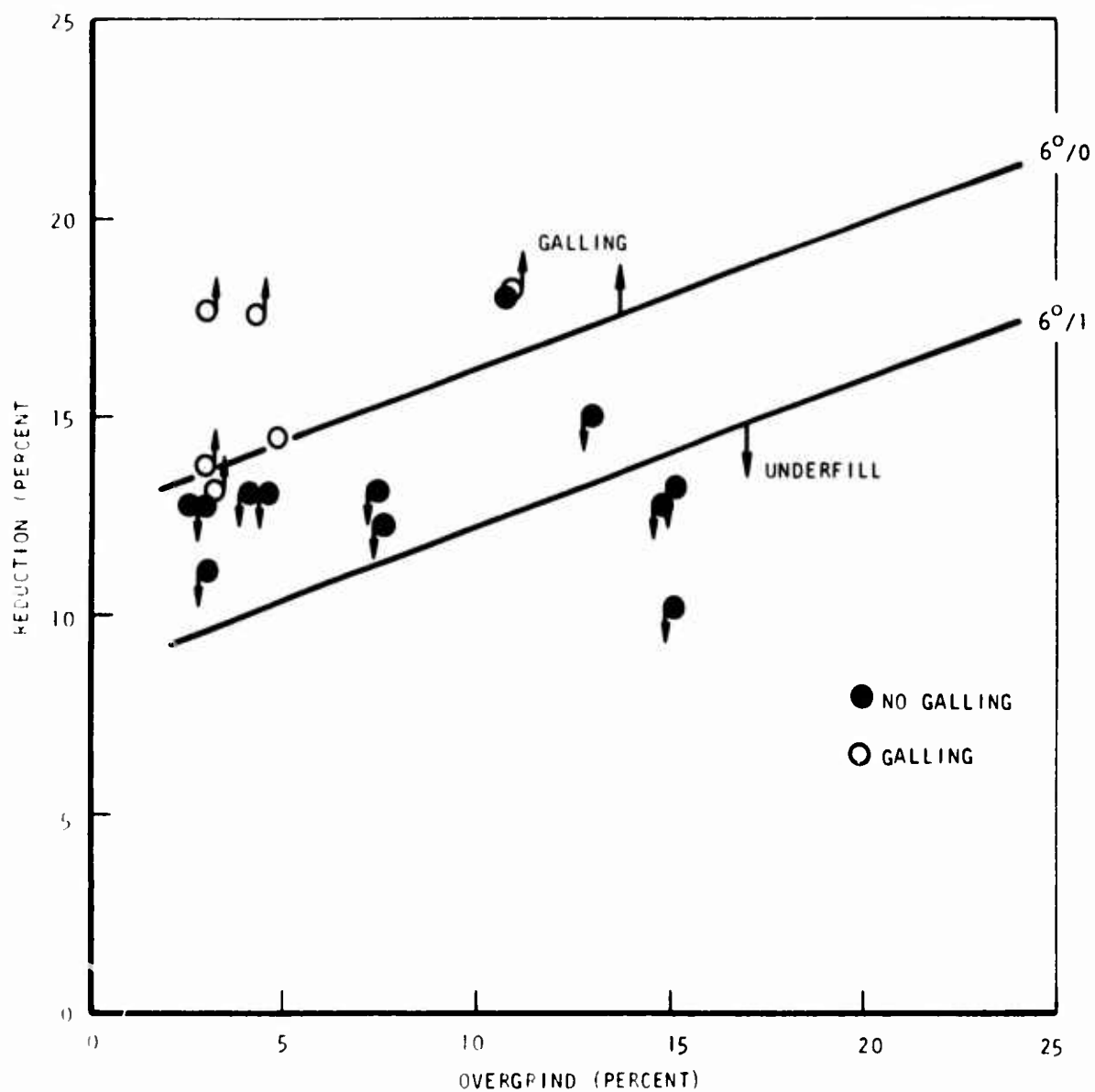
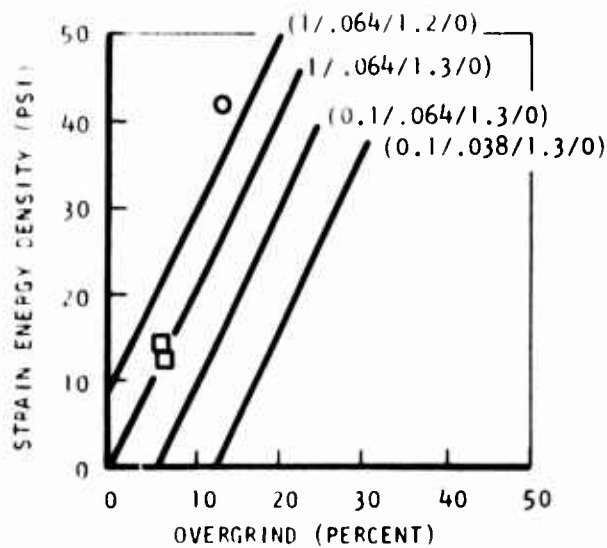


Figure 25. The dependence of the Quality Factor on reduction and overgrind.

curves and show good agreement with the predictions. The arrows on the points correspond to an underfill (arrows point in direction of decreasing reduction) or an overfill (i.e., bore dimensions smaller than the mandrel) condition. In general underfill occurs in the direction of increasing Q and is associated with the lack of tearing. Fill only occurred near $Q = 0$ and only for two cases without tearing, one at Q greater than 0 and the other at Q less than 0. The five data points at reductions in the range of 12.9 ± 0.2 percent illustrate some important observations for the 61S2 and 61S4 dies. As the overgrind was decreased fill was achieved at a 13.1 percent reduction, but with galling; at nearly the same overgrind (3.9 percent), but slightly lower reduction (12.7 percent) underfill was experienced; at the same reduction, but a 0.4 percent smaller overgrind, fill was achieved. These observations demonstrate the very critical relations among overgrind reduction and rifling quality at one die angle. All of these measurements had high mandrel forces, which might be considered typical of incipient galling. Good quality rifling under the described conditions appeared impossible at values of overgrind below about 5 percent.

The third product quality parameter, strain energy density, has been briefly discussed and illustrated in Figure 19 where the dependence of U on percent overgrind was shown. The general relation which was shown demonstrates that increasing overgrind increases the strain energy density. Since each data point required definition of 9 independent process parameters to describe the conditions used to produce the rifled blank, the obvious spread of the data in Figure 19 was affected by the dependence of U on the 8 other process parameters. As with the previous evaluations, multiple regression analysis was used to determine the individual effects of the process parameters on U . The resulting equations are shown in Table IX and the first equation for U is plotted in Figure 26. Three sets of curves, one for each die angle of 3° , 6° and 8° , are presented for the dependence of U on overgrind for the specified conditions of land length, feed rate, tube diameter and mandrel reduction. Data points for these specific conditions are shown on the curves to demonstrate the agreement between the experimental observations and predictions. This agreement appears to be very good. The regression results show that U decreases with decreasing overgrind, land length, feed rate, back pressure, die angle and secondary mandrel and die reductions, and with increasing tube diameter and total reduction of area. However, the most significant design parameters are overgrind, land length, feed rate, tube diameter, die angle and secondary die reduction. The minimum possible value of U is zero, which is the most desirable value based on barrel stability. Two parameters which affect U and quality (Q) are feed rate and tube diameter. These parameters lead to desirable changes of U and Q with a simultaneous increase in product cost (i.e., decreased feed rate reduces productivity and increased tube diameter increases material and finishing costs). The units of feed rate, inch per machine revolution, and the effect of feed rate indicate that the volume of material enclosed between the dies on closing is proportional to residual stress or U . Therefore, a short stroke

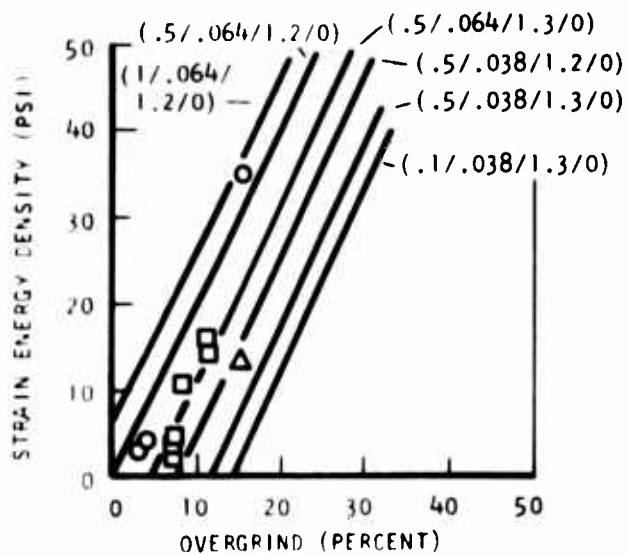


8° (LAND LENGTH/FEED RATE/
TUBE DIA./MANDREL RED.)

DATA

○ (1/.064/1.2/0)

□ (1/.064/1.3/0 & .17)



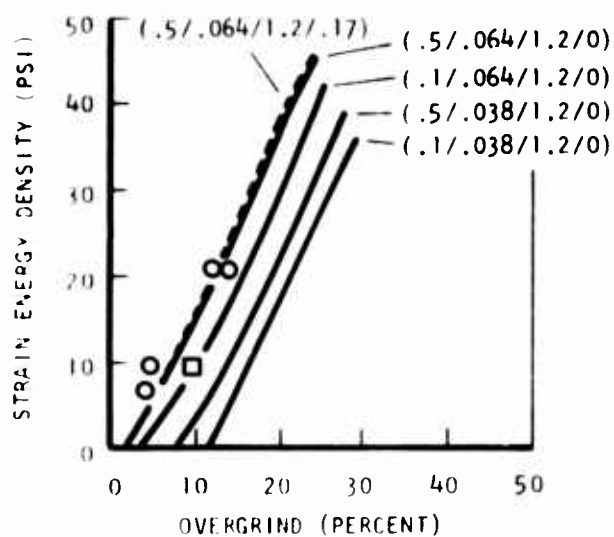
6° (LAND LENGTH/FEED RATE/
TUBE DIA./MANDREL RED.)

DATA

○ (.5/.064/1.2/0 & .17)

□ (.5/.064/1.3/0 & .17)

△ (.5/.038/1.3/0)



3° (LAND LENGTH/FEED RATE/
TUBE DIA./MANDREL RED.)

DATA

○ (.5/.064/1.2/0 & .17)

□ (.1/.064/1.2/0)

Figure 26. The dependence of strain energy density on process parameters.

machine of high rpm appears most desirable for producing low stress values at reasonable production rates because of the strong dependence of U on feed rate (as inch per machine revolution). The desirable effect of increasing tube diameter on both U and Q is probably associated with the shear strain gradient which exists through the tube wall during swaging. This gradient may also be proportional to the total contact length of the workpiece and mandrel and certainly the land length (e.g., increasing land length produces undesirable changes in both U and Q). Because the mandrel produces a circumferential shear in addition to the radial contraction and axial extension produced by the dies, a thick-walled tube can cushion the effect of this shear on the average deformation required to achieve the product. As the wall thickness decreases, the pure radial and axial flow imposed by the dies interacts more strongly with the effect of the mandrel on the deformation and probably imposes a greater force on the right hand side of the mandrel to achieve the net axial flow. With this line of reasoning thin-walled tubes and increased twists should result in lower quality and increased residual stress.

The analysis of residual stress was based on a principal system of normal stresses directly related to the cylindrical coordinate system of the tube. Such an analysis for swaged barrels is somewhat empirical or semi-quantitative because of the high probability that the rifling imparts residual shear stresses. These stresses would produce an under or over-twisting of the tube, in addition to the radial and axial displacements, during boring out. This twisting was not evaluated during the residual stress measurements.

The most desirable value for the strain energy density is, of course, zero which may be impossible to achieve and/or maintain. Other values of U are associated with values of diametral expansion ΔD and axial expansion ΔL which can promote distortion. The results in Figure 20 showed that ΔD and ΔL approached zero as U approached zero. Within the experimental scatter, the dependence of ΔL on U appeared approximately linear, but the values for ΔD exhibited a precipitous drop at low values of U (less than about 5) where ΔD became small in absolute magnitude but with both positive and negative values. The dependence of ΔD on overgrind as shown in Figure 21 was significantly more continuous indicating a possible dependence of ΔD on process parameters. The dependence of both ΔD and ΔL on the processing variables were analyzed; however, only ΔD exhibited a significant relation. The best regression equation for ΔL exhibited a standard error equal to nearly one-fourth the average of the measured values and, therefore, was not used for process design. This finding and the results in Figure 20 indicate that ΔL is most strongly dependent on the value of U and, otherwise, relatively independent of the process design parameters. In contrast to this observation, ΔD was strongly dependent on the process parameters as shown by the regression equation in Table IX. Since ΔD can

be either positive or negative, processing conditions should be established from this relation for $\Delta D=0$ while simultaneously achieving a low value of U to minimize the total strain energy density and ΔL . The values of overgrind and reduction which satisfy these conditions $\Delta D=0$ and $U=0$ for $Q=0$ and a land diameter of 0.3002 inch are shown in Figure 27. This figure can be used as a working diagram for process design. Because the relations were developed for $Q=0$, $U=0$, and $\Delta D=0$, any significant departures from the curves should be in a direction to make Q more positive and to leave U and ΔD relatively unchanged. Since the variation of the process parameters is linear over the range between the lines in Figure 27, a scale can be used to interpolate between the values shown on the figure. For example, a die with a 6.2° entrance angle, 9 percent overgrind and 0.1 inch land length would require a feed rate of 0.04 inch/rev., a reduction of 15.3 percent with a minimum tube diameter of 1.207 inch. Increasing tube diameter would increase both Q and ΔD , therefore, requiring a compromise. But for $Q=0$, it is conceivable that a lower reduction could be used to increase Q without affecting ΔD or U .

The complicated nature of a diagram such as Figure 27 makes its use objectionable. However, it can be used to establish approximate process design conditions for selecting tooling from an available inventory. Subsequent precise specification of the processing conditions, particularly to insure $Q>0$ and $U=\Delta D=0$, should be performed from the regression equations.

The parametric relations for machine performance factors (push rod force and mandrel force) and barrel quality (land diameter, quality factor and residual stress) as affected by process design parameters provide a basis for quantitative optimization of the process design. The objective of this program was to optimize the relevant processing parameters to produce improved quality precision swaged barrels. Therefore, the primary concern of the program was process design optimization and not cost. If cost were explicitly considered, design factors affecting productivity and the cost of raw material, tube preparation and finishing, etc., would have been explicitly considered. However, the necessary basic parametric relations for relating swage process design to cost are identical to those for process optimization.

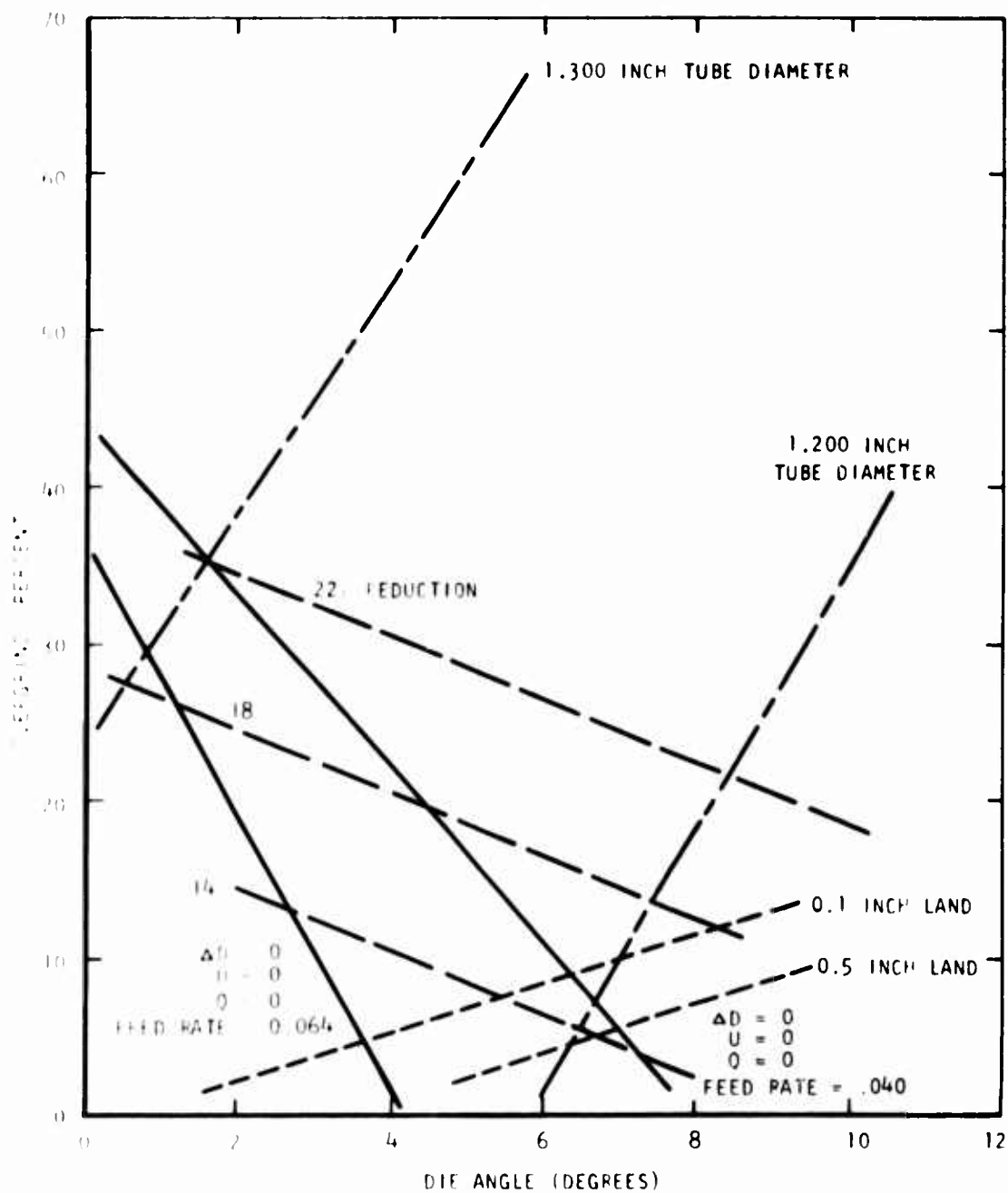


Figure 27. The dependence on overgrind and reduction of the significant processing parameters required to produce a land diameter of 0.3002 inch with minimum distortion and a Quality Factor value of 0.

5.0 Process Optimization

The results of this program have shown that the attainment of good quality rifling at low values of residual stress is not easy to achieve by swaging, but can be obtained under rather specific conditions. Rounded corners on the lands may be the best quality bore form under a specific set of design conditions because increased reductions necessary for fill can result in galling before fill is achieved. This condition is usually indicative of high mandrel rod forces. In general, the reduction range over which complete fill can be achieved is either not attainable or very narrow. A high quality bore form with dimensional precision is achieved and maintained in the swaged blank when the mandrel form is filled and the bore surface "wipes" or is burnished by the mandrel. When this condition is achieved, excellent surface finishes and dimensional precision are obtained at the bore provided the back pressure can be maintained constant during the swaging cycle. Straightness achieved by swaging is most significantly affected by bushing design and can be maintained at values better than 0.0005 inch/foot by proper bushing design. All of these quality features can be destroyed by residual stress produced in the barrel blank during swaging as a result of process design and by the lack of care in the barrel finishing operation.

The process optimization which was performed was based on the following empirical observations:

1. The maximum push rod force should be maintained below about 7000 pounds for safe and comfortable machine operation and the back pressure should be sufficient to avoid full recoil of the push rod (loose contact with the work-piece).
2. The tube diameter should be selected to produce a finished blank close to the maximum finished dimension of the barrel regardless of the quality benefits of a large diameter tube.
3. Straightness control is most significantly provided through proper bushing design and alignment.
4. A low mandrel force is desirable because this force increases with the tendency toward galling and may be indicative of wear rate.

Therefore, with these general considerations optimization was performed to obtain the processing conditions which provided the lowest levels of strain energy density while producing the completely filled rifling form at a high value of quality from a tube which could be swaged to near finished dimensions. The following analytical procedure was used:

1. The regression equation for land diameter was set equal to 0.0001 inch less than the mandrel diameter (0.3003 inch) and the reduction-overgrind relations determined for each die angle. This procedure was followed to insure fill without corner rounding. These relations are shown in Figure 28 for 3°, 4°, 6° and 8° die angles as the solid lines in this figure.
2. The required tube diameters for values of $Q = +1$ and 0 were determined from the overgrind - reduction - die angle relations in the preceding by using the equation for Q in Table VII and solving for X_5 with secondary die and mandrel reductions set equal to zero (i.e., nearly conventional dies and conventional mandrels were used). These calculations are shown as the broken lines, $Q = +1$ and the dash lines, $Q = 0$, in Figure 28.
3. The overgrind-reduction relations for $U = 10$ and $U = 0$ were determined from the equations for U with a land length of 0.1 inch and expressions for die angle and tube diameter obtained from the equations for land diameter, which was set equal to 0.3002 inch, and Quality Factor, which was set equal to +1. These relations for U are shown as the heavy lines as indicated in Figure 28.

The plotted relations in Figure 28 provide the range over which good quality barrels can be produced and the anticipated strain energy density. For example, for a 20 percent overgrind with a 4° die angle, a reduction of 17 percent would be required. The quality factor Q would range from +1 for a tube diameter of 1.340 inch to 0 for a diameter of 1.190 with a U value in the range of 5 to 10 respectively. Smaller tube diameters would reduce the quality factor and increase the strain energy density. Tube diameters smaller than 1.190 inch would probably result in galling and those larger than 1.340 inch would not satisfy the fill requirements and, therefore, would result in rounded corners. Therefore, it is usually desirable to start with a tube diameter significantly greater than the diameter for $Q = 0$, but less than the diameter for $Q = +1$.

Figure 28 was used to select the final processing conditions in the following manner:

1. As-hot-rolled and centerless-ground bar was heat treated, sand blasted to remove any adhering scale, gun drilled (0.3125 inch diameter hole), honed to 0.3140 inch diameter and ground on centers to provide 23 inch long tubes with a 0.314 inch I.D. and 18+6 microinch AA bore finish, a 1.220 inch O.D. and a maximum T.I.R. of 0.005 inch. These dimensions were selected before the final fabrication procedures were established to facilitate the program schedule.

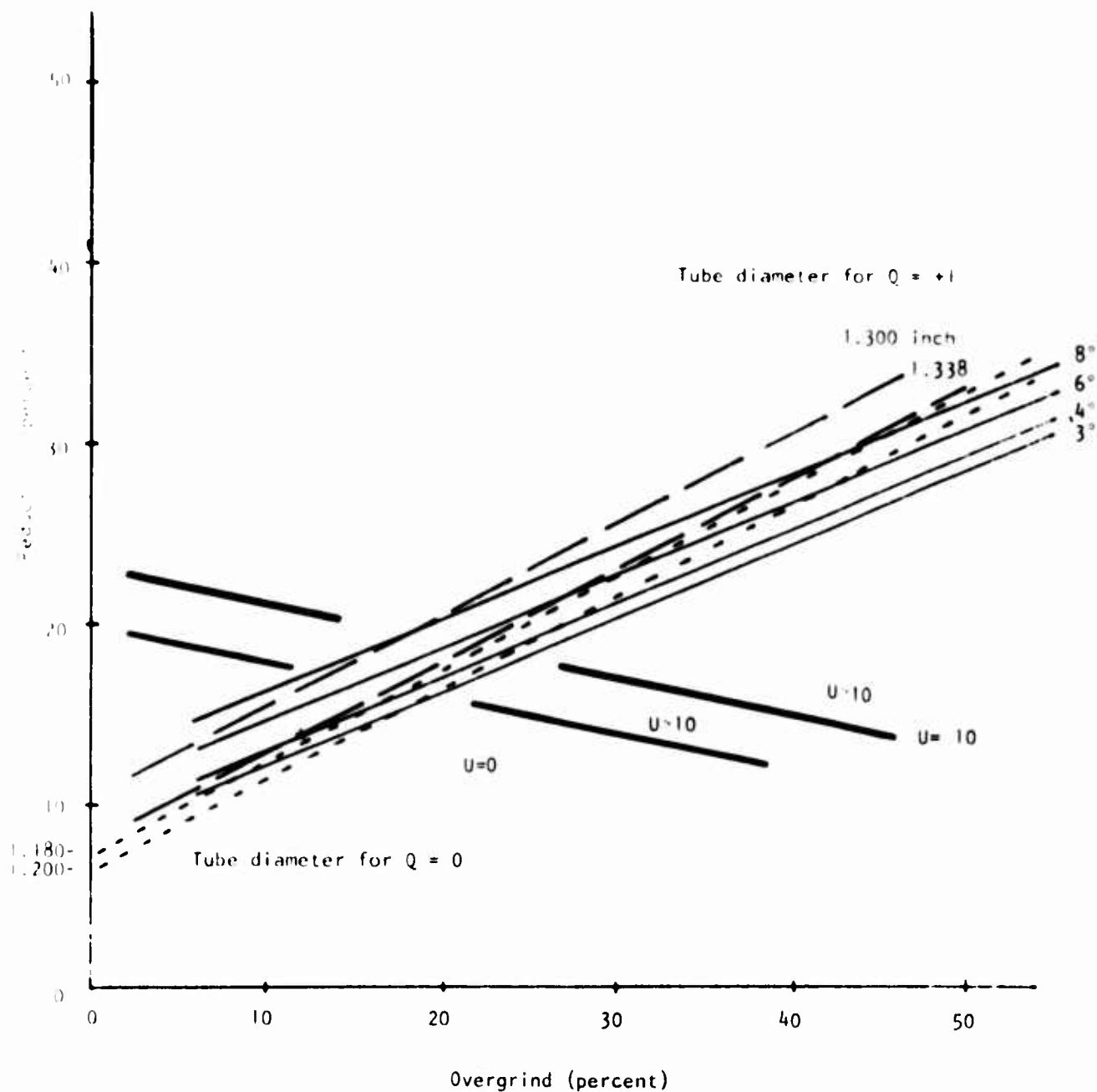


Figure 28. The dependence of tube diameter, die angle and strain energy density on reduction and overgrind for defining optimum process design conditions.

2. The results in Figure 28 indicated that overgrinds below about 20 percent were desirable for producing low levels of residual stress with a 0.1 inch land length. Further restrictions were placed on the range of overgrinds, reductions and die angles which could be used because of the mandrel rod force (see Figure 24). A mandrel force of 300 pounds was selected as a desirable maximum which further restricted the range of the design parameters to the following:

<u>Die Angle</u>	<u>Overgrind (%)</u>	<u>Reduction (%)</u>
3°	6 to 20	12 to 18
6°	7 to 12	15 to 17
8°	7.5 to 8.5	17

All of these conditions were found to be satisfactory; however, the smaller die angles were preferred to produce the smallest push-rod force and lowest values of strain energy. Based on this quantitative selection of the possible range of processing conditions, a 4° die with a 10 percent overgrind at the nominal maximum barrel diameter of 1.100 was selected because a diametral change ΔD of approximate ± 0 could be obtained.

3. The 1.220 inch diameter tubes were swaged over a smooth mandrel (0.3110 inch diameter) to a diameter of 1.187 inch to improve the bore surface and provide a quantitative test of the validity of the results in Figure 28. These conditions corresponded to a Q value of +0.3 for 13.7 percent reduction from 1.187 to 1.103 inch diameter.

4. The barrels were forged under the following conditions:

Overgrind - 10%
Land Length - 0.1 inch
Feed Rate - 0.040 in/rev.
Back Press. - 2100 lbs.
Tube Dia. - 1.187
Reduction - 13.7%
Die Angle - 4°

Mandrel Red. - 0%

Secondary Die reduction - 0%

$Q = +0.3$

$U = 0$

$\Delta D = 0$

6.0 Barrel Fabrication and Evaluation

Eight tubes were prepared according to the preceding set of optimum processing conditions. However, during the fabrication of these blanks, difficulty was encountered in the back pressure hydraulic cylinder from the combined effects of cylinder-wall pitting and wear of the piston. This back pressure variation produced a corresponding variation of the land diameter. Four blanks were run and rejected before this condition was properly repaired. Repair necessitated honing of the cylinder wall and replacement of the piston assembly. The remaining four blanks were run after this repair of the equipment. Because a total of six blanks was required for final barrel fabrication, three previously swaged blanks (61S4R9-1, 61S4R9-2 and 61S4R9-3) were selected for further processing. These blanks were swaged with slightly rounded corners, but with near zero strain energy density and ΔD . The rounded corners were removed by diamond lapping using a cylindrical lap (0.3001 inch original diameter and 0.50 inch long) and six micron diamond paste. Measurements before and after machining the 61S4 series of blanks which had been lapped and the blanks swaged under the optimum conditions are shown in Table XI. The "Runout from Q" recorded in Table XI was obtained on blanks rotated on centers located off chamfers machined with a piloted center drill. The blanks were 22.35 ± 0.05 inches long. The measurements after machining were obtained on 22.00 ± 0.02 inch long barrels before chambering. The chamber end of the barrel was located off the chamfer and the muzzle was held in a collet. Measurements on Blank No. 41S1-3 after machining have been omitted because this blank was used for setup and some of its dimensions are not correct. The comparatively large runout of the 41S1 series of blanks resulted from the inadvertent use of an oversize rear guide bushing (1.200 inch diameter).

Machining of the barrels was performed in accordance with the test results (i.e., a maximum speed of 150 surface feet per minute, maximum depth of cut of 0.03 inch and a feed rate of 0.005 inch per revolution). The runout of the barrels during roughing increased to a maximum of 0.014 inch which necessitated straightening before final machining. Obviously, with more elaborate fixturing, which could be justified for production fabrication, this runout could have been averted.

All blanks exhibited a bore contraction after machining as shown by the results in Table XI for the maximum/minimum land and groove diameters. The maximum contraction was 0.00014 inch, although the variation of bore dimensions along the entire length of both the blanks and barrels was less than 0.00009 inch. These contractions resulted from machining the swaged blanks from nominally 1.1 inch diameter to a contour which varied between 1.1 inch to 0.4795 inch diameter.

TABLE XI

Measurements on Swaged Blanks and
the Corresponding Fabricated Barrels

Blank No.	Measurement before Machining (in)				Measurement after Machining (in)		
	Land Dia.	Groove Dia.	Runout from ϕ	Outer Dia.	Land Dia.	Groove Dia.	Runout from ϕ
41S1-1	$\frac{.30074}{.30078}$.30860	0.0045	1.102	$\frac{.30073}{.30065}$	$\frac{.30852}{.30846}$.002
41S1-2	$\frac{.30050}{.30049}$.30868	0.0025	1.102	$\frac{.30049}{.30043}$	$\frac{.30862}{.30855}$.0015
41S1-3	$\frac{.30047}{.30045}$.30868	0.003	1.102			
41S1-4	$\frac{.30047}{.30045}$.30868	0.0025	1.103	$\frac{.30043}{.30038}$	$\frac{.30838}{.30832}$.0035
61S4R9 2	$\frac{.30035}{.30033}$.30843	0.002	1.105	$\frac{.30033}{.30024}$	$\frac{.30831}{.30828}$.006
61S4R9-3	$\frac{.30035}{.30032}$.30818	0.0016	1.104	$\frac{.30031}{.30025}$	$\frac{.30810}{.30807}$.002
61S4R9-4	$\frac{.30036}{.30035}$.30818	0.003	1.101	$\frac{.30028}{.30022}$	$\frac{.30816}{.30812}$.0015

Six barrels of the M21 configuration were submitted to the Marine Corps Base, Quantico, VA. for test firing. The test firing was conducted under the supervision of Mr. Snodgrass of the GEN Thomas J. Rodman Laboratory, Rock Island Arsenal. His Memorandum For Record, dated 8 Jul 74, which gives the results of the test firing, is attached to this report as an Appendix. All six barrels performed satisfactorily. The test firing on these barrels will be continued throughout next year and complete records of performance and bore dimensional decay will be maintained. At the conclusion of these tests, a separate technical report on the performance of these barrels will be published.

7.0 Conclusion

An experimental-analytical program was performed which provided parametric relations for rifle barrel quality and machine performance measurements in terms of nine process design variables for the use of a precision swage. The parametric relations formed the basis for defining optimum process design procedures for swaging precision barrels.

The experimental observations showed that stress-free barrels of good bore form and dimensional precision to meet the requirements of the M21 barrel can be achieved by swaging. Bushing design was found to be the most significant factor affecting blank straightness. Although a broad range of process design variables were shown to produce low levels of residual stress (i.e., equivalent to the stress relieved product) the requirement of good bore quality (dimensional precision and, particularly, tear-free, complete fill) greatly restricted this range. This narrow processing range resulted from the opposing effects of the major process variables, e.g., overgrind and die angle, on residual stress and tearing or galling. The critical factor with residual stress for the M21 barrel is diametral expansion which can produce a variation of the bore diameter in excess of the 0.0001 inch tolerance band. This expansion was reduced to near zero values by selection of appropriate process design parameters. Loss of straightness was related to both tool force and residual stress, but was avoidable by machining with light feeds and depths of cut at the expense of productivity or by using lateral support of the blank during machining.

The results of this program demonstrated that very specific process design parameters must be selected to achieve the quality and precision required for the M21 barrel. The fact that these conditions can be obtained is demonstrated by the results in Table XI.

8.0 REFERENCES

1. Rock Island Arsenal personnel, private communications (February 1972).
2. R.L. Suffredini, "How Swaging Affects Mechanical Properties of Steel," Metal Progress, ASM (Aug. 1963) 109.
3. A.L. Hoffmanner, "Rotary Swaging of Precision Barrels," First Quarterly Report on U.S. Army Contract No. DAAF03-73-C-0005 (December 1972).
4. TRW Inc., Manufacturing Data on M 14 (January 1963).
5. A.A. Denton, "Measurement of Residual Stresses," Techniques of Metals Research, Vol. V, Part 2, "Measurement of Mechanical Properties," R.F. Bunshah, Editor, Interscience (1971) 234
6. N.R. Draper and H. Smith, Applied Regression Analysis, John Wiley and Sons, Inc., New York, N.Y. (1963).
7. R.J. Fiorentino, et al., "Development of the Manufacturing Capabilities of the Hydrostatic Extrusion Process," Interim Engineering Progress Report No. IR-8-195(ix), Battelle Memorial Institute, Columbus Laboratories. March 1967.
8. J.K. Misra and N.H. Polakowski, "In-Process Control of Residual Stress in Drawn Tubing," TASME, J. of Basic Engineering (Dec. 1969) 810.
9. System 360, Scientific Subroutine Package 360-A-CM-03X Version 2, IBM Corp., White Plains, N.Y. (1971).

APPENDIX

TRAVEL MEMORANDUM FOR RECORD

8 July 1974

SUBJECT: Travel to MCB, Quantico, VA, 24-28 Jun 74, T.O. #4-2383

1. PURPOSE: To determine the accuracy level and dimensional stability of prototype rotary swaged M14/M21 Rifle barrels.

2. BACKGROUND: Although rotary swaging of rifle barrels is not necessarily a new process, considerable study went in the optimizing the processing of these barrels to provide the best possible dimensional control and the minimum of residual stress. Each of these barrels exhibited different dimensions ranging from the smallest .3080 groove .3001 lands to .3066 groove .3005 lands, the variation within anyone of the barrels was less than .00015 inches and the internal bore finish averaged 8 micro inches. This can be considered outstanding in comparison to the present match/sniper rifle barrels.

Present mfg. M14 match rifle barrels (the sniper rifle barrel is a select match rifle barrel) exhibits .3076 + .001 groove .3000 + .001 barrel with no requirement for uniformity through the bore length. Experience requires these barrels be air gaged and selected for use presently about 65 out of each 100 barrels are considered suitable for use. Of the 65 selected barrels, about two or three may be considered excellent barrels and should be used in a sniper or a premium grade match rifle.

These barrels would exhibit the dimensions, and uniformity of the provided prototype barrels.

3. SUMMARY OF MODIFICATIONS: The barrels were received at Marksmanship Training Unit on 14 June. MSgt Sweet, GSgt McGee, SSgt Gregorg and Sgt Sterling started building rifles around the barrels on 17 June. Total time expended in assembly of the rifles was 118 hrs with an additional 8 hours of time spent on 25 and 26 June with some final adjustments. The following comments were provided relative to the barrels and assembly:

			<u>Barrel No.</u>
M14 Serial No.	299297	was assembled with	61S4R9-4
M14 Serial No.	300531	was assembled with	41S1-2
M14 Serial No.	541779	was assembled with	41S1-4
M14 Serial No.	544093	was assembled with	61S4R9-2
M14 Serial No.	546B05	was assembled with	61S4R9-3
M14 Serial No.	119464	was assembled with	41S1-1

It was noted, none of the barrels provided had an extractor clearance cut or feed ramps. All required machining prior to assembly. One barrel required the shoulder to be rolled back to obtain proper "draw". The receivers had been previously assembled and were not new. Consideration should be given to tolerancing the shoulder to provide proper draw on any action.

Bearing areas for the gas cylinder and flash suppressor were rather tight; threads for gas cylinder lock and flash suppressor nut were oversized. Splines for flash suppressor required modification prior to assembly.

4. PERFORMANCE: Accuracy testing of the rifle was accomplished at 300 yds fired from the shoulder, rapid fire cadence. The ammunition used was 7.62mm Nato Match Lot LC 20-29, and a hand load utilizing LC 20-24 case, primer and charge, with a Sierra 168 gr. ball substituted for the 172 gr. ball. This hand loaded lot is designated 24-68 by the Marksmanship Training Unit.

The following table indicates the average of 3 ten shot groups obtained out of 4 trials with each rifle/shooter/barrel and ammunition combination:

a. Rifle #544093, Barrel No. 6154R9-2

Groove dimension of .3082 to .3083

Land Dimension of .3002

Shooter MSgt Martin

Lake City LC 20-29

Handload Lot 24-68

6 X 6.8

4.3 X 4.5

b. Rifle #299297, Barrel No. 6154R9-4

Groove dimension of .3080

Land Dimension of .3081

Shooter CW03 Neal Crane

Lake City LC 20-29

Handload Lot 24-68

7.6 X 5.8*

10.3 X 3.7*

*Note this rifle was later found to have a loose rear sight.

c. Rifle #119464, Barrel No. 4151-1

Groove dimensions of .3081 to .3080

Land Dimensions of .3001

Shooter MSgt Carlson

Lake City LC 20-29

Handload Lot 24-68

7.4 X 6

4.6 X 3.5

d. Rifle #541779, Barrel No. 4151-4

Groove dimensions of .3085
Land dimensions of .3005 to .3004
Shooter CW0-3 David Luke
Lake City LC 20-29 Handload Lot 24-68
7 X 6.2 5.7 X 3.4

e. Rifle #546305, Barrel No. 6154R9-3

Groove dimensions of .3085 to .3084
Land dimensions of .3007
Shooter MSgt Frank Kruk
Lake City LC 20-29 Handload Lot 24-68
6.5 X 6.7 6.3 X 4

f. Rifle #300531, Barrel No. 4151-2

Groove dimensions of .3086 to .3085
Land dimensions of .3005
Shooter CW0-3 Sargeant
Lake City LC 20-29 Handload Lot 24-68
6.9 X 6.5 4.7 X 4.7

Excluding the rifle found to have a loose rear sight (the recoil was relocated after each shot) the guns averaged 6.7 inches Vertical and 6.8 Horizontal with no correction for wind using LC 20-29. The groups with the handloads as would be expected, were much better, 5.1 inches Vertical, 4.0 inches Horizontal.

Usually a rifle re-built to MTU standards requires about 300 to 400 rounds history before this kind of performance is obtained.

5. OBSERVATIONS: The present cost of the Match Rifle barrel is over \$43.00 per copy. These 100 barrels then cost \$4,300.00; if 65 are serviceable, they cost \$66.00 each and the three real good premium barrels cost over \$1,400.00 each.

Since the last procurement of barrels, the drawings have been changed to allow only 1/2 the previous tolerance. The new drawings do not control the variation of dimensions within any one barrel. Bids on production of barrels to the present drawings have been received at \$74.00 each or \$7,400.00/100 barrels. Selection will probably yield the same percentage of serviceable barrels that will make them worth \$113.00 each and the premium quality barrel (with less than .0001 variation throughout) will then cost over \$2,400.00 each.

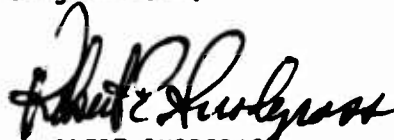
6. CONSLUSIONS: The prototype rotary swaged barrels provided appear to be more uniform in dimensions, exhibit a better bore finish and shoot as well if not better than the standard cut rifled barrels. Considering that 100% of the samples would meet the most stringent dimensions, and exhibited better than average performance within the initial 100 rounds history, consideration should be given to production of a larger sample for a more extensive test.

7. RECOMMENDATIONS: Simplifying the outside configuration of the barrel, doing away with some of the fancy milling operations now required would provide a heavier, stiffer barrel and probably increase the performance significantly. (See attached drawing). It has been estimated barrels of the same quality provided for this test could be produced in the \$20 to \$30.00 price range and a higher yield of serviceable barrels could be expected.

8. FOLLOW-ON ACTION REQUIRED: The Marksmanship Training Unit will continue testing these six barrels through 500 rounds history. One of the barrels (the worst one) will be returned to RIA for further metallurgical evaluation. The remaining five barrels will be tested to destruction.

9. COORDINATION: Liaison will be maintained with the Marksmanship Training Unit to obtain any data generated.

Incl
as



ROBERT SNODGRASS
Mech. Engr. Tech.
Individual Weapons Division



1	2	3	4	5	6	7	8	9	10	11	12	13	14	15	16	17	18	19	20	21	22	23	24	25	26	27	28	29	30	31	32	33	34	35	36	37	38	39	40	41	42	43	44	45	46	47	48	49	50	51	52	53	54	55	56	57	58	59	60	61	62	63	64	65	66	67	68	69	70	71	72	73	74	75	76	77	78	79	80	81	82	83	84	85	86	87	88	89	90	91	92	93	94	95	96	97	98	99	100
---	---	---	---	---	---	---	---	---	----	----	----	----	----	----	----	----	----	----	----	----	----	----	----	----	----	----	----	----	----	----	----	----	----	----	----	----	----	----	----	----	----	----	----	----	----	----	----	----	----	----	----	----	----	----	----	----	----	----	----	----	----	----	----	----	----	----	----	----	----	----	----	----	----	----	----	----	----	----	----	----	----	----	----	----	----	----	----	----	----	----	----	----	----	----	----	----	----	----	-----

Technical drawing of a cross-section of a pipe. The drawing shows a central rectangular area labeled "NO. 3 MESH SIEVE (60 MESH ON DIA PER INCH OF LENGTH)". To the left of this area, the dimension "6.62" is indicated. Below the central area, the dimension "4.50" is indicated. To the right of the central area, the dimension "1.50" is indicated. At the bottom left, the dimension "845-007" is indicated. At the bottom center, the dimension "1.00 DIA DOZ" is indicated. At the bottom right, the dimension "12" is indicated. The overall width of the drawing is labeled "24.00" on the left side. The overall height of the drawing is labeled "700 DIA" on the right side. The drawing also includes a vertical dimension line on the right side labeled "800 DIA".

[illegible]

96